ผลกระทบของตัวแปรของกระบวนการกัดผิวที่มีต่อรอยตำหนิแบบเส้นบนอะโนไดซ์อลูมิเนียม

นางสาวศิริกานต์ สัตถวิชยพิชญ์

วิทยานิพนธ์นี้เป็นส่วนหนึ่งของการศึกษาตามหลักสูตรปริญญาวิศวกรรมศาสตรมหาบัณฑิต
สาขาวิชาวิศวกรรมเคมี ภาควิชาวิศวกรรมเคมี
คณะวิศวกรรมศาสตร์ จุฬาลงกรณ์มหาวิทยาลัย
ปีการศึกษา 2559

EFFECT OF ETCHING PROCESS PARAMETERS ON STREAK DEFECT IN ANODIZED ALUMINUM

Miss Sirikarn Sattawitchayapit

A Thesis Submitted in Partial Fulfillment of the Requirements
for the Degree of Master of Engineering Program in Chemical Engineering
Department of Chemical Engineering
Faculty of Engineering
Chulalongkorn University
Academic Year 2016

Thesis Title	EFFECT OF ETCHING PROCESS PARAMETERS ON STREAK DEFECT IN ANODIZED ALUMINUM
By	Miss Sirikarn Sattawitchayapit
Field of Study	Chemical Engineering
Thesis Advisor	Assistant Professor Amornchai Arpornwichanop, D.Eng.

Accepted by the Faculty of Engineering, Chulalongkorn University in Partial Fulfillment of the Requirements for the Master's Degree

....Dean of the Faculty of Engineering
(Associate Professor Supot Teachavorasinskun, D.Eng.)

THESIS COMMITTEE

....Chairman
(Assistant Professor Sorada Kanokpanont, Ph.D.)

....Thesis Advisor
(Assistant Professor Amornchai Arpornwichanop, D.Eng.)

....Examiner
(Paravee Vas-Umnuay, Ph.D.)

....External Examiner
(Sasawat Mahabunphachai, Ph.D.)

ศิริกานต์ สัตถวิชยพิชญ์ : ผลกระทบของตัวแปรของกระบวนการกัดผิวที่มีต่อรอยตำหนิแบบเส้นบนอะโนไดซ์อลูมิเนียม (EFFECT OF ETCHING PROCESS PARAMETERS ON STREAK DEFECT IN ANODIZED ALUMINUM) อ.ที่ปรึกษาวิทยานิพนธ์หลัก: ผศ. ดร.อมรชัย อาภรณ์วิชานพ, 112 หน้า.

รอยตำหนิแบบเส้น (Streak defect) บนอะโนไดซ์อะลูมินัมเป็นปัญหาหลักในอุตสาหกรรมการผลิตอะลูมินัมแบบอัดขึ้นรูป รอยตำหนินี้ทำให้สีพื้นผิวของอะลูมินัมหลังการอัดขึ้นรูปไม่สม่ำเสมอกัน สังเกตเห็นได้ด้วยตาเปล่า สาเหตุที่ทำให้เกิดรอยตำหนินี้เกิดมาจากหลายปัจจัยด้วยกัน เช่น ผิวของแม่พิมพ์ที่ใช้ในการอัดขึ้นรูปมีคุณภาพไม่ดี การเปลี่ยนพื้นที่ผิวสัมผัสของน้ำโลหะที่แม่พิมพ์ขาออก (Bearing) ในการอัดขึ้นรูปอย่างรวดเร็ว เป็นต้น ในส่วนของการแก้ปัญหาเชิงเทคนิคในปัจจุบัน มีการใช้วิธีการลองผิดลองถูกในระหว่างกระบวนการกัดผิว (Etching process) เพื่อกำจัดรอยตำหนิแบบเส้น ซึ่งวิธีนี้ทำให้เสียค่าใช้จ่ายและใช้เวลาในกระบวนการผลิตเพิ่มขึ้น ดังนั้นงานวิจัยนี้จึงมุ่งเน้นการศึกษาผลกระทบของตัวแปรควบคุม (Controllable factors) ของกระบวนการกัดผิว ได้แก่ ความเข้มข้นของโซเดียมไฮดรอกไซด์ อุณหภูมิและเวลาของกระบวนการกัดผิว ที่มีต่อตัวแปรตอบสนอง (Response variables) ได้แก่ น้ำหนักที่หายไป ความแตกต่างของความเงาพื้นผิวของก่อนและหลังการกัดผิว และความขรุขระของพื้นผิวของชิ้นงานอะลูมินัมหลังการกัดผิว การทดลองทั้งหมด 20 ครั้งที่ได้ดำเนินการถูกออกแบบโดยใช้หลักเซ็นทรัลคอมโพสิต (Central Composite Design, CCD) วิธีการแสดงผิวตอบสนองแบบโครงร่างพื้นผิว (Response Surface Methodology, RSM) ถูกใช้ในการสร้างแบบจำลองและวิเคราะห์สมการถดถอย (Regression equation) สำหรับตัวแปรตอบสนองที่มีตัวแปรของกระบวนการกัดผิวเป็นตัวแปรควบคุม การวิเคราะห์ความแปรปรวน (Analysis of variance, ANOVA) ถูกใช้ในการหาอิทธิพลของตัวแปรควบคุมเหล่านี้ เพื่อที่จะหาสมการถดถอยซึ่งจะนำไปใช้เป็นแบบจำลองทำนายค่าตัวแปรตอบสนอง สำหรับการตรวจสอบแบบจำลอง (Model validation) ผลการทำนายที่ได้มีค่าความแม่นยำสูง โดยมีค่าผิดพลาดของน้ำหนักที่หายไป 0.55% และค่าความแตกต่างของความเงาของพื้นผิวของก่อนและหลังการกัดผิว 18% นอกจากนี้ยังมีการนำกราฟแสดงความสูง - ต่ำ (Contour plot) และกราฟพื้นผิว (Surface plots) ที่ได้จากการใช้วิธี RSM มาใช้ในการอธิบายผลกระทบหลักและผลกระทบร่วมของปัจจัยด้วย อีกทั้งวิธีการซ้อนทับกราฟแสดงความสูงต่ำ (Overlaid contour plot) ใน CCD สามารถนำมาใช้หาสภาวะของการกัดผิวเพื่อลดรอยตำหนิแบบเส้นได้ จากผลการทดลองในงานวิจัยนี้ สามารถหาแนวทางสภาวะของตัวแปรควบคุมของกระบวนการกัดผิวเพื่อลดรอยตำหนิแบบเส้นของชิ้นส่วนอะลูมินัมแบบอัดขึ้นรูปที่เหมาะสมได้

ภาควิชา วิศวกรรมเคมี	ลายมือชื่อนิสิต ....
สาขาวิชา วิศวกรรมเคมี	ลายมือชื่อ อ.ที่ปรึกษาหลัก ....
ปีการศึกษา 2559	

5771010021 : MAJOR CHEMICAL ENGINEERING
KEYWORDS: STREAK / ALUMINUM EXTRUSION / ETCHING / RESPONSE SURFACE METHODOLOGY / CENTRAL COMPOSITE DESIGN / ANOVA / OVERLAID CONTOUR PLOT / SURFACE GLOSS

SIRIKARN SATTAWITCHAYAPIT: EFFECT OF ETCHING PROCESS PARAMETERS ON STREAK DEFECT IN ANODIZED ALUMINUM. ADVISOR: ASST. PROF. AMORNCHAI ARPORNWICHANOP, D.Eng., 112 pp.

A streak defect on anodized aluminum is a major problem in the aluminum extrusion industry. It causes uneven color (dull or bright) on the surface of the extruded parts and can be easily observed. Many factors can contribute to the streak defect, such as poor surface quality of the extrusion die, abrupt change of bearing on the extrusion die, etc. In the current practice, a trial and error method is used during the etching process to eliminate the streak defect and this approach increases the production cost and time. The aim of this study is to experimentally investigate the effect of etching process parameters, i.e., concentration of NaOH, etching temperature and etching time on response variables (i.e., material loss, surface gloss difference and final surface roughness) of etched aluminum parts. The experiment was conducted in a total of 20 runs designed using Central Composite Design (CCD). Response Surface Methodology (RSM) was used to model and analyze regression equations for the response variables with the etching process parameters as the controllable factors. Analysis of Variance (ANOVA) was used to investigate the significance of these parameters to determine the regression equations as the predictive models. For the model validation, the predicted results showed high accuracy with maximum errors of 0.55% and 18% in weight loss and difference in surface gloss, respectively. Additionally, contour and 3D surface plots were obtained from RSM and were used to discuss the main effects and the interaction effects of the process parameters. Moreover, the overlaid contour plots in CCD analysis were used to determine an operational range for the removal of streak defect on extruded aluminum. Based on these results, guidelines for suitable etching process parameters to eliminate the streak defect on aluminum extrusion parts are provided.

Department:	Chemical Engineering	Student's Signature	....
Field of Study:	Chemical Engineering	Advisor's Signature	....
Academic Year:	2016		

ACKNOWLEDGEMENTS

Firstly, I would like to express my sincerest gratitude and deep appreciation to my advisor, Asst. Prof. Dr. Amornchai Arpornwichanop, for his kindness, invaluable supervision, guidance, advice, and encouragement throughout the course of this study.

I also gratefully thank Asst. Prof. Dr. Sorada Kanokpanont, Dr. Paravee Vas-Umnuay, and Dr. Sasawat Mahabunphachai, as the thesis committee, for their invaluable comments.

I would like to thank the National Metal and Materials Technology Center (MTEC), Thailand, for generous and continuous supports on laboratory equipment and Alumet Co., Ltd., Thailand, for providing examples of the aluminum profiles used in this study. The support from the Computational Process Engineering Research Unit is acknowledged.

Additionally, I would like to thank Dr. Tongjai Chookajorn from the National Metal and Materials Technology Center (MTEC) for his kind support on the thesis checking and consulting, and also to every person who deserves thanks for encouragement and support.

Finally, my deepest respect to my parents and family, who have always been the source of my unconditional love, understanding, and generous encouragement during my studies.

CONTENTS

Page

Page

LIST OF FIGURES

Page

LIST OF TABLES

Page

CHAPTER 1

INTRODUCTION

1.1 General Introduction

Aluminum has been widely used in modern buildings and architecture due to its unique characteristics as a lightweight construction material, such as low volumetric mass density, high strength-to-weight ratio, and good formability as well as reformability. Moreover, because of its high index of light reflection, aluminum has an attractive surface gloss, which when combined with its high corrosion resistance, offer a lasting attractive surface finish suitable for decorative usage [1]. Although its high strength-to-weight ratio makes aluminum an interesting structural material, its aesthetics is often the important characteristic that makes aluminum an appealing material for architectural applications.

Different parts made from aluminum and aluminum alloys can be manufactured by several methods, such as casting, rolling, stamping, and extruding. Then, these aluminum and alloys can be coated using various methods such as anodized coating, powder coating and wet coating for decorative visual appearance as well as protective purposes [2].

The aluminum extrusion process is commonly used for fabricating aluminum profiles by squirting the material out through a die. Therefore, extruded products are long with a uniform cross-sectional profile that has the shape of the die opening. During the extrusion process, defects on the surface of aluminum are major problems, especially for the required decorative surface finishing. Such defects include dying lines, pitting, pick up and streaking.

A streak defect often occurs on the surface of aluminum profiles and can be observed clearly, especially after the anodizing process as shown in Figure 1-1. Different shades of bands usually occur on the surface (e.g., darker or lighter, brighter or duller) due to the difference in surface gloss and surface roughness values on the extruded parts, resulting in different reflections of light in those regions [3]. The streak defect might have originated from the extrusion process due to an improper die design, a non-uniform alloy deformation or a non-uniform distribution of friction force, consequently building up different amount of heat in different regions [4].

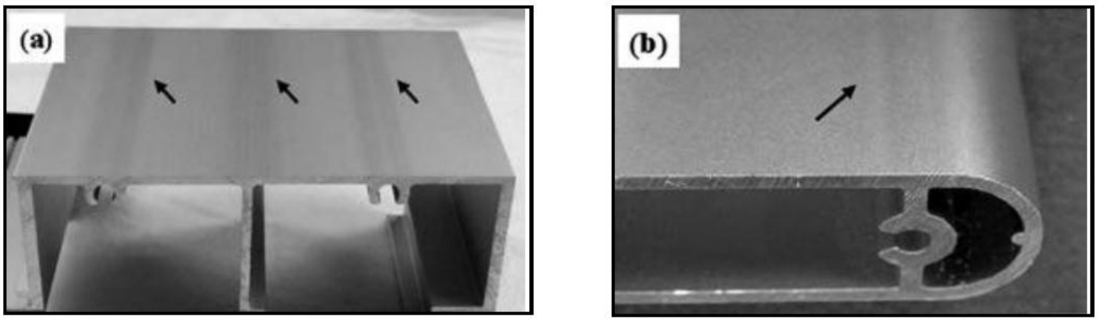

Figure 1-1: Streak defects on anodized aluminum extrusions [5].

In the actual production process, a trial and error approach has been used for streak defect elimination, often by re-processing the aluminum extrusion parts. The etching process, which is the surface preparation step before anodizing, is another method used for eliminating the streak defect. However, these approaches increase the production cost and time. Based on available information in the literature, no guidelines or predictive models have ever been developed to predict the occurrence or elimination of the streak defect.

It is well known that etching step plays a major role in the surface preparation before anodizing because the etching process can eliminate surface defects, i.e., die lines, pitting, streaking, etc. Hence, this study focuses on the etching process conditions that can eliminate the streak defects in the aluminum extrusion parts. Specifically, the effect of the following etching process parameters, namely, concentration of NaOH etchant, etching temperature and etching time, on the surface of etched aluminum, the amount of material loss, the different surface gloss after etching and the final roughness value of extruded aluminum parts are investigated. Response Surface Methodology (RSM) is used to provide the etching conditions. In the experiments, Central Composite Design (CCD), which is a subset of RSM, is applied to model and analyze regression equations for the predictive response variables with the etching process parameters as the input variables. The Analysis of Variance (ANOVA) results are used to investigate the significance of these parameters to determine the predictive equations. In addition, the contour and 3D surface plots obtained from RSM are used to describe the main effects and the interaction effects. The overlaid contour plots in the CCD analysis are used for determining an operational range to remove the streak defect on extruded aluminum. Based on the experimental data and statistical analyses, guidelines and predictive models are provided for selecting a set of suitable etching process parameters that can be used to reduce the streak defect on extruded aluminum parts without sacrificing too much of material loss in the process.

1.2 Research Objectives

1) To investigate the effect of etching process parameters, i.e., concentration of NaOH etchant, etching temperature and etching time, on the amount of material loss, the surface gloss value and the surface roughness value of extruded aluminum parts.
2) To provide guidelines for the elimination of the streak defect while minimizing the amount of material loss in the etching process.

1.3 Scopes of the Research

1) Investigate the effect of etching process parameters on streak defect in aluminum by using the response surface methodology.
2) Examine the qualities of etched aluminum regarding the weight loss after etching, and the resulting surface gloss and surface roughness.

3) Determine the relation of etched aluminum with the etching parameters.
4) Develope a predictive model based on etching parameters analysis for reduction of the streak defect on extruded aluminum parts.

1.4 Benefits Obtained from the Research

1) Cost and energy saving from re-processing or re-melting extrusion parts with streak defect.
2) Prevention of over-etching or under-etching scenario on the defective extrusion parts since suitable etching parameters will be selected based on guidelines provided in this study.

CHAPTER 2
THEORY

Recently, aluminum profiles have been used in many modern constructions, for example, as decorations in condominium in Wisconsin and marine operation centers in the United Kingdom, and as the main structure in McDonald's in France. It is because aluminum has remarkable properties as follows:

2.1 Aluminum and Aluminum Alloys

Aluminum and aluminum alloys are widely used metals in engineering and architecture due to its remarkable properties as follows [6]:

- Lightness: Its density is 2.7 g/cm^3.
- Strength: The yield strength of pure aluminum is 7–11 MPa and aluminum alloys have yield strengths ranging from 200 MPa to 600 MPa.
- Corrosion resistance: A protective oxide coating is naturally generated on aluminum surface.
- Conductivity: Its thermal conductivity is 237 W/(m•K) and it is a good conductor of heat and electricity.
- Ductility: Its low density and melting point allow aluminum products to be formed up until the last stage of a product design.
- Reflection: As a reflector (approximately 92%) of visible light and an excellent reflector (as much as 98%) of medium and far infrared.
- Impermeable and odorless: Releasing no taste or toxins, aluminum is ideal for food and pharmaceutical packaging.
- Recyclability: Aluminum is 100% and infinitely recyclable with no deterioration in quality.

These properties are belonging to general aluminum which may change due to other metals adding.

For aluminum alloys, they compose alloy of aluminum, copper, magnesium, manganese, tin, silicon, and zinc, with aluminum being the dominant metal. These elements are added into cast aluminum in order to give suitable characteristics for each application.

Aluminum alloys naming scheme are given in a four-digit number, where the first digit indicates the major alloying elements as follows:

Table 2-1: Aluminum alloy series [6]

Aluminum alloy series	Description
1000	99-100 wt.% aluminum content

Aluminum alloy series	Description
2000	alloyed with copper
3000	alloyed with magnesium and can be work hardened.
4000	alloyed with silicon
5000	alloyed with magnesium
6000	with magnesium and silicon
7000	alloyed with zinc
8000	alloyed with other elements such as lithium

In addition, aluminum alloys are used in many typical applications, as follows in Table 2-2. The series of alloys most widely used in construction are the 6000 series heat-treatable magnesium silicone alloys due to the 6000 series are improved high strength.

Table 2-2: The application of some aluminum alloys [7].

Alloy	Application
Work-hardening Alloy	
1060	Chemical equipment, tankers
1100	Cooking utensils, decorative panels
3003, 3004	Chemical equipment, storage tanks, beverage can bodies
5005, 5050 5052, 5657	Automotive trim, architectural applications
5085, 5086 5454, 5456 5182, 5356	Marine structures, storage tanks, rail cars, pressure vessels, armour plate, cyrogenic tanks, beverage can ends
Heat Treatable Alloys	
2219	High temperature (e.g., high speed aircraft)
2014, 2024	Airframes, autobody sheet
6061, 6063 6082, 6351 6009, 6010	Marine structures, heavy road transport, rail cars, autobody sheet
7004,7005 7019, 7039	Missiles, armour plate, military bridges

2.2 Extrusion Process

2.2.1 Introduction to Extrusion Process

Aluminum extrusion is a plastic deformation process for aluminum which converts a block of aluminum billet as shown in Figure 2-1 into a required shape of product.

Figure 2-1: Aluminum billets [8].

The aluminum extrusion process begins with melting and treatment of aluminum scrap. Alloying element is added during this step to adjust to required aluminum properties. Then, melted aluminum is converted to billets. Before extrusion, these billets are homogenized in order to change the stress concentration and to control grain sizes. This is performed in the step of billet preheating where billets are heated at temperature between 300 and 400 °C in order to soften the billets in order to reduce the friction force during extrusion process. Then, billets pushed through extrusion die opening by forging action into the required aluminum profiles. The extruded profile is passed through cooling, stretching, and cutting into a required length. After that, aging process is used to increase hardness increasing (strengthening) and then passed into anodizing process for surface finishing. After anodizing, aluminum profiles are packed and sealed for transport to customers. These steps are shown in Figure 2-2.

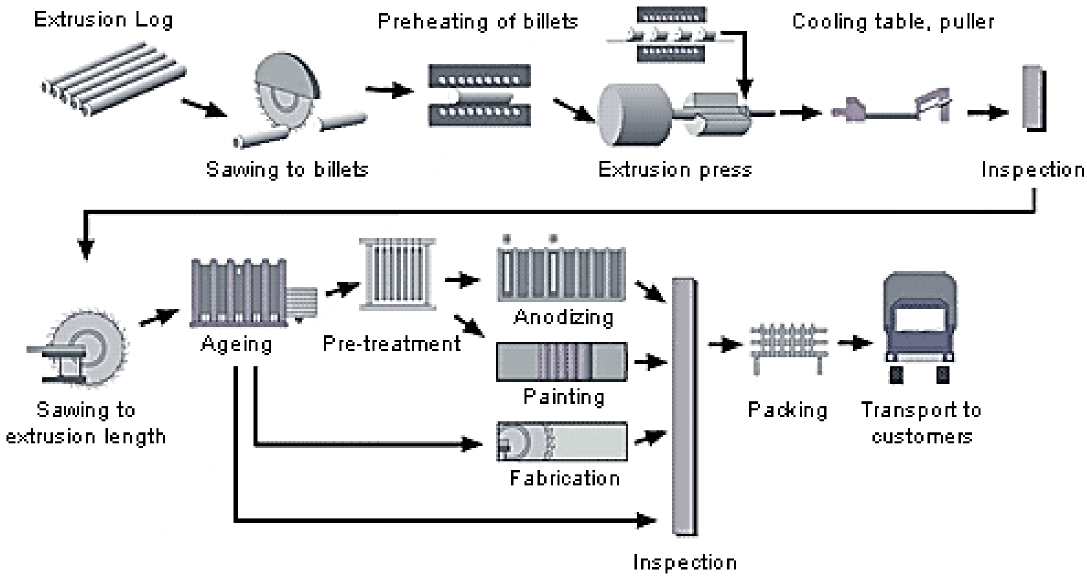

Figure 2-2: Schematic representation of extrusion process [9].

Aluminum profiles are aluminum alloys with a long and uniform cross-section shape with unique physical properties and used in many applications, for examples, window, door and building structures that glasses are attached as shown in Figure 2-3.

Figure 2-3: Aluminum profiles [10].

The two basic types of extrusion are direct and indirect extrusions:

- Direct extrusion is the process where the material being extruded through the die is moved in the same flow direction with the direction of compression.

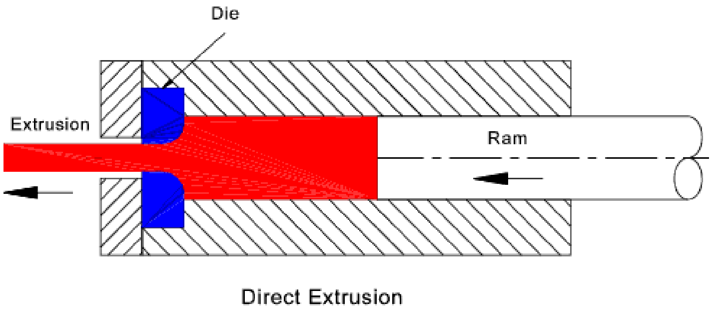

Figure 2-4: Direct extrusion [11].

- Indirect extrusion is the process where the material being extruded though the die is moved in opposite direction to the direction of compression.

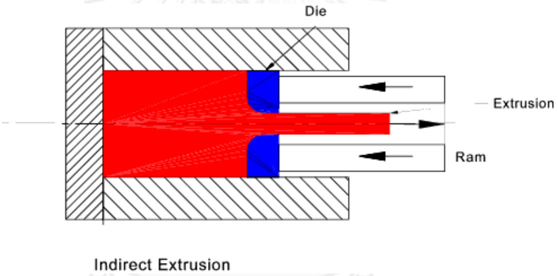

Figure 2-5: Indirect extrusion [11].

2.2.2 Advantages of Aluminum Extrusion Process

Aluminum is considered the best of all around extrusion metal because of its unique combination of properties. In addition, the advantages of extrusions are as follows [12]:

- Can be designed for high strength because metal can be placed where it is needed.
- The most economical way to make parts with a constant cross section.
- Extrusion dies are relatively inexpensive.
- Extrusion dies have a relatively long production life, reducing die replacement cost.
- Extrusion dies produce faster than forming dies and casting molds.
- Short lead times - faster production than most other metal forming processes.

2.3 Anodizing Process

Anodizing process is a general method to create protective anodic film on the aluminum profile after extrusion in order to enhance aluminum corrosion resistance properties to corrosion by using an electrochemical method. Aluminum oxide (Al_2O_3) as coating is generated to coat on the aluminum surface (Figure 2-6) and it has high porosity and matte surface. These properties are made to improve adhesion of paint or glue adhesion [10].

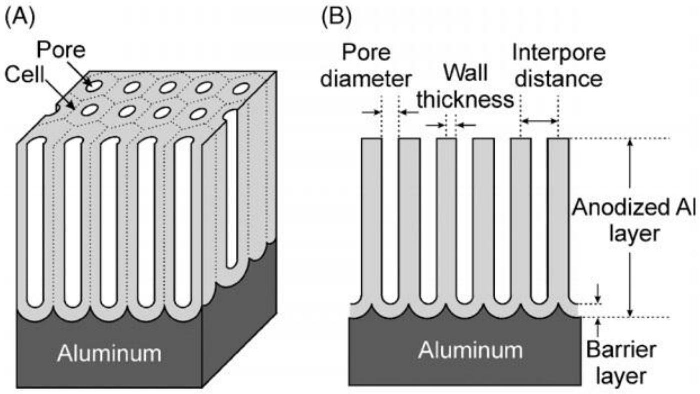

Figure 2-6: Aluminum oxide film structure.

The process has been used in the industry as early as 1923 [13] until the present time due to its low cost and simplicity to control. The anodizing process is consisted of five main steps as follows:

Table 2-3: Industrial anodization process steps [14].

Process Step	**Step description**
1. Cleaning	Remove contaminants such as lubricants, grease, dust and fingerprints.
2. Etching	Dissolve the aluminum surface to remove embedded impurities and develop a smooth, uniform surface.
3. Desmutting	Remove surface oxides, and loosely adhered metal, metal oxides, and associated compounds.
4. Anodizing-Anodic Alumina Layer Growth	Produce a porous, stable oxide film through electrochemical oxidation of the aluminum surface.
5. Sealing	Close the pore structure of the alumina layer and render the film generally inert.

In the aluminum anodizing steps, etching is the most important step that affects surface imperfection prior to anodic film formation since etching can reduce the defects such as pitting, pick up, and streaking. Thus, this study is focused on the etching process.

2.4 Etching Process

2.4.1 Basic of Etching

Etching of aluminum has 2 main steps, which are etch to clean and etch to create matte surface etching. Each step is described as follows:

1) Etch Cleaning

Most chemical cleaners for aluminum are alkaline and based on mixtures of caustic soda and diluted acid. These chemical dissolve contaminants such as dust, dirt, or lubricants from the aluminum surface to prepare surface before anodizing. There are two general etch cleaning solution as follows:

i) De-smut solutions

The caustic soda etch solutions is used that is immersed in solution for longer than 30 seconds. After that a smut due to impurities or alloying elements is formed on the surface, which in most cases can be removed by a short dip in cold nitric acid.

ii) Acid cleaning

Acid cleaning is used for particular applications, which are often thickened during thermal treatment of aluminum as removing magnesium oxides found on components made from aluminum alloys. These chemicals are containing of sulfuric and phosphoric acid.

2) Matte Etching of Aluminum

The matte etching of aluminum is a process to produce the matte aluminum surface before the anodic coating. During extrusion, defects may occur on its surface. Thus, these defects are removed along with the creation of matte surface is producing by chemicals reaction between etchant and aluminum surface. There are two kinds of chemical etchants as alkaline and acid etching.

i) Alkaline Etching

A typical process of alkaline etching was used caustic soda (NaOH) for it is the cheapest of all etchant. The general process use NaOH at concentration of 5 wt.%, at temperature 50-65 °C, for 10-20 minutes.

The alkaline etching reactions of aluminum (Al) with NaOH etchant are mainly these three reactions as follows:

Reaction 1: $2Al + 2NaOH + 2H_2O \rightarrow 2NaAlO_2 + 3H_2$ (2.1)

Reaction 2: $NaAlO_2 + H_2O \rightarrow Al(OH)_3 + NaOH$ (2.2)

Reaction 3: $2Al(OH)_3 \rightarrow Al_2O_3 + {}_3H_2O$ (2.3)

These reactions show that aluminum on the surface reacts with NaOH and water to form aluminate and release hydrogen gas. Finally, the final appearance will depend on the extent of etching and on the size and shape of the pits. In addition, it depends on the etching temperature, etching time and concentration of etchant.

ii) Acid Etching

Etching in acids is not so frequently used. Sometimes it is used in the case of high silicon content, due to the fact that silicon is insoluble in caustic soda. A typical acid solution is composed of nitric and hydrofluoric acid [15].

In this study, NaOH was used in aluminum etching because NaOH are widely used chemical in the aluminum extrusion plant.

2.4.2 Etching Process Parameters

Generally, there are many parameters in etching process that can influence the quality of the final surface of the extruded parts, such as types of etchant, concentrations of etchant, temperature, time, specimen area and etching rate, etc. However, the three main process parameters in the aluminum etching process are concentration of etchant, etching temperature and etching time [16]. A small change in each of these parameters will result in reducing a streak defect on extruded aluminum. The nature of these parameters is the main concerns in order to obtain good results, and provide optimum conditions for streak defect elimination. Due to responses of etched aluminum (i.e., weight loss, surface gloss and surface roughness); its values are changed at low-level conditions. Thus, aluminum etching study is always etched begin with low-level of process condition.

In this study, the specimens were tested under different combined conditions of the concentration of NaOH, etching temperature and etching time. The highlights are not all materials were etched in all conditions and only specific concentrations, temperature and time are suited for certain materials.

2.5 Extrusion Defects

The most common defects may be described as pitting, streaking or general non-uniform appearance. Causing of some defects can be originating on the surface aluminum profiles as a result of the thermo-mechanical extrusion process or during etching process for surface preparation before anodizing. These defects are resulted from poor die design, contamination in solution, or lack of control process in the various steps into aluminum profile production. Main defects on extrusion parts have been classified into general section as follows [17]:

2.5.1 Pitting Defect

Pitting can be generated on the anodized aluminum surface throughout the process due to corrosive media attacking the exposed surface of the aluminum. Pitting is often occurred on the weakest of national protective oxide film as shown in Figure 2-7. This type of corrosion can be removed by etching in case of less depth of defect. Therefore, handling and storing must be done correctly to reduce the pitting.

Figure 2-7: Typical pitting corrosion.

2.5.2 Die Line

Die line is a physical line or band of lines in the extrusion direction that may be resulted from poor die design or the condition die bearing. This defect is clearly observed and has a larger depth than streaking. Figure 2-8 shows the die line on the extruded aluminum.

Figure 2-8: Die line defect on the extruded aluminum.

2.5.3 Streaking

Streak defect is a major problem of the extrusion that its root causes cannot be identified due to streak defect can be generated in various steps of the extrusion process. Sometimes streak defect is related to the non-uniform metallurgical structure in the extruded aluminum, or physical damage in the process.

Structural streaking is resulted from the various grain size and grain orientation between the streak regions and the normal regions that affect difference of light scattering on both regions. Hence, both regions are obvious the different color of shades of both regions by naked eyes.

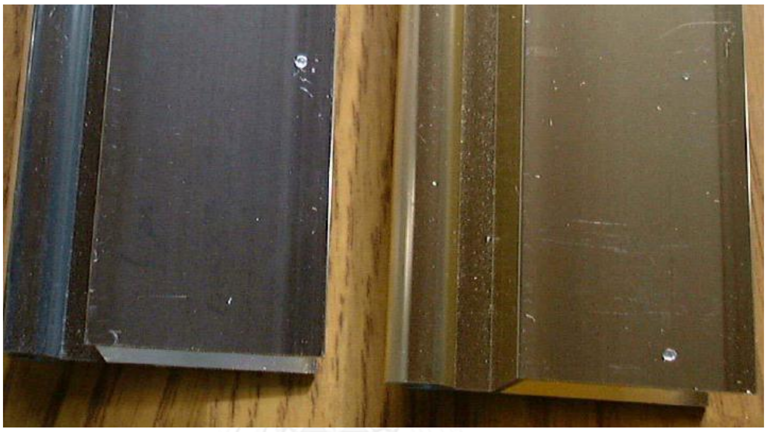

Figure 2-9: Structural of die design streaking

For streak defect, there is no method for streak elimination besides; using re-process that is a trial and error method has been used for this problem in the process. Therefore, it is an important solution to reduce the production cost and time.

2.6 Surface Gloss and Surface Roughness

2.6.1 Surface Gloss

The most observable differences in surface gloss is at the edge of the streak region. Thus, the difference in surface gloss between the streak and surrounding regions are used as an indicator of the streak defects. Therefore, the surface gloss was measured in this study in order to investigate the effect of different etching conditions, both before and after the etching process. Surface glosses is measured by directing a constant intensity light beam, at a fixed angle, on to the test surface and then monitor the amount of reflected light from the same angle. This specular reflectance is measured using a gloss meter, expressed as gloss units (GU). Measurement angle refers to the angle between the incident light and the perpendicular. Note that different surfaces require different reflective angles. In general, three measurement angles (20°, 60°, and 85°) are used which can cover the majority of industrial coating applications. The angle is selected based on the anticipated gloss range, as shown in Figure 2-10 [18].

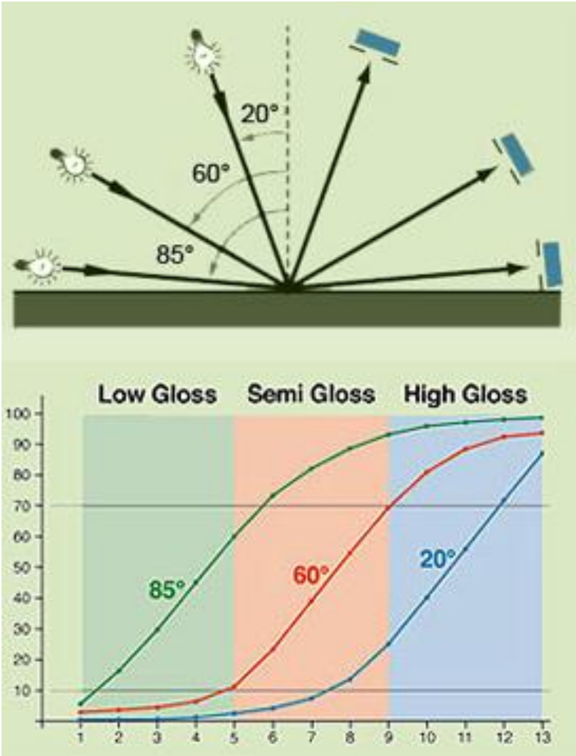

Figure 2-10: The angle of surface gloss measurement.

2.6.2 Surface Roughness

The surface roughness is usually measured in a direct method by using Profilometer, which is a stylus probe instrument moved vertically in contact with a surface sample and then moved laterally across the sample for a specified distance and specified contact force. However, this method is can cause some scratches on the surface specimen. Therefore, 3D Measuring Laser Microscope is sometimes preferred to measure the surface roughness, which is a non-contact measurement and can give accurate surface roughness measurement regardless of surface texture conditions [19].

Figure 2-11: Non-contact surface roughness measurement.

Surface Roughness is a measurement of the aluminum surface after etching, which measures the small scale variation. The main results of the measurement are the arithmetic mean (Ra) and the mean point roughness (Rz) that was studied in this research.

The arithmetic mean (Ra) is an average of deviations of the series of points on the center-line (Figure 2-12) that can be calculated the Ra values as equation 2-4 in microns (μm).

$$Ra = \frac{a + b + c + d + e + f + ...}{n} \quad (2.4)$$

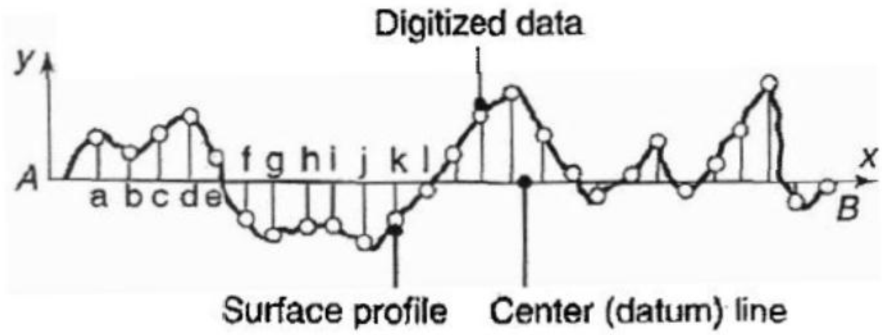

Figure 2-12: Pattern for surface roughness measurement calculation [20].

2.7 Design of Experiments

Design of experiments (DOE) is a statistical tool for the individual and interactive effects of many factors that could affect the output results in any design. In addition, DOE also provides a full insight of interaction between design elements; hence, it helps to fix the sensitive parts and sensitive areas in designs that cause problems in responses. There are various method used as DOE, i.e., Factorial Design, Taguchi method, Response Surface Method (RSM), etc. [21] In this work, RSM was used to optimize the etching conditions for streak defect elimination.

2.7.1 Response Surface Methodology (RSM)

Response Surface Methodology (RSM) is usually used to develop, improve, and optimize problems in a process. The analysis of these types of designs requires some knowledge of analysis of variance, regression, and optimization techniques. Generally, experimental condition is possible to represent independent factors as given in Equation 2-5. These factors are related with response in function as follows [22]:

$$Y = \phi(x_1 + x_2, ... + x_k) \pm e_r \quad (2\text{-}5)$$

where:

Y is response

$x_1 + x_2, ... + x_k$ are quantitative factors

ϕ is the response function

e_r is the experimental errors

Independent variables are given to set, a characteristic surface is responded. Therefore, it can be approximated within the experimental region by a polynomial, if the mathematical form of ϕ is not known.

In general, RSM can be visualized graphically. The graph is useful to see the shape of response surface. Therefore, the response function, ϕ, can be plotted versus the level of x_1 and x_2 as shown in Figure 2-13 [22]. This 3D graph represents the response surface the side and it can call a response surface plot.

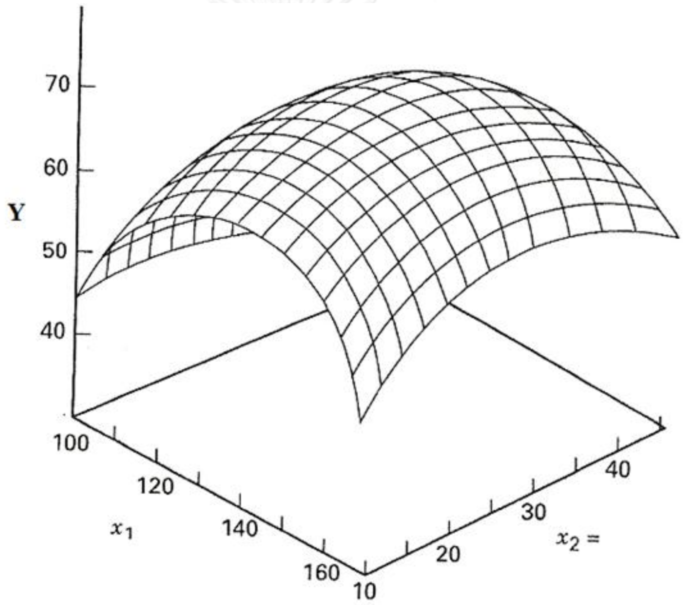

Figure 2-13: Response surface plot [23]

Additionally, the response surface plot can be viewed in 2D graphs to reduce complicated plots. It is call a contour plot. The contour plots represent the contour lines of x_1 and x_2 pairs that have co-Y value. Figure 2-14 illustrates a contour plot as a function of x_1 and x_2.

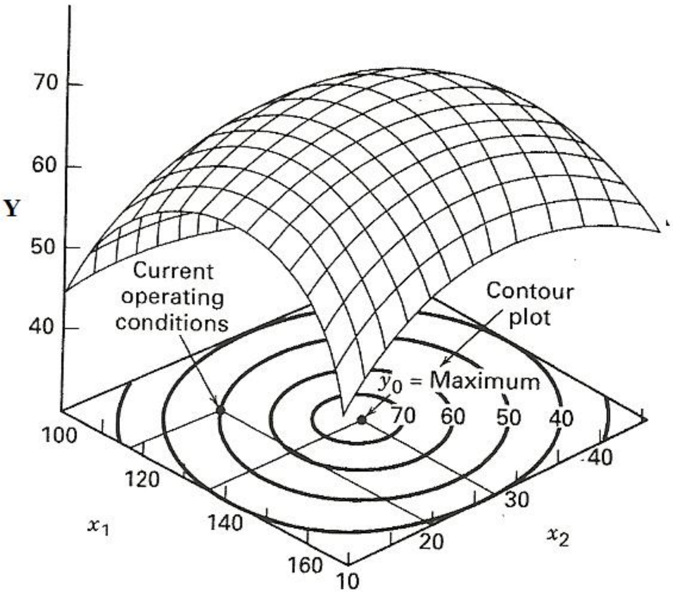

Figure 2-14: Contour plot [23].

2.7.2 Central Composite Design (CCD)

Central composite design (CCD) is the most usual experimental design tool that is applied from the second-order model. CCD techniques have various types such as central composite circumscribed (CCC), central composite inscribed (CCI) and central composite face centered (CCF). CCD consists of 2^k factorial design with nj runs, 2k axial runs, and n_c center runs [24]. CCD can be subdivided in three parts as follows:

- Points related to 2k design, where k is the number of parameters and 2 is the number of levels at which the parameters is kept during experimentation.
- Extra points called star points positioned on the co-ordinates axes to form a central composite design with a star arm of size α.
- Few more points added at the center to give roughly equal precision for response Y with a circle of radius one.

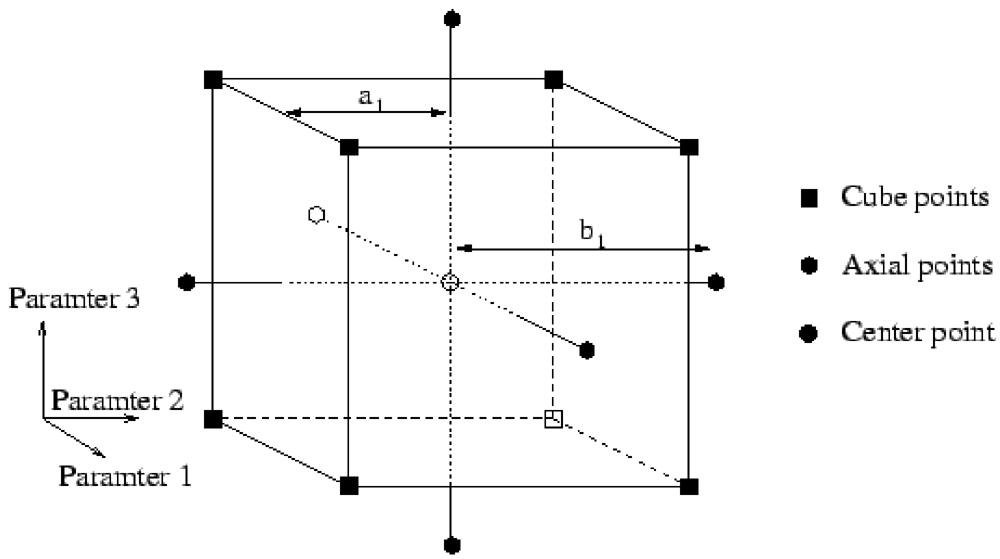

Figure 2-15: Central composite model with three input parameters.

In Figure 2-15, a 2k model is used, CCD with 3 input parameters that is k = 3, it means 6 center points are generally selected to get 20 runs for experiments including 8 cube points, 6 axial points, and center point. Moreover, the factor α is the radius of the circle or sphere on which the star points line. The components of central composite design for different number of variables are given in Table 2-4.

Table 2-4: Components of central composite design

Variables (k)	**Factorial Points (2^k)**	**Star Points (2k)**	**Center Points (n)**	**Total** (N)**	**Value of α*** **
2	4	4	5	13	1.414
3*	8	6	6	20	1.682
4	16	8	7	31	2.000

* This row is used in the present work.

** For total run are 2^k+2k+n.

*** For **Rotatable design** $\alpha = (nF)^{1/4}$ where, matrix **F** obtained from the factorial experiment.

2.7.2 Analysis of Variance (ANOVA)

For the ANOVA, the total sum of squares may be divided into four parts:

1) The contribution due to the first order terms.

2) The contribution due to the second order terms.

3) A lack of fit component which measures the deviations of the response from the fitted surface.

4) Experimental error which is obtained from the center points.

Table 2-5: Analysis of variance for central composite second order rotatable design [24].

No.	Source	Sum of Squares	Degree of freedom
1	First order terms	$\sum_{q=1}^{k} b_i \left(\sum_{q=1}^{N} x_{iq} Y_q \right)$	K
2	Second order terms	$b_0 \left(\sum_{q=1}^{N} Y_q \right) + \sum_{i=1}^{k} b_{ii} \left(\sum_{q=1}^{N} x_{iq}^2 Y_q \right) + \sum_{i<j}^{k} b_{ij} \left(\sum_{q=1}^{N} x_{iq} x_{jq} y_q \right) - \frac{\left(\sum_{q=1}^{N} y_q \right)^2}{N}$	$\frac{k(k-1)}{2}$
3	Lack of fit	Found by subtraction	$N - n_0 - \frac{k(k+3)}{2}$
4	Experimental error	$\sum_{i=1}^{n_0} \left(y_i - \bar{y}_0 \right)^2$	n_0-1
5	Total	$\left(\sum_{q=1}^{N} y_q \right)^2 - \left[\frac{\left(\sum_{q=1}^{N} y_q \right)^2}{N} \right]$	N-1

The F ratio is calculated from Equation 2-7:

$$F(1, n_0) = \frac{\left(b_i^2 / c_{ii} \right)}{S_e^2} \qquad (2.7)$$

where:

b'_i is the regression coefficients.

c_{ii} is the element of the error matrix $(X'X)^{-1}$.

S_e is the standard deviations of experimental error calculated from replicating observations at zero level as:

$$S_e^2 = \frac{1}{n_0 - 1} \sum_{s=1}^{n_0} \left(y_s - \overline{y_o} \right)^2 \qquad (2\text{-}8)$$

Where: $y_0 = \frac{1}{n_0} \sum_{s=1}^{n_0} y_s$

Y_s is s^{th} response value at the center.

This calculated value of F can be compared with theoretical value of F at 95% confidence level. If for a coefficient the computed value of F is greater than the theoretical value, then the effect of that term is significant. The insignificant second order terms can be deleted from the equations and remaining co-efficient can be recalculated [25].

Additionally, degrees of freedom in ANOVA results are the number of values in a study that have the freedom to vary. They are commonly described in relationship to various forms of hypothesis testing in statistics.

CHAPTER 3
LITERATURE REVIEWS

This section presents previous research studies related with root cause analysis of streaking on the anodized aluminum, and method used for the streaking elimination and anodizing. Beginning with causes of streaking, there are many researchers who are interested in the formation of streaking. Zhu et al. [26] focused their study on the influencing factors involved in various process steps (i.e., billet quality, extrusion process, die design and etching process). From this research, it can be summarized as follows:

i) Effect of billet quality on the formation of streaking can be implying that resulted from some chemical elements in the billet alloy, distribution and morphology of intermetallic particles. Conducting the experiment, the different amount of iron were added to the billet alloy to obtain content of 0.17 wt.% (low-iron) and 0.29 wt.% (high-iron) before extrusion. From the experimental results, the grain boundary grooves of the low-iron extrusion in streak region are deeper and wider than the normal region (Figure 3-1). On the other hand, the high-iron adding was not be differenced on grain boundary groove of both regions. In addition, color of shade on streak region which low-iron extrusion, had brighter than the normal region whereas there were no differed in high-iron extrusion. Therefore, the difference in these morphologies affected the intensity of streaking.

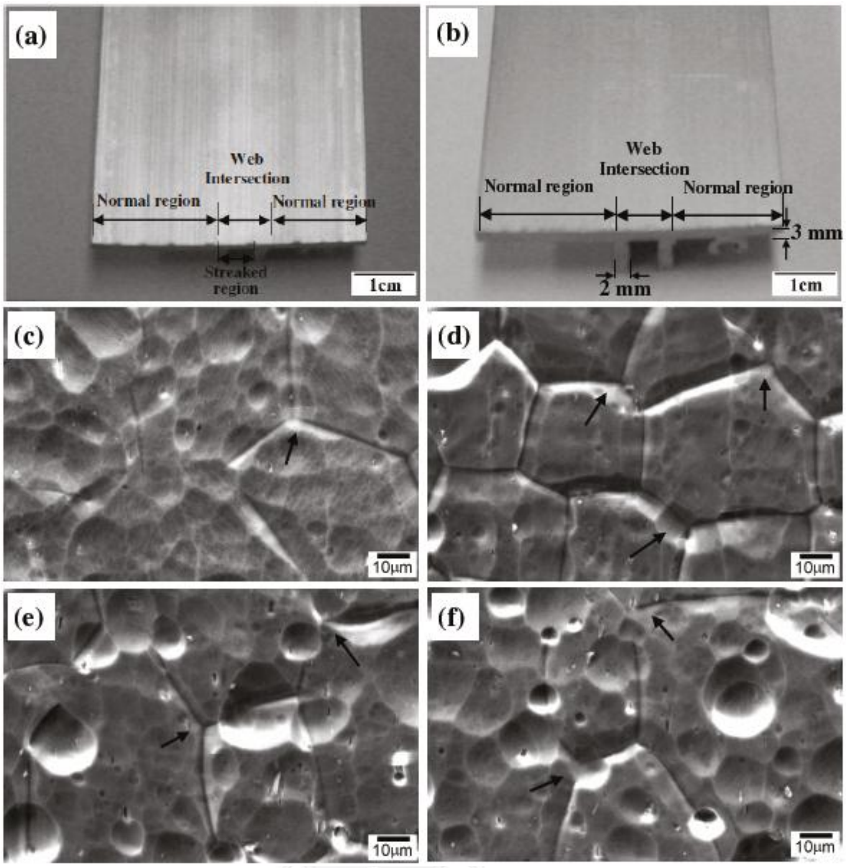

Figure 3-1: Profiles of anodized aluminum extrusions with (a) 0.17 wt.% Fe and (b) 0.29 wt.% Fe, and SEM morphology of anodized low-iron extrusion in (c) web streak region and (d) normal region, and high-iron extrusion in (e) web streak region and (f) normal region.

ii) Effect of extrusion process such as process imperfections, process parameters and extrusion surface defects can be result in the longitudinal or transverse weld, non-uniform metal flow through the die and surface defects of extruded aluminum, respectively. These causes were affect streaking and difficult to eliminate completely. Therefore, optimum operating process and cleaning container can be reducing the intensity of streaking.

iii) Effect of die design on the streaking formation has many important factors which can be reducing or eliminating the streaking as follow: good design to flow uniformly, adjusting die bearing length, avoiding the abrupt changes and smooth bearing transitions.

iv) Effect of etching process was an important step to result in the streak defect and other defects.

In a recent year, Ma et al. [27] investigated an origin of streaking on anodized aluminum alloy extrusions (grade AA6063) by using optical microscope (OM) and scanning electron microscopy (SEM) for microstructural features analysis. For experiment, AA6063 specimen which appeared streaking on the surface (Figure 3-2), were prepared under stripped the anodic film by immersing in 10 wt.% of NaOH at 60°C for 2 minutes. Then, the microstructure of aluminum was determined.

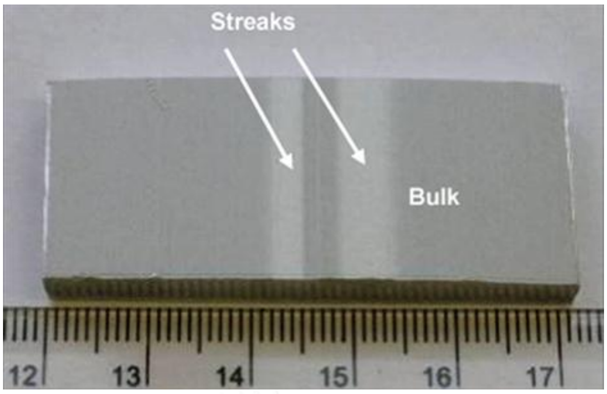

Figure 3-2: Optical image of aluminum specimen with streaking.

After that the specimen was anodized in 2M sulfuric acid at current density of 1.5 A dm-2 at 20°C for 20 minutes. Then, specimen was analyzed by SEM. Before SEM analysis, specimens were prepared through mechanical grinding with silicon carbide paper.

It was found that the surface of etched and anodized aluminum alloy is related with grain boundary groove and etching steps which are determined by the distribution of grain size and crystallographic orientations. From this research, it can be concluded that the different microstructures of the streaking may be caused by the non-uniform alloy deformation and non-uniform distribution of friction force in the extrusion process.

Further, many research studies in used new chemical of etchants in order to improve the process as seen in Cakir [28]. This research used experimental method by using FeCl3 with a concentration of 1.25 moles because it is cheap and easy to control as the etchant. In their the experiment, AA7075 was used as specimens and were cleaned in an Autoclean pulver powder mixed with distilled water at 30°C for 30 minutes. Then, the etching in $FeCl_3$ was carried out at 4 etching temperatures of 20, 30, 40 and 50°C for 20 minutes. Experimental setup was put a water jacket to control uniformly temperature of system as shown in Figure 3-3. After the etching step, the depth of etch and surface roughness were measured by Mitutoyo micrometer and Taylor-Hobson Surtronic 3+, respectively.

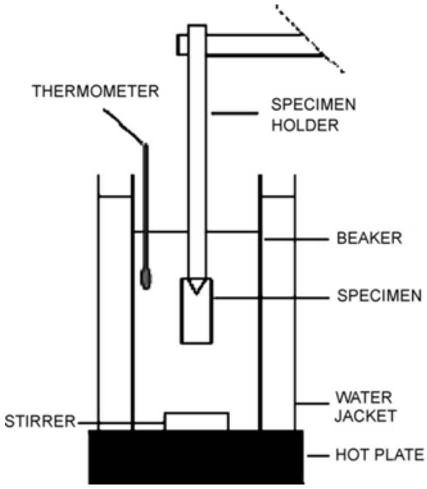

Figure 3-3: Experimental setup of aluminum beaker etching.

From the results, it was found that the chemical reaction of aluminum etching with $FeCl_3$ can be written as follows:

$$3FeCl_3 + Al \rightarrow 3FeCl_2 + AlCl_3 \quad (2.8)$$

The reaction steps occurred as following: $FeCl_3$ attacks aluminum, etchant contacts with metal surface and electron transfer starts. Then, Fe ions spread into etchant. Based on the test results, the depth of etch was affected by etching time and etching temperature. That is longer etching time and a higher etching temperature would produce the higher depth of etch as shown in Figure 3-4. Similar trend was also observed for the surface roughness. As a result, this research showed that $FeCl_3$ is one of the most effective etchants.

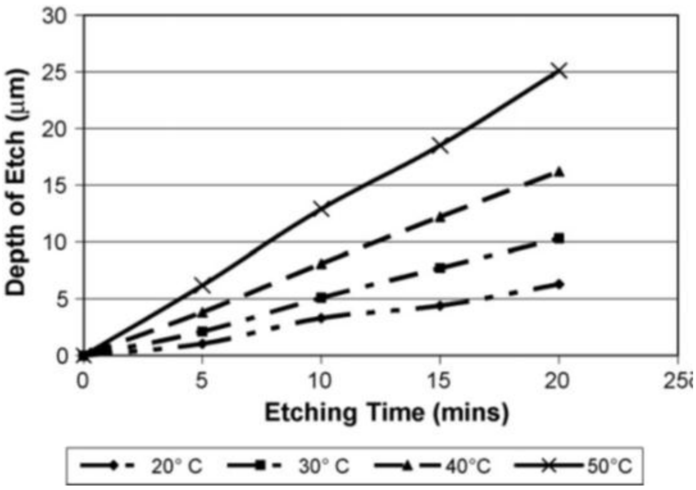

Figure 3-4: Examination of depth of etch.

Despite a proven effectiveness of an etchant like $FeCl_3$ as shown in the research, the industry still uses NaOH because of its lower cost and availablability than other etchants. On the other hand, researchers are also interested in using NaOH as etchants. In 2014, Zhu studied etching behavior of aluminum extrusions and investigated the influence of various factors (i.e., etching process parameters, Fe-rich particles, and extrusion profiles) on weight loss during aluminum etching. In their study, AA6060 was used as specimen. The specimens were immersed in an etchant of 10 wt.% NaOH at the etching temperature between 40°C and 90°C for 1 to 20 minutes. The surface morphology after etching is shown in Figure 3-5. Based on the results, a lot of die lines were still observed on the etched aluminum surface when the etching time was between 5 and 10 minutes (Figure 3-5b and Figure 3-5c). However, etched aluminum with etching time of 10 minutes has different on kinetic of dissolution that affects grain boundary grooves formation. In addition, die lines were completely removed on the surface when etching at high temperatures (70 and 90°C). Moreover, at 90°C, the grain boundary grooves were not obversed, but many pits were clearly found on the etched aluminum (Figure 3-5f).

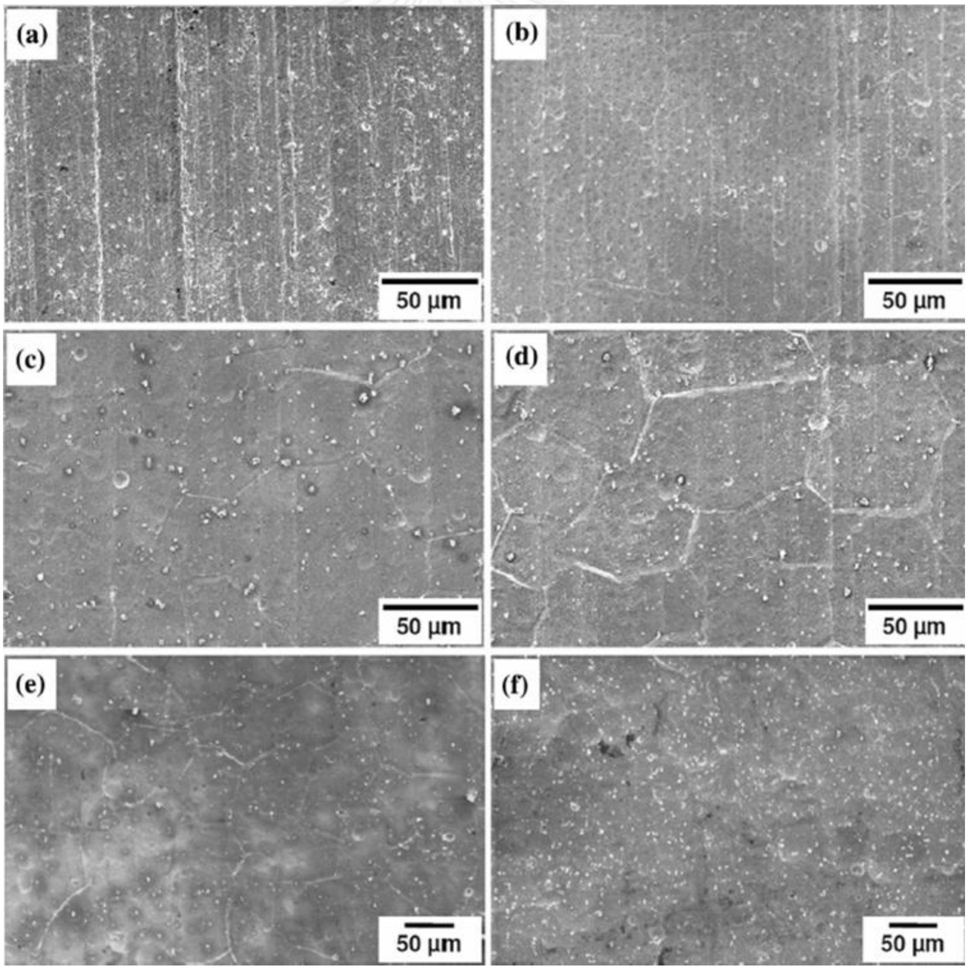

Figure 3-5: Surface morphology of etched 6060 aluminum alloy extrusions with etching at (a) 40°C/1 min, (b) 40°C/5 min, (c) 40°C/10 min, (d) 40°C/15 min, (e) 70°C/5 min, and (f) 90°C/5 min.

In addition, effect of Fe-rich particles can be concluded that the different amounts of Fe-rich particles adding in the billets could cause inhomogeneous distribution of Fe-rich particles. By adding move Fe-rich particles, the amount of weight loss, the formation of grain boundary grooves, and the dimension of etching pits also increase since Fe particles have a larger atomic number (55.845u) than aluminum (26.982u). Thus, the detachment of Fe-rich particles can directly increase the weight loss of aluminum specimen as shown in Figure 3-6.

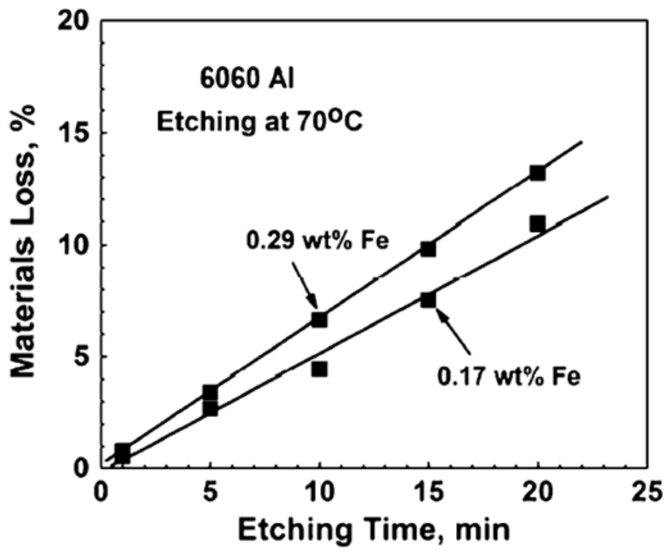

Figure 3-6: Effect of Fe content on etching behavior of 6060 aluminum alloy extrusions.

On the other hand, the effect of different shapes of extrusion profiles on etching process also has a significant effect on the surface microstructure and surface quality of the aluminum parts after etching. Based on the results in Figure 3-7, extrusion 2 has a larger weight loss than the extrusion 1. Hence, a larger surface profile (extrusion 2) would lead to a faster reaction rate and more weight loss than a less surface profile (extrusion 1).

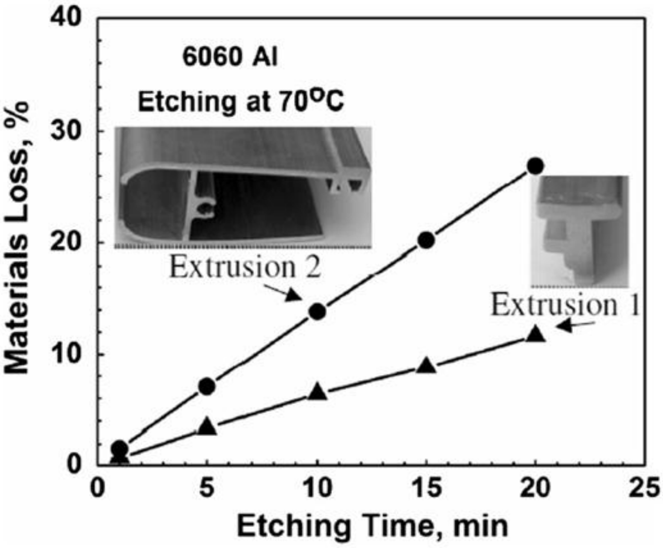

Figure 3-7: Effect of extrusion profile on etching behavior of 6060 aluminum alloy extrusions.

In the RSM, CCD is widely used to provide a second-order response surface model. Many researches have used CCD to improve the process. For example, Nikolett et al. [29] studied the primary task of DOE such as minimize and maximize analysis in case of aluminum alloy machining. Two experiment design methods, the full factorial design (FF) and the central composite design (CCD), were compared. The results could assist the machinability research development engineer for the suitable experimental design selecting. In their study, the cutting speed and the feed rate were selected, and the response was the cutting force. In the experiments, AA6082 with a size of 60×60×100 mm^3 was tested by chamfering using a three-axis B640 type Kondia machine tool (Figure 3-8). The cutting force was detected with a force sensor and the data was collected by KISTER Dyno Ware software.

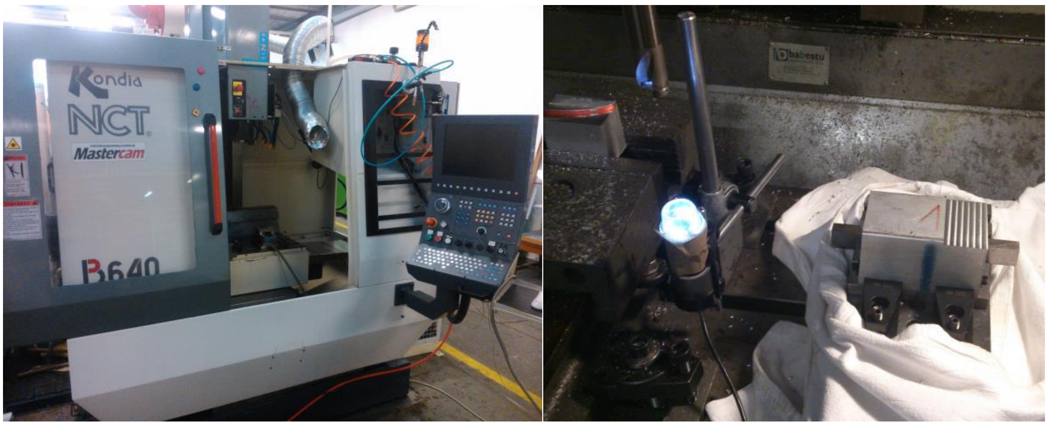

Figure 3-8: The used machine tool and the machining environment [29].

The results were fed into Minitab 17 and Microsoft Excel software. The FF results were showed that increasing of feed rate (vf) value would increase the strength value (Figure 3-9). On the other hand, the cutting speed (vc) was shown to be less prominent.

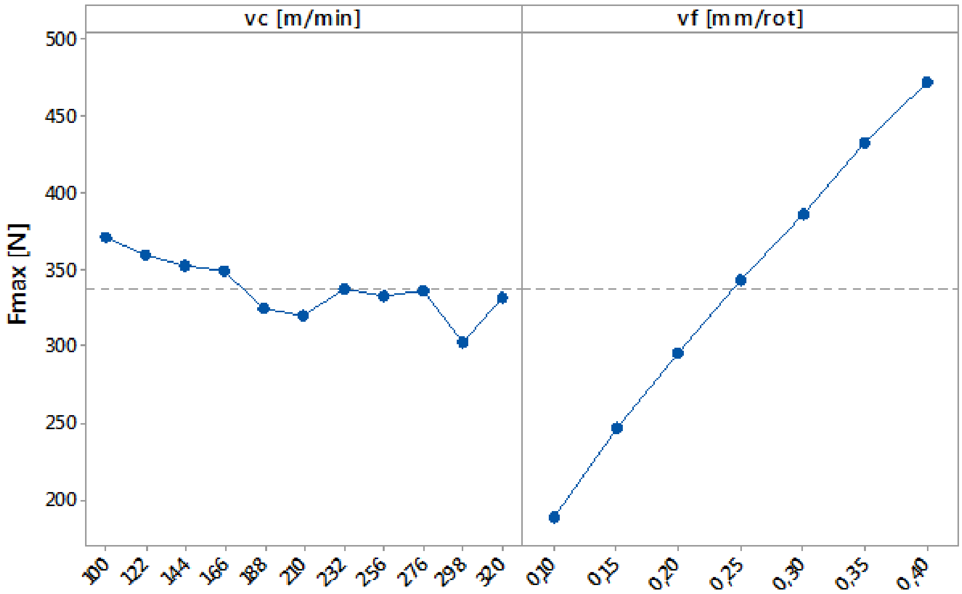

Figure 3-9: Main effect plot used the full factorial experiment design.

From the interaction effect (Figure 3-10), the cutting speed and the feed rate has low interaction as can be observed from the line on the plot that was quite a linearly.

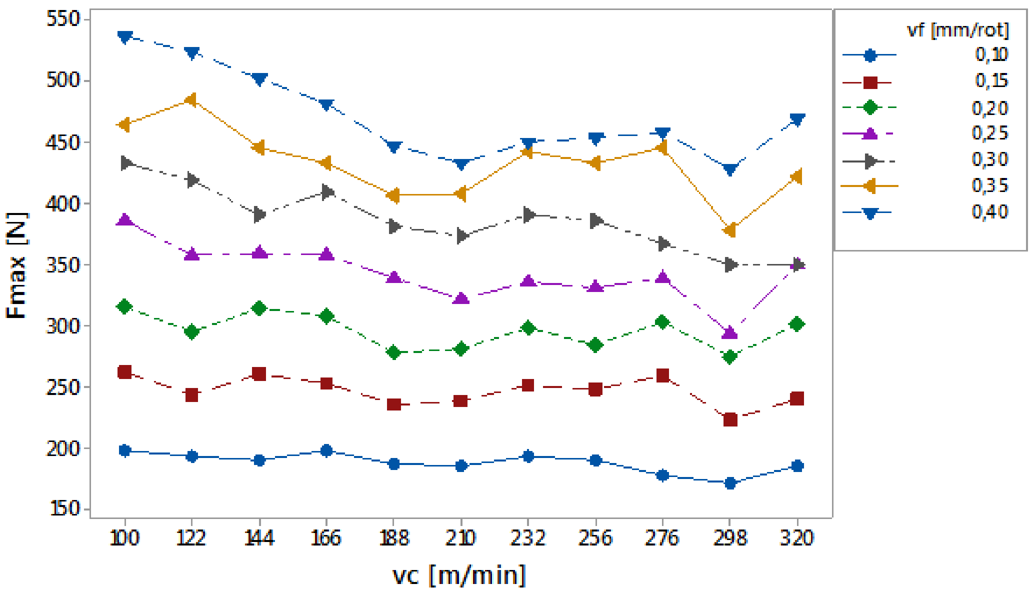

Figure 3-10: Interaction effect plot used the full factorial experiment design.

For CCD results, the main and interaction effects as shown in Figure 3-11 and Figure 3-12, was shown to be similar to the results obtained by using the full factorial method.

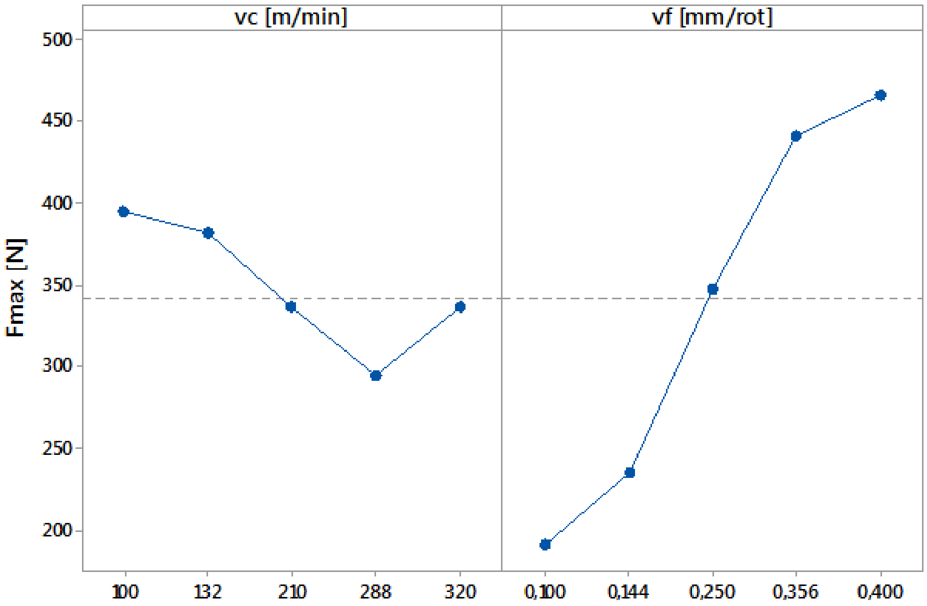

Figure 3-11: Main effect plot used the full central composite design.

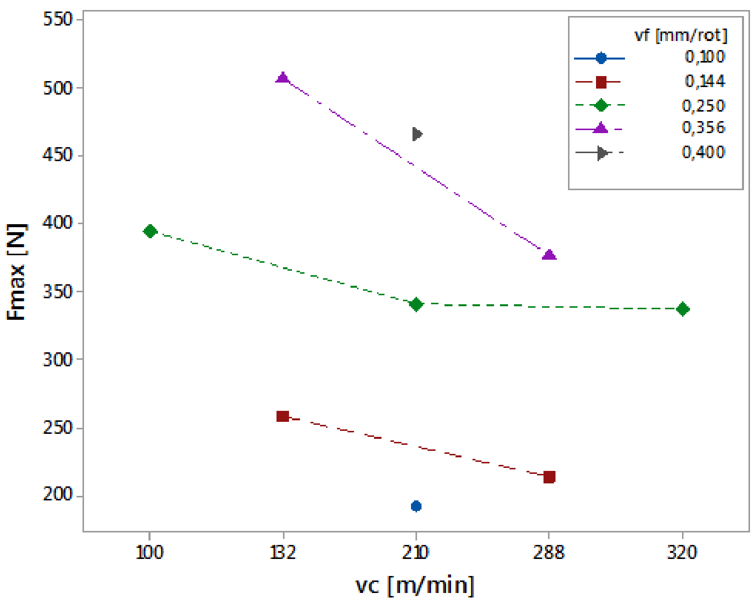

Figure 3-12: Interaction effect plot used the full central composite design.

Therefore, by comparing their results, it can be concluded that the CCD method is more cost-effective, since it requires less experimental run and less time (about 70%).

CHAPTER 4
RESEARCH METHODOLOGY

The effect of etching process parameters on reduction of streak defect on extruded aluminum was studied using the central composite design (CCD) approach under response surface methodology (RSM) to provide predictive models of aluminum etching process that may be used as guidelines for user application.

4.1 Specimen preparation

Extruded AA6063 profiles from Alumet Co., Ltd. with streak defect on the surface (Figure 4-1) were selected for the current study. The specimens were cut into 2 cm long pieces by a cutting wheel as shown in Figure 4-2. The chemical composition of this alloy is given in Table 4-1. The specimens were first cleaned with soap and tap water before etching experiment.

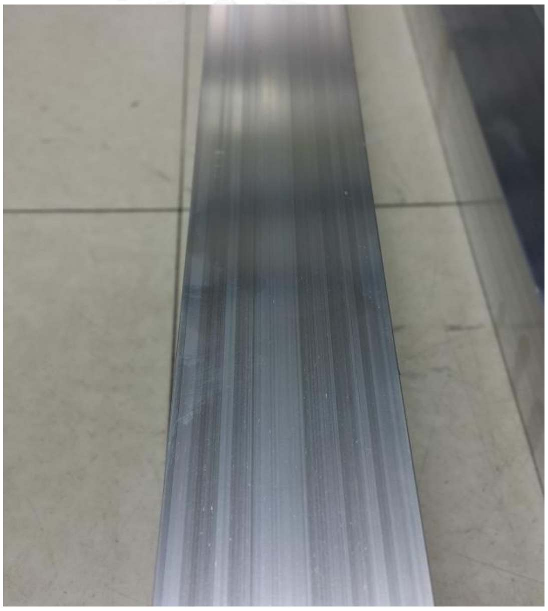

Figure 4-1: Extruded AA6063 profile with streak defects.

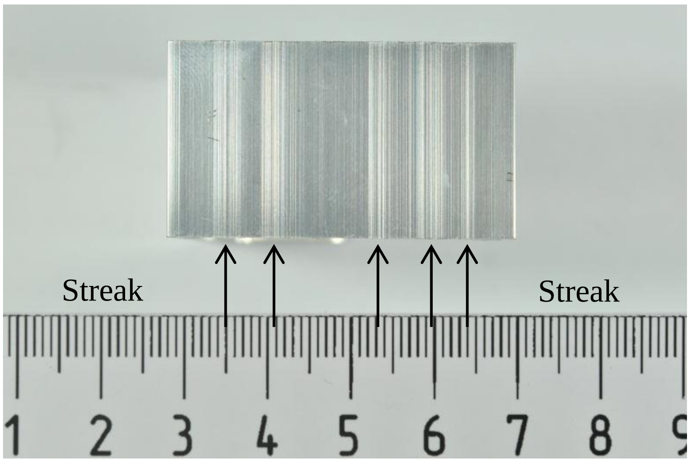

Figure 4-2: an AA6063 specimen.

Table 4-1: Chemical composition of the aluminum profile specimen(wt.%).

Element	**Wt.%**
Silicon, Si	0.62
Iron, Fe	0.18
Copper, Cu	<0.01
Manganese, Mn	0.06
Magnesium, Mg	0.47
Chromium, Cr	<0.01
Zinc, Zn	<0.01
Titanium, Ti	0.02

4.2 Experimental Apparatus and Chemicals

The etching process was performed using a laboratory setup shown in Figure 4-3. The experiments were conducted using a water bath system that heats a hot water beaker to the input temperature value using a hot plate and monitors the temperature using a thermocouple placed inside the hot water beaker. The thermocouple readings were used to acquire all temperature data. The etchant was contained in a 500 ml beaker placed inside the water bath.

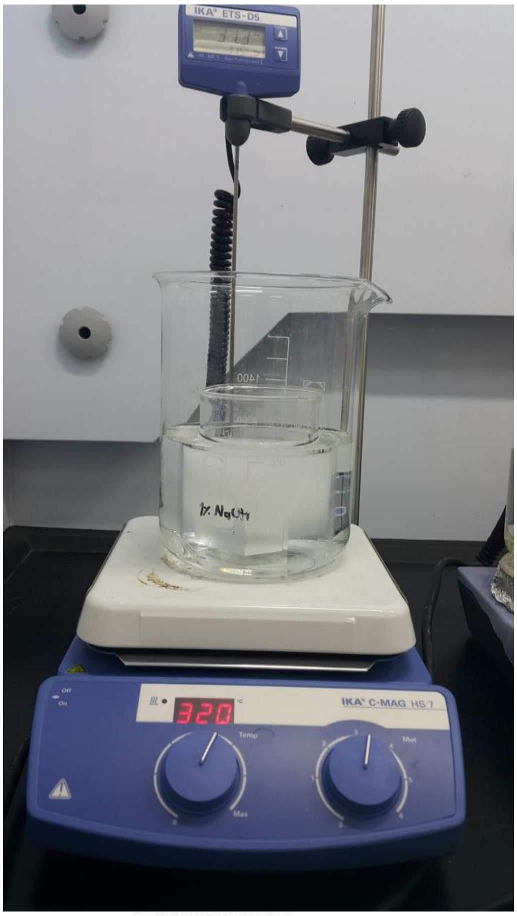

Figure 4-3: Experimental setup for etching process.

The chemicals used in the etching experiments are as follows:

- Sodium hydroxide (caustic soda)
- Acetone
- Nitric acid
- Sulfuric acid

4.3 Experimental Procedures

Before conducting the experiment, the specimens had undergone the following pretreatment: rinsing with deionized water, degreasing in acetone for 5 minutes in order to produce a cleaned surface, and rinsing with deionized water at room temperature. Then, the specimens were etched in NaOH using different concentrations, etching temperatures and etching time.

After etching, specimens were rinsed in deionized water and desmutted in 5%HNO_3 at room temperature for 5 minutes (in order to remove non-aluminum constituents from the surface of the specimen), then submersed with deionized water for approximately 10 minutes and drying in a stream of air at room temperature, and stored in a desiccator before being taken out for surface quality measurement. For each etching condition, three repetitions were performed to ensure good reproducibility.

The aluminum etching steps are performed as shown in Figure 4-4 and Figure 4-5.

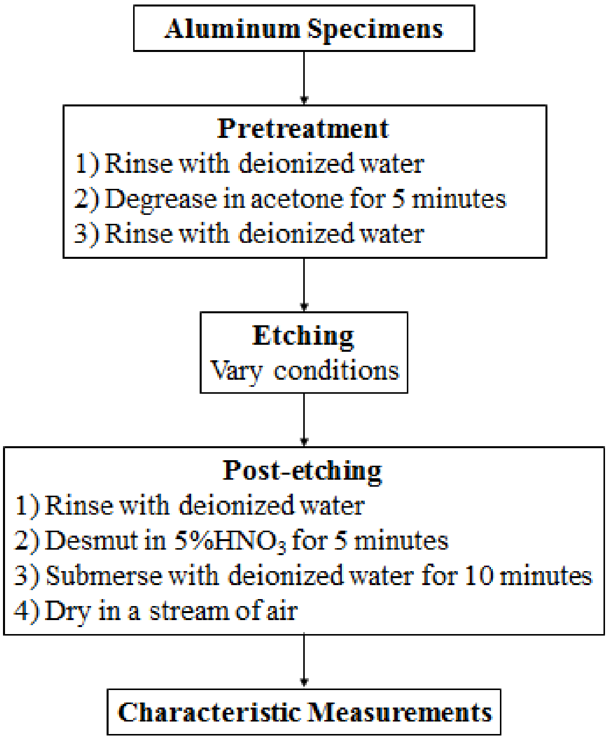

Figure 4-4: Experimental procedure flow chart.

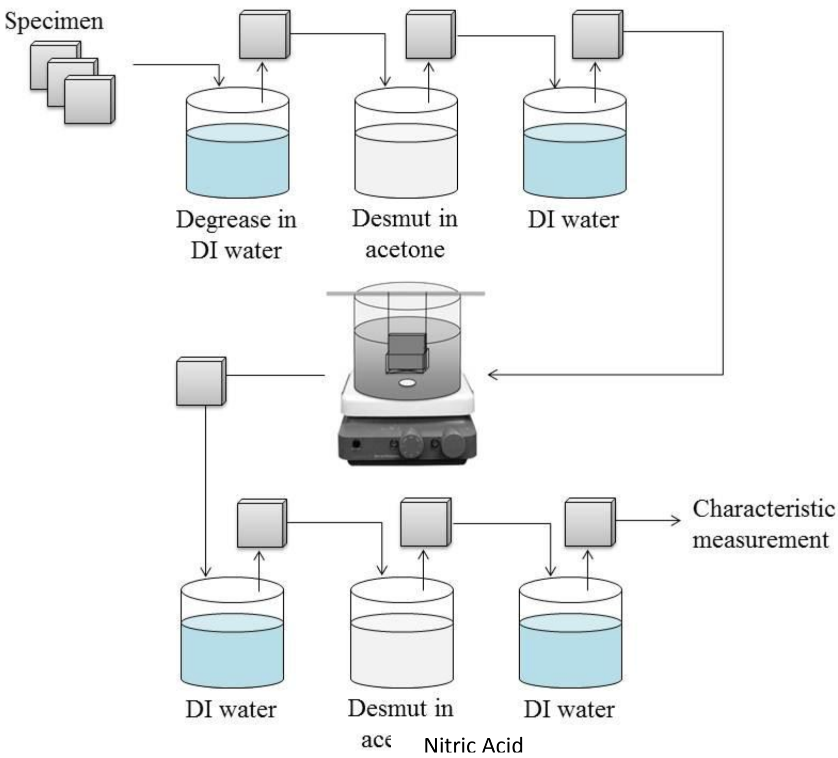

Figure 4-5: Experimental setup for etching process.

4.4 Characteristic Analysis

Physical properties (i.e., weight loss, morphologies, surface gloss, and surface roughness) of the etched parts were measured with a weighing scale, an optical microscope, a gloss meter, and a confocal laser scanning microscope (CLSM), respectively. Morphologies of etched surface were measured by optical microscope both before and after the etching process. Weight loss analysis was conducted by weighing each specimen before and after the etching process. Surface gloss measurements and surface roughness measurements were taken at the location of the streak band.

Characteristic of the etched parts are measured with various instruments as follows:

Table 4-2: Characteristic measurement.

Characteristic measurement	**Instrument/analysis**
Weight loss	Digital scale (4 digit) – Sartorius BSA224S-CW
Surface gloss	Gloss meter – KSJ 3-Gloss
Surface roughness	Confocal laser scanning microscopy (CLSM) – LEXT Olympus OLS4100
Streak appearance	DSLR camera

For weight loss analysis, it was weighed the specimen before the aluminum etching and after the aluminum etching. Then, weight loss percentage for every experiment can be calculated as equation as follows:

$$\%\text{weight loss} = \left(\frac{wt_{before} - wt_{after}}{wt_{before}} \right) \times 100 \qquad (4\text{-}1)$$

For surface gloss difference measurement, it was measured using glossmeter that selected the reflective angle at 60°. Due to aluminum surface is a semi-gloss as the angle can select based on the anticipated gloss range, as shown in the following Table 4-3: The angle of glossmeter.

Table 4-3: The angle of glossmeter.

Gloss Range	60° Value	Measure with
High Gloss	>70 GU	20°
Medium Gloss	10 - 70 GU	60°
Low Gloss	<10 GU	85°

Additionally, surface gloss difference was measured comparing with the streak region (Figure 4-6 – Loc1) and the surrounding region (Figure 4-6 – Loc2) of both before the etching and after the etching values as calculated as following equation 4-2.

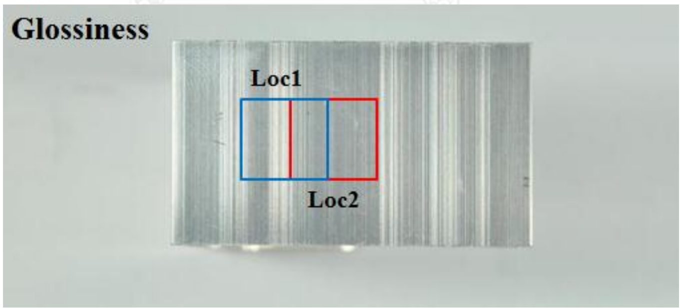

Figure 4-6: Surface gloss measurement regions

$$\Delta gloss = \left| \left(\left| gloss_{loc1} - gloss_{loc2} \right| \right)_{before} - \left(\left| gloss_{loc1} - gloss_{loc2} \right| \right)_{after} \right| \qquad (4\text{-}2)$$

For surface roughness measurement, it was measured using Confocal laser scanning microscopy (CLSM) that had detected 1 cm distance through the streak region as shown in Figure 4-7. The results from CLSM measurement was the average roughness (Ra).

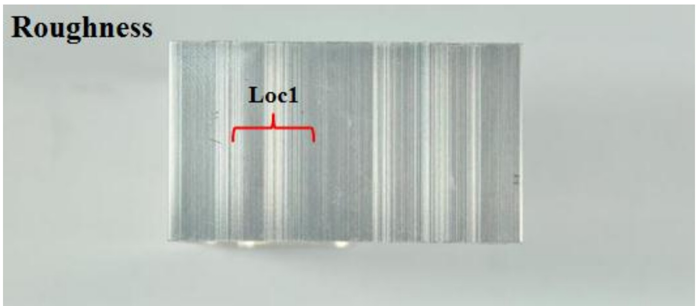

Figure 4-7: Surface roughness measurement region

4.5 Layout of Experiments for RSM

In this study, RSM has been used for providing the mathematical models in the form of multiple regression equations for the characteristic of aluminum etching process. During the evaluation of the results, the independent variables have been looked as a surface to which a mathematical model is fitted in second-order polynomial form using RSM. For the RSM regression, the general form of the second-order polynomial is described by Equation 4-3 [22].

$$Y = b_0 + \sum_{i=1}^{n} b_i x_i + \sum_{i=1}^{n} b_{ii} x_{ii}^2 + \sum_{i=1}^{n-1} \sum_{j=i+1}^{n} b_{ij} x_i x_j \pm e_r \tag{4-3}$$

where:

x_i are input variables.

$x_i x_j$ are interaction of those input variables.

b_0 is a constant.

b_i, b_{ii} and b_j are regression coefficents.

e_r is an accidental error.

Y is design optimization.

This assumed surface Y can be estimated the regression coefficients; a number of experimental design techniques are available. The aim of the scheme based on central composite design is fitted the second order response surfaces quite accurately [23].

In this study, the central composite design (CCD) approach, which is a subset of response surface method (RSM), was used to study the effect of etching process parameters on streak defects on aluminum parts. Specifically, CCD was applied to study the relationships between the variables and the responses. The experimental layout was obtained in accordance with the 3-level full-factorial CCD with 8 cube points, 6 axial points, 4 center points, and 2 center points in axial, resulting in a total of 20 runs and was replicated 3 times. The three variables were: concentration of NaOH (x_1), etching temperature (x_2), and etching time (x_3). The range and central point values of the three independent variables used in these studies are summarized in Table 4-4: Factors for central composite DOE and their levels..

Table 4-4: Factors for central composite DOE and their levels.

Factors (Independent Variables)	**Uncoded levels**				
	-1.68	-1	0	1	1.68
Concentration of NaOH: x_1 (wt.%)	1	2	5	8	10
Etching Temperature: x_2 (°C)	30	38	50	62	70
Etching Time: x_3 (min)	1	2	5	8	10

The run numbering continues from the end of the Central Composite experiments as follows Table 4-5. Then, the three responses tested for were weight loss (Y_1), the difference in surface gloss before and after etching (Y_2), and the final surface roughness (Y_3).

Table 4-5: Experimental conditions for central composite DOE (uncoded values).

Run	**Concentration of NaOH (wt%)**	**Etching Temperature (°C)**	**Etching Time (min)**
1	2	38	2
2	8	38	2
3	2	62	2
4	8	62	2
5	2	38	8
6	8	38	8
7	2	62	8
8	8	62	8
9	1	50	5
10	10	50	5
11	5	30	5
12	5	70	5
13	5	50	1
14	5	50	10

Run	Concentration of NaOH (wt%)	Etching Temperature (°C)	Etching Time (min)
15	5	50	5
16	5	50	5
17	5	50	5
18	5	50	5
19	5	50	5
20	5	50	5

Finally, the experimental method can be concluding as following flowchart:

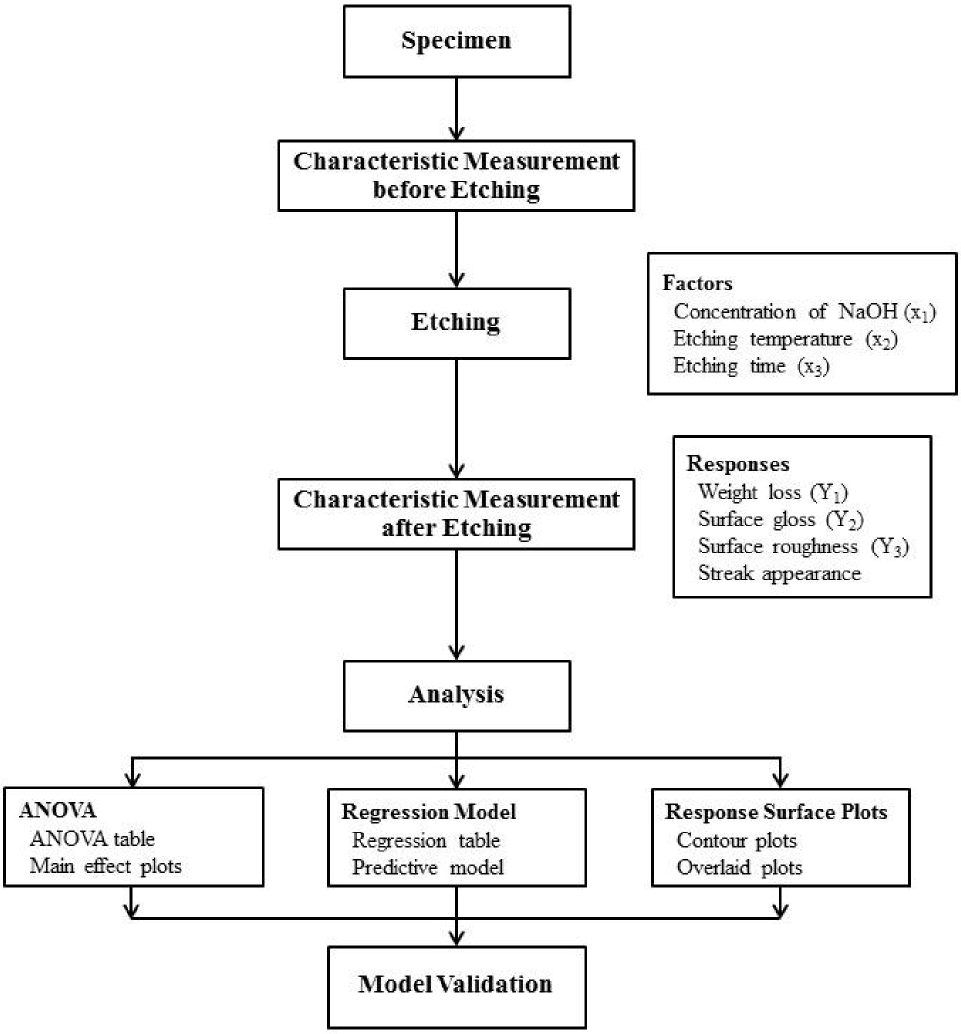

Figure 4-8: Flowchart for experimental method

CHAPTER 5
RESULTS AND DISCUSSION

In this study, RSM are used to develop and improve the aluminum etching process in order to provide the analysis of variance and the model regression for streak defect elimination. The relationship between responses and etchinf process parameters are illustrated as follows:

5.1 Streak Appearance Results

From the study of the effect of concentration of NaOH (Conc, x_1), etching temperature (Temp, x_2) and etching time (Time, x_3) on the weight loss of aluminum etching, is shown in Figure 5-1.

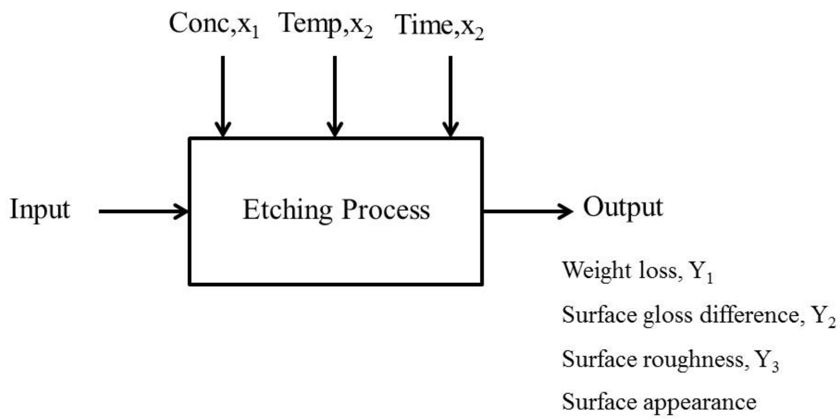

Figure 5-1: Controllable factors for etching process.

In this study, the streak appearances after the etching are shown in the Table 5-1. It can be conclude that the streak defects cannot eliminate at low level value of the etching parameters (Concentration of NaOH, etching temperature, and etching time), nonetheless, they were disappeared on the surface when increasing the etching parameters.

Table 5-1: Streak observation results.

Run	**Conc of NaOH [wt%], x_1**	**Etching Temp [°C], x_2**	**Etching Time [min], x_3**	**Streak observation**
1	2	38	2	observed
2	8	38	2	observed

Run	Conc of NaOH [wt%], x_1	Etching Temp [°C], x_2	Etching Time [min], x_3	Streak observation
3	2	62	2	observed
4	8	62	2	disappeared
5	2	38	8	observed
6	8	38	8	disappeared
7	2	62	8	disappeared
8	8	62	8	disappeared
9	1	50	5	observed
10	10	50	5	disappeared
11	5	30	5	observed
12	5	70	5	disappeared
13	5	50	1	observed
14	5	50	10	disappeared
15	5	50	5	disappeared
16	5	50	5	disappeared
17	5	50	5	disappeared
18	5	50	5	disappeared
19	5	50	5	disappeared
20	5	50	5	disappeared

The specimens after etching were sent to the aluminum production plant to assess the streak by expert user’s observation. An example of a specimen that still showed the streak after etching is shown in Figure 5-2. This particular sample was from Run13 experiment, using the NaOH concentration of 5 wt.%, etching temperature of 50°C, and etching time of 1 minute.

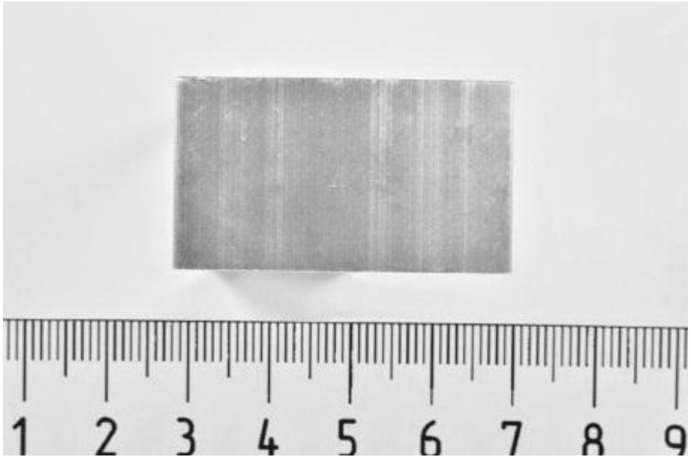

Figure 5-2: Specimen with the streak appearance on the surface.

In contrast, the specimen that does not have streak appearance on the surface after etching is shown as example in Figure 5-3. This particular sample was from Run18 experiment, using the NaOH concentration of 5 wt.%, etching temperature of 50°C, and etching time of 5 minutes.

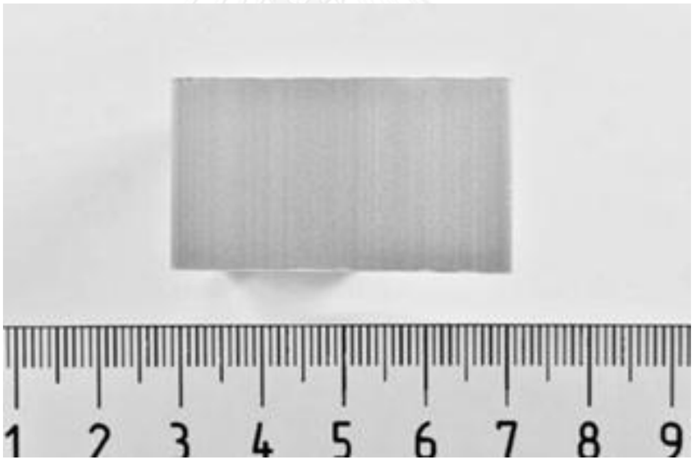

Figure 5-3: Specimen without the streak after the etching.

5.2 Effect of Etching Process Parameters on Weight Loss

5.2.1 Experimental Results Table for Weight Loss

In section 4.5 the experimental conditions for a three-level, three-factor Central Composite Design was outlined. The results of this series for average weight loss are outlined in Table 5-2.

Table 5-2: Results of the weight loss from central composite design.

Run	Concentration of NaOH [wt.%], x_1	Etching Temperature [°C], x_2	Etching Time [min], x_3	Average weight loss [%], Y_1	Standard deviation, SD
1	2	38	2	0.19	0.02
2	8	38	2	0.49	0.02
3	2	62	2	0.88	0.06
4	8	62	2	2.48	0.40
5	2	38	8	1.01	0.20
6	8	38	8	2.67	0.85
7	2	62	8	3.93	0.16
8	8	62	8	11.59	0.92
9	1	50	5	0.77	0.13
10	10	50	5	3.72	0.47
11	5	30	5	0.59	0.15
12	5	70	5	8.83	1.03
13	5	50	1	0.36	0.02
14	5	50	10	5.07	0.52
15	5	50	5	2.21	0.07
16	5	50	5	2.23	0.14
17	5	50	5	2.29	0.13
18	5	50	5	2.31	0.28
19	5	50	5	2.38	0.28
20	5	50	5	2.46	0.24

From the results, the main chemical reaction between aluminum (Al) and NaOH etchant can be described by Equation 5-1.

$$2Al + 2NaOH + 2H_2O \rightarrow 2NaAlO_2 + 3H_2 \tag{5-1}$$

In this reaction, the aluminum specimen reacts with NaOH and water to form aluminate and release hydrogen gas. As the reaction goes on, aluminum will become aluminate and hydrogen gas. As a result, the weight of the extruded part will decrease.

Table 5-2 shows the effect of concentration of NaOH, etching time and etching temperature on the weight loss. It can be clearly seen that, as expected, the weight loss increases with increasing concentration of NaOH, etching time and etching temperature since the aluminum etching effect is reaction rate-limited; when the etching temperature increases, the reaction rate will also increase.

5.2.2 Analysis of Variance (ANOVA)

The CCD results obtained from the experiments were fed into MINITAB®16 in order to analyze the variance of data and develop a predictive model for optimum conditions of aluminum etching. The first step of analysis is ANOVA table as shown in Table 5-3.

Table 5-3: The ANOVA for response surface quadratic model of weight loss.

Source	**DF**	**Adj SS**	**Adj MS**	**F-value**	**P-value**
Regression model	9	454.929	50.5476	113.64	0.000
Linear	3	46.157	15.3856	34.59	0.000
Conc	1	9.054	9.0541	20.36	0.000
Temp	1	35.631	35.6315	80.11	0.000
Time	1	15.465	15.4652	34.77	0.000
Square	3	31.007	10.3357	23.24	0.000
Conc*Conc	1	1.435	1.4349	3.23	0.079
Temp*Temp	1	28.833	28.8329	64.82	0.000
Time*Time	1	0.05	0.0499	0.11	0.739
Interaction	3	72.087	24.029	54.02	0.000
Conc*Temp	1	19.984	19.9842	44.93	0.000
Conc*Time	1	20.69	20.6903	46.52	0.000
Temp*Time	1	31.412	31.4124	70.62	0.000
Residual Error	50	22.24	0.4448		
Lack-of-Fit	5	14.802	2.9604	17.91	0.000
Pure Error	45	7.439	0.1653		
Total	59				

Here, DF is degree of freedom, SS is sum of squares, MS is means of square, F-value is fixation indices and P-value is probability values. Based on the P-value determination, it can be concluded that these etching parameters at various conditions significantly affect the weight loss of aluminum after etching since the P-value of the model is less than the significant value (α=0.05), as shown in

Table 5-3. Additionally, comparisons with F-values from the regression model and the lack-of-fit were made.the F-value of the lack of fit is less than the F-value of the regression model. It can be concluded that the model is adequate for further usage.

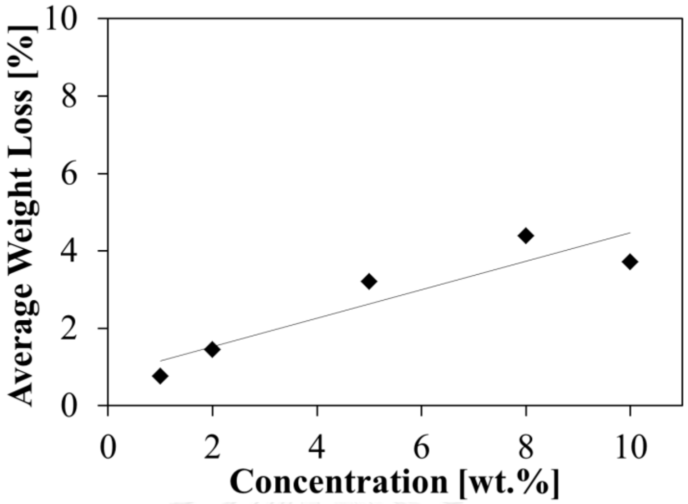

Figure 5-4: Main effect plot of concentration of NaOH on weight loss

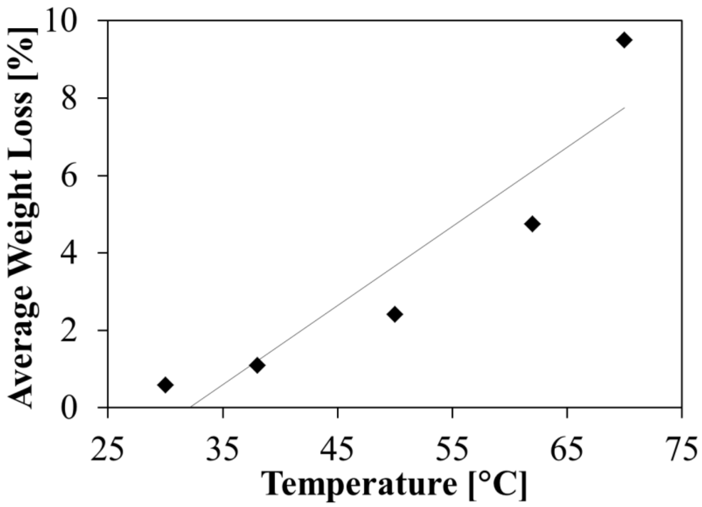

Figure 5-5: Main effect plot of the etching temperature on weight loss.

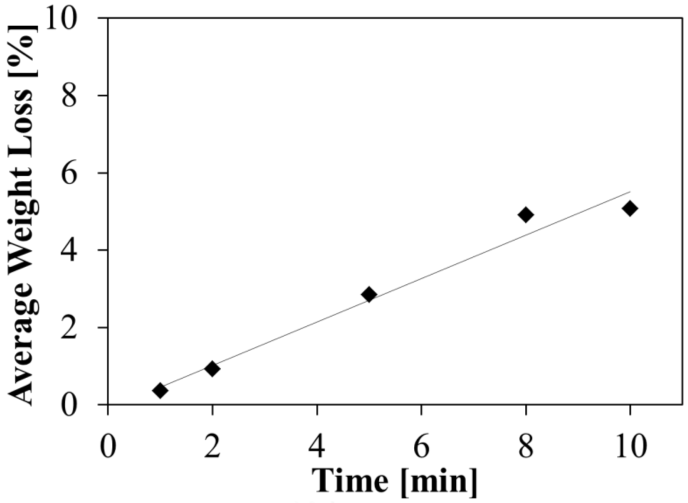

Figure 5-6: Main effect plot of the etching time on weight loss.

Moreover, the concentration of NaOH, etching temperature and etching time are shown to affect the weight loss of aluminum, there are 2 square terms i.e., Conc*Conc and Time*Time, which do not significantly affect the weight loss. From the main effect plots (Figure 5-4, Figure 5-6), it was found that etching temperature is the most influential parameter affecting the weight loss of aluminum etching.

5.2.3 Regression Model Analysis for Weight Loss

The regression coefficients for weight loss of aluminum etching obtained from MINITAB®16 are laid out in Table 5-4.

Table 5-4: The estimated un-coded regression coefficients for weight loss.

Term	**Coef**	**SE Coef**	**T**	**P**
Constant	19.0171	2.30477	8.251	0.000
Conc	-1.1208	0.24843	-4.512	0.000
Temp	-0.6833	0.07634	-8.95	0.000
Time	-1.4649	0.24843	-5.896	0.000
Conc*Conc	-0.0236	0.01312	-1.796	0.079
Temp*Temp	0.0057	0.00071	8.051	0.000
Time*Time	-0.0044	0.01312	-0.335	0.739
Conc*Temp	0.0253	0.00378	6.703	0.000
Conc*Time	0.1032	0.01513	6.82	0.000
Temp*Time	0.0318	0.00378	8.404	0.000

Since the output response with 95% ($\alpha = 0.05$) confident level was assumed and the experiment degree of freedom (DF) was 2n - 2 = 116, the significant t-value, t, of variable term equal to 1.9832 refer the table of t distribution percentage point . If a t-value of observed term is large enough, $|t| \geq 1.9832$, it can be concluded that the observed term is significant. The absolute t-values of each coefficient are shown as Figure 5-7.

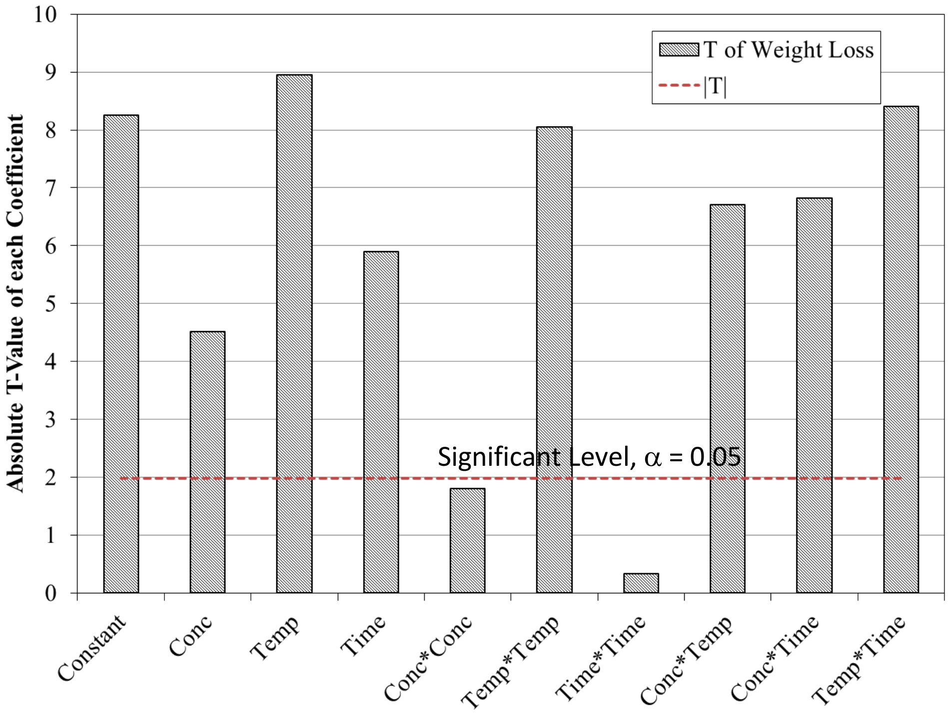

Figure 5-7: The significance of individual regression coefficients.

The results of the predictive model were used to determine the optimum conditions for aluminum etching using CCD, in order to provide guideline to minimize weight loss of etching for streak defects elimination. CCD was applied for the development of the polynomial regression equations which were all quadratic expressions as suggested by the software. The final predictive model equation for weight loss response is given as Equations 5-2

Regression equation in un-coded units:

$$Y_1 = 19.017 - 1.121x_1 - 0.683x_2 - 1.465x_3 + 0.006x_2^2 + 0.025x_1x_2 + 0.103x_1x_3 + 0.032x_2x_3 \quad (5\text{-}2)$$

where:

x_1 = concentration of NaOH [wt.%]

x_2 = etching temperature [°C]

x_3 = etching time [min]

Y_1 = weight loss [%]

5.2.4 Residual Plots for Weight Loss

The analysis of variance can be adequacy check the hypothesis to ensure that the model can be effectively used in etching process. The model is found to be adequate as represented by residual plots shown in Figure 5-8, Figure 5-9. There are key points as follows;

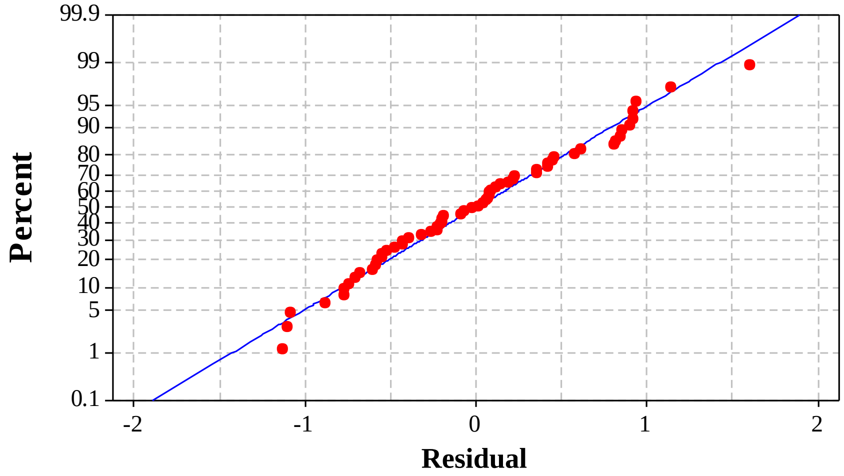

Figure 5-8: Normal probability plot for weight loss response.

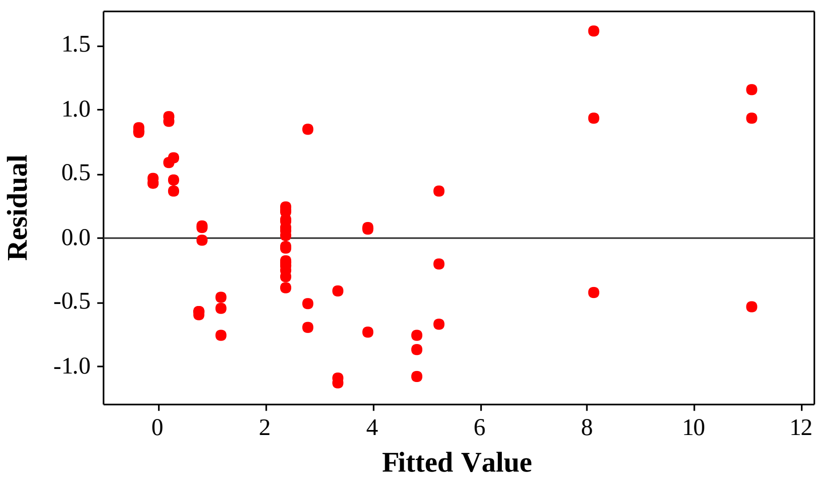

Figure 5-9: Residuals versus fits plot for weight loss response.

- A normal distribution checking was shown using the normal probability plot in Figure 5-8, which appears to align with a linear trend line. Hence, the results can be represented by a normal distribution.
- Hypothesis testing of the correlation plots between the error values and predicted response variable (versus fits), as shown in Figure 5-9, that analyzed from average residual of zero and the variance of data is stable and normal distribution.

5.2.5 Relationship between Experimental and Predicted Weight Loss

From the mathematical model equation for weight loss of aluminum etching with different concentrations of NaOH from 1 to 10 wt.%, the etching temperatures from 30 to 70 °C and the etching time ranging between 1 minute and 10 minutes, Figure 5-10 shows the predicted values versus the experimental values for weight loss of aluminum etching, and the correlation was indicated by the model's R^2 value of 0.9273.

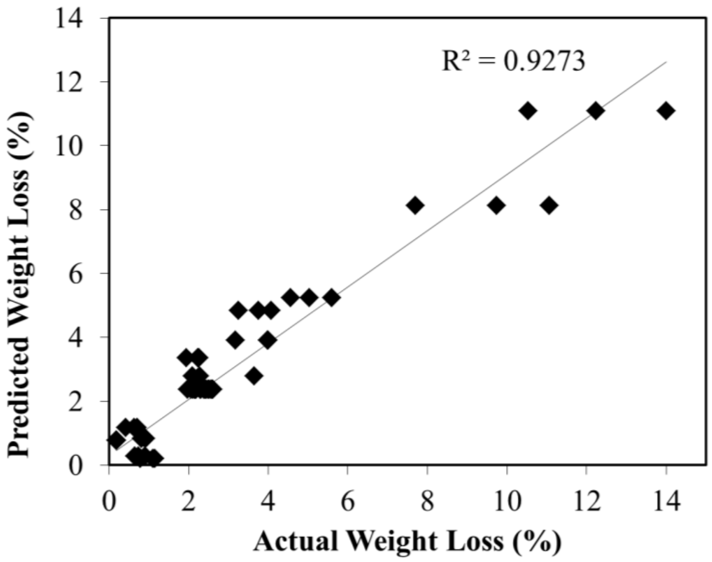

Figure 5-10: Relationship between predicted and experimental data for weight loss of aluminum etching.

5.2.6 Contour Plots and 3-D Surface Plots for Weight Loss Response

In the contour plots and the 3-D response surface plots for the parameters on the weight loss of the aluminum etching, the concentration of NaOH and the etching temperature mainly affect weight loss. The peak value was the maximum weight loss point in these 3-D plots. When the etching time was fixed at low value (Figures 5-11, 5-12), the influence of concentration of NaOH and etching temperature on the weight loss of aluminum etching was observed; the increase of each parameters resulted in the increased weight loss value, the results were also likely with etching temperature was fixed at low value (Figures 5-13, 5-14) and concentration of NaOH was fixed at low value (Figures 5-15, 5-16).

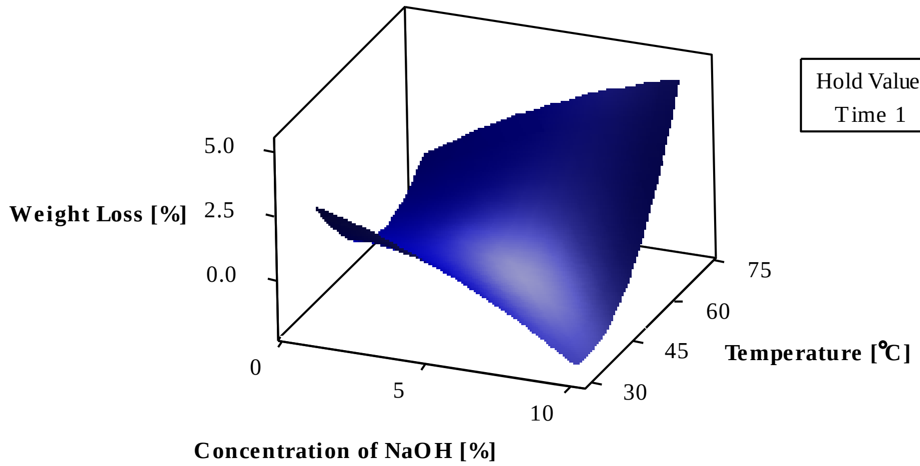

Figure 5-11: 3-D response surface plot for the influence of concentration of NaOH and the etching temperature when the etching time was fixed at 1 minute.

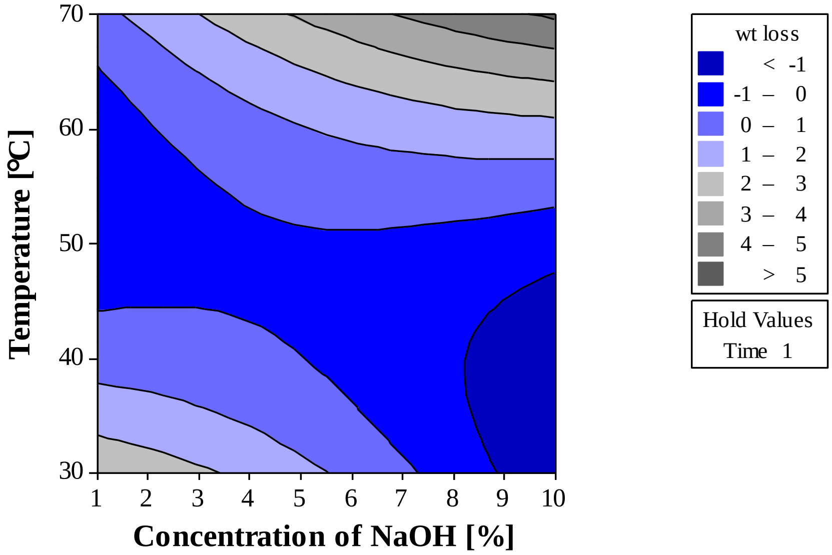

Figure 5-12: Contour plot for the influence of concentration of NaOH and the temperature when the etching time was fixed at 1 minute.

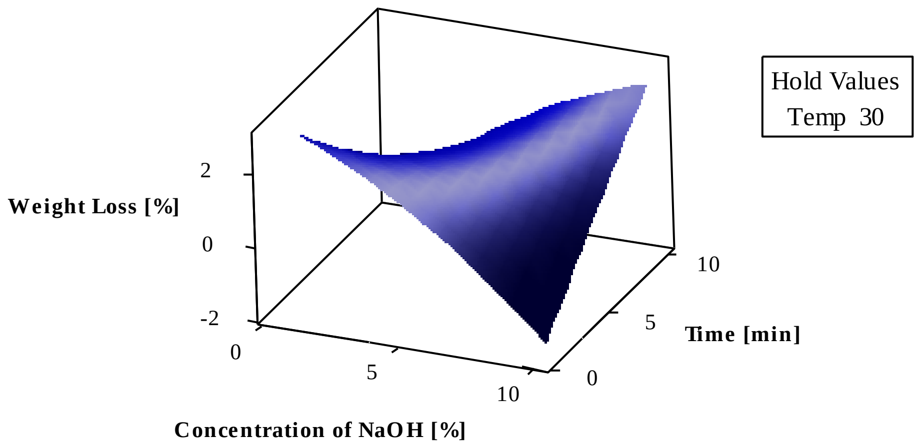

Figure 5-13: 3-D response surface plot for the influence of concentration of NaOH and the etching time when the etching temperature was fixed at 30°C.

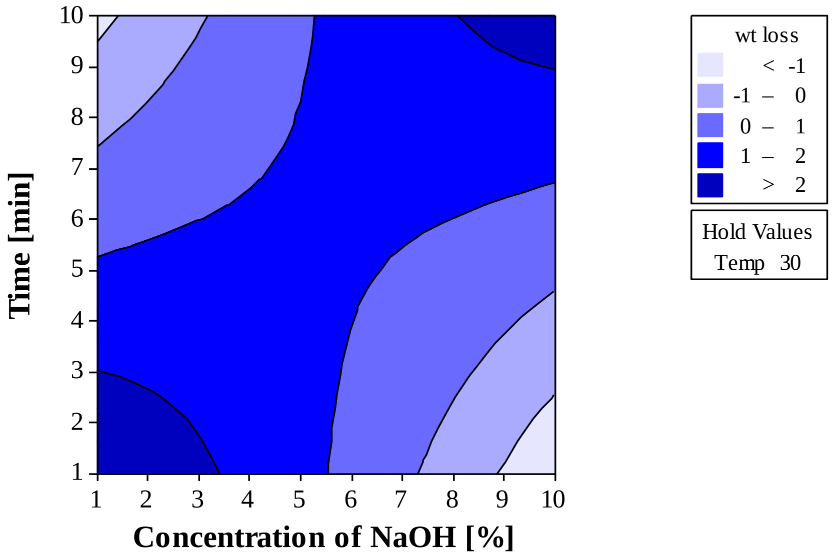

Figure 5-14: Contour plot for the influence of concentration of NaOH and the etching time when the etching temperature was fixed at 30°C.

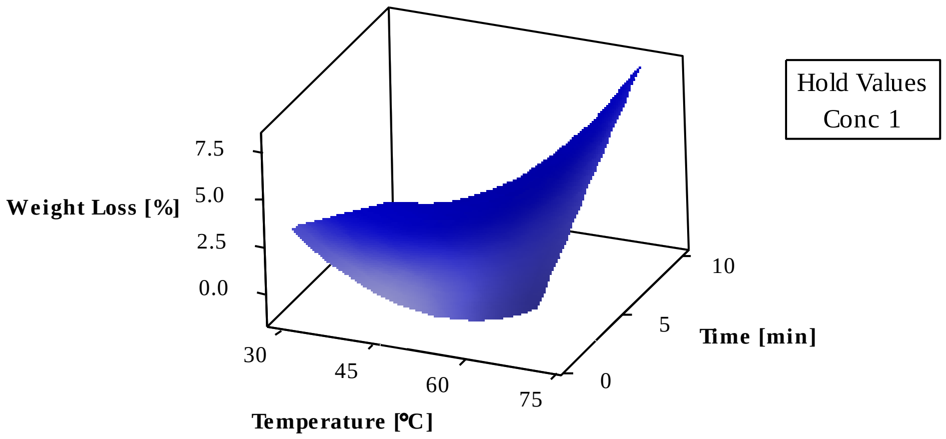

Figure 5-15: 3-D response surface plot for the influence of the etching temperature and the etching time when the concentration of NaOH was fixed at 1%.

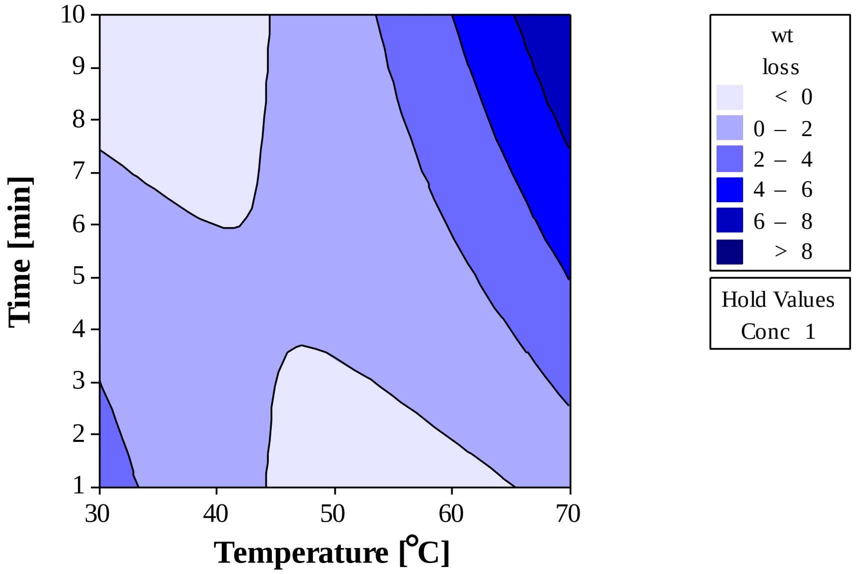

Figure 5-16: Contour plot for the influence of the influence of the etching temperature and the etching time when the concentration of NaOH was fixed at 1%.

5.3 Effect of Etching Process Parameters on Surface Gloss Difference

5.3.1 Experimental Results Table for Surface Gloss Difference

In CCD experiments, the results of this series for average surface gloss differences are outlined in Table 5-5.

Table 5-5: Results of the surface gloss difference from central composite design.

Run	**Concentration of NaOH [wt.%], x_1**	**Etching Temperature [°C], x_2**	**Etching Time [min], x_3**	**Average Surface Gloss Difference [GU], Y_2**	**Standard deviation, SD**
1	2	38	2	6.20	0.26
2	8	38	2	4.33	0.06
3	2	62	2	14.60	2.51
4	8	62	2	19.57	2.22
5	2	38	8	8.70	1.83
6	8	38	8	20.67	3.54
7	2	62	8	24.53	5.66
8	8	62	8	23.64	3.01
9	1	50	5	11.17	0.60
10	10	50	5	28.50	2.05
11	5	30	5	10.87	3.96
12	5	70	5	29.53	5.40
13	5	50	1	8.77	2.83
14	5	50	10	29.83	4.88
15	5	50	5	19.20	7.30
16	5	50	5	23.73	6.23
17	5	50	5	14.40	7.76
18	5	50	5	18.97	4.57
19	5	50	5	24.40	8.50
20	5	50	5	23.80	6.16

5.3.2 Analysis of Variance (ANOVA)

From Table 5-6, the three parameters (concentration of NaOH, etching temperature, and etching time) can also be concluded to significantly affect the difference in surface gloss before and after etching (Δgloss) of aluminum etching because the P-value of the model is 0.000, which is less than the significant value (α=0.05).

Table 5-6: The ANOVA for response surface quadratic model of the surface gloss difference.

Source	**DF**	**Seq SS**	**Adj SS**	**Adj MS**	**F-value**	**P-value**
Regression model	9	3057.01	3057.01	339.668	64.9	0.000
Linear	3	2483.81	275.37	91.791	17.54	0.000
Conc	1	351.6	52.65	52.652	10.06	0.003
Temp	1	1391.56	200.17	200.169	38.24	0.000
Time	1	740.65	107.86	107.856	20.61	0.000
Square	3	506.09	506.09	168.696	32.23	0.000
Conc*Conc	1	208.61	213.1	213.096	40.71	0.000
Temp*Temp	1	101.87	112.74	112.745	21.54	0.000
Time*Time	1	195.6	195.6	195.602	37.37	0.000
Interaction	3	67.11	67.11	22.371	4.27	0.009
Conc*Temp	1	2.05	2.05	2.053	0.39	0.534
Conc*Time	1	62.79	62.79	62.791	12	0.001
Temp*Time	1	2.27	2.27	2.269	0.43	0.513
Residual Error	50	261.7	261.7	5.234		
Lack-of-Fit	5	193.87	193.87	38.775	25.72	0.000
Pure Error	45	67.83	67.83	1.507		
Total	59	3318.72				

The main effects for the difference in surface gloss before and after etching (Δgloss) are shown in Figure 5-17 to Figure 5-19, and it can be concluded that the surface gloss difference increases with these input parameters until at a center point of conditions, then it slightly decreases and rises again with further increase in the three parameters, whereas the interaction of these factor terms, i.e., Conc*Temp, Temp*Time, insignificantly affect the surface gloss difference, except for the term Conc*Time.

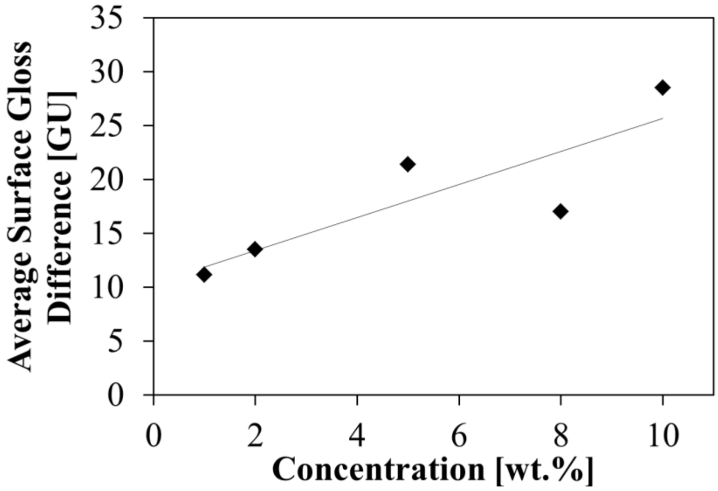

Figure 5-17: Main effect plot of the concentration of NaOH on the surface gloss difference.

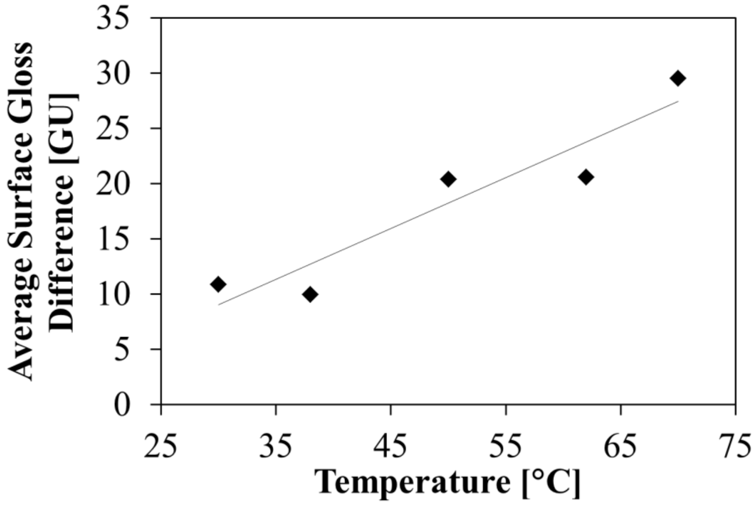

Figure 5-18: Main effect plot of the etching temperature on the surface gloss difference.

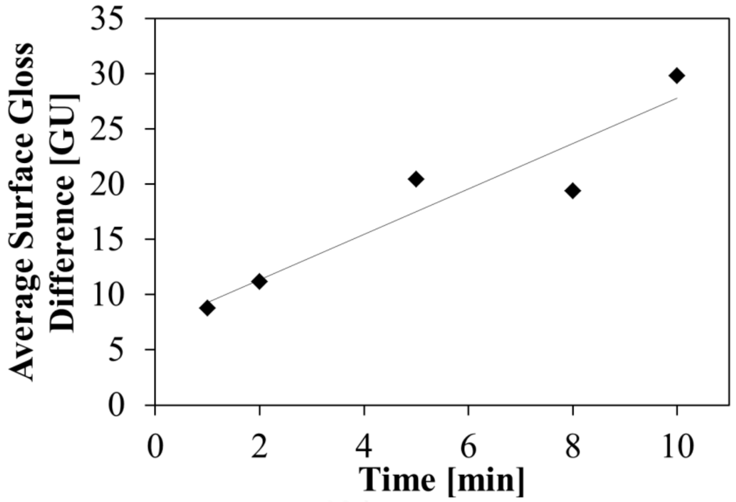

Figure 5-19: Main effect plot of the etching time on the surface gloss difference.

5.3.3 Regression Model Analysis for Surface Gloss Difference

The regression coefficients for difference in surface gloss before and after aluminum etching obtained from MINITAB®16 are laid out in Table 5-7.

Table 5-7: The estimated un-coded regression coefficients for the surface gloss difference.

Term	**Coef**	**SE Coef**	**T**	**P**
Constant	-53.3767	7.90609	-6.751	0.000
Conc	2.7029	0.85219	3.172	0.003
Temp	1.6195	0.26188	6.184	0.000
Time	3.8685	0.85219	4.539	0.000
Conc*Conc	-0.2871	0.045	-6.381	0.000
Temp*Temp	-0.0113	0.00243	-4.641	0.000
Time*Time	-0.2751	0.045	-6.113	0.000
Conc*Temp	0.0081	0.01297	0.626	0.534
Conc*Time	0.1797	0.05189	3.464	0.001
Temp*Time	-0.0085	0.01297	-0.658	0.513

From the table of t distribution percentage point, the significant t-value of variable term is equal to 1.9832. Since the t-value of observed term is large enough, $|t| \geq 1.9832$, this can be concluded that the observed term is significant. The absolute t-values of each coefficient are shown in Figure 5-20. The results can be concluded that the interaction terms of Conc*Temp and Temp*Time are insignificant.

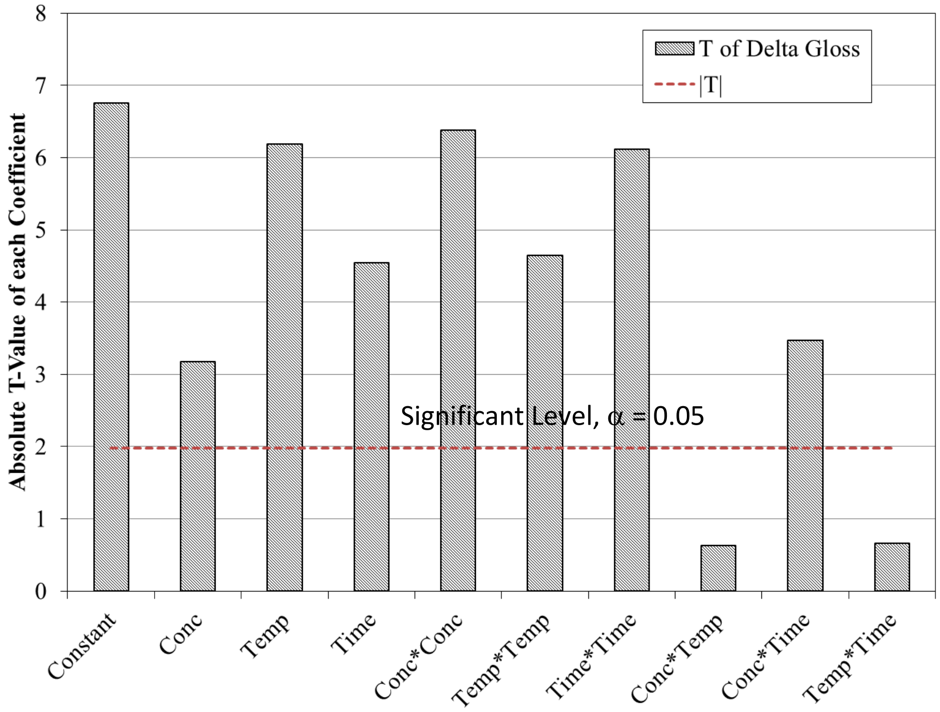

Figure 5-20: The significance of individual regression coefficients.

The predictive model for difference in surface gloss before and after etching is used to determine the optimum conditions for aluminum etching and provide a guideline to optimum range of the surface gloss difference for streak defects elimination. From the CCD analysis, the final predictive model equation for weight loss response is given as Equation 5-3.

Regression equation in un-coded units:

$$Y_2 = -53.377 + 2.703x_1 + 1.620x_2 + 3.869x_3 - 0.287x_1^2 - 0.011x_2^2 - 0.275x_3^2 + 0.178x_1x_3 \quad (5\text{-}3)$$

where:

x_1 = concentration of NaOH [wt.%]

x_2 = etching temperature [°C]

x_3 = etching time [min]

Y_2 = difference in surface gloss value before and after etching [GU]

5.3.4 Residual Plots for surface gloss

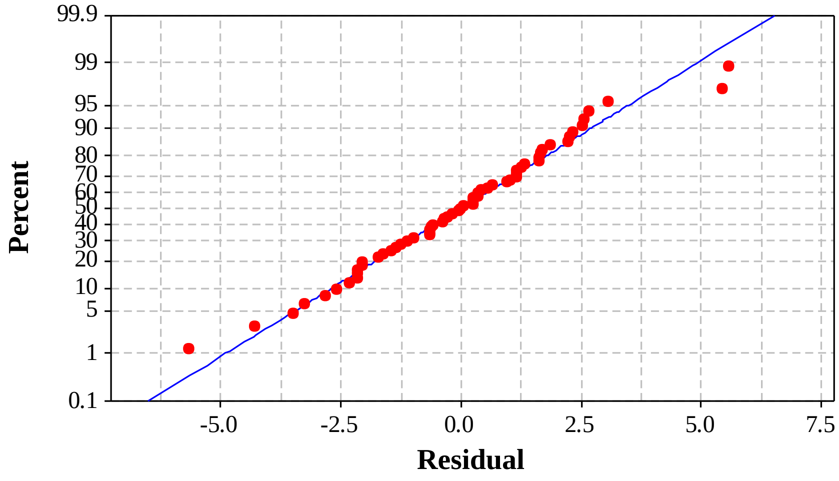

Figure 5-21: Normal probability plot for surface gloss difference response.

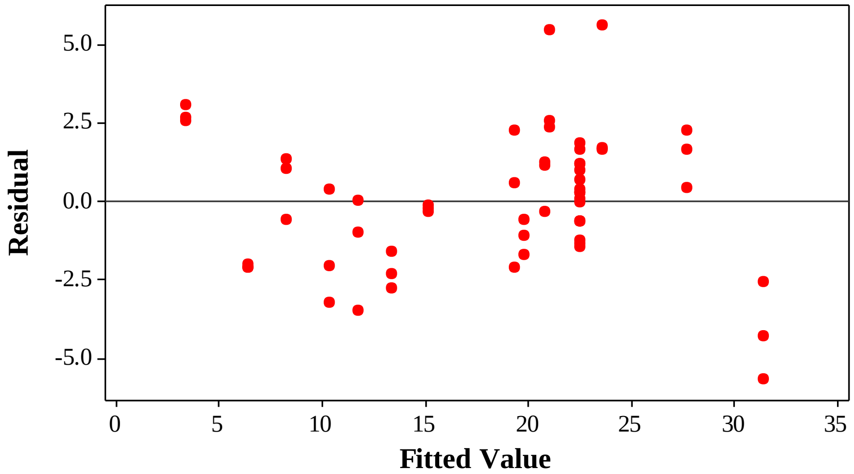

Figure 5-22: Residuals versus fits plot for surface gloss difference response.

From the residual plots shown in Figure 5-21, Figure 5-22, it can be concluded that:

- From the normal probability plot, the points are aligned linearly. Therefore, the results are normal distribution.
- Hypothesis testing of the correlation plots (versus fits) shows that the variance of data are stable distribution.

5.3.5 Relationship between Experimental and Predicted Surface Gloss Difference

From the predictive model equation for difference in surface gloss after aluminum etching using different concentrations of NaOH, etching temperatures and etching time ranges, the predicted values versus the experimental values for surface gloss difference are shown in Figure 5-23, and the correlation was indicated by the model's R^2 values of 0.8286.

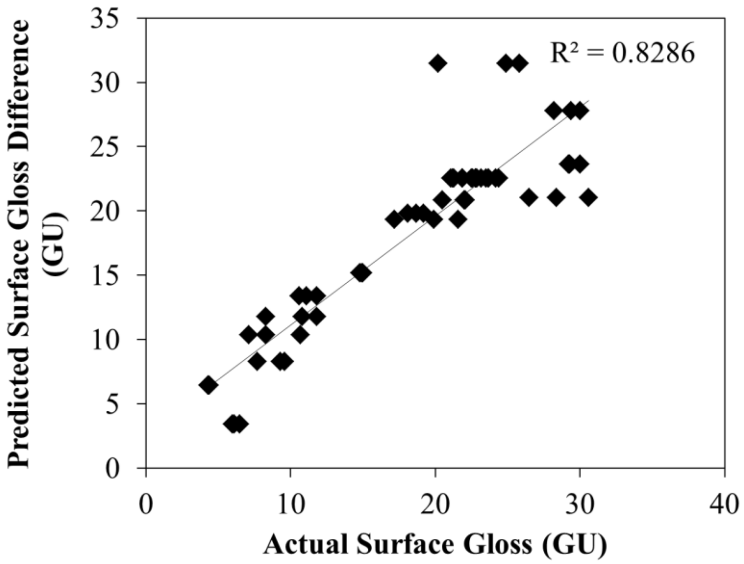

Figure 5-23: Relationship between predicted and experimental data for surface gloss of aluminum etching.

5.3.6 Contour Plots and 3-D Surface Plots for Surface Gloss Difference Response

In addition, the contour plots and 3-D response surface plots of the surface gloss difference show that when etching time was fixed at low value (Figures 5-24, 5-25), the value of surface gloss difference rapidly changes as the concentration of NaOH and the etching temperature increase, especially, at high values. In the case of fixed etching temperature at low value, the surface gloss difference value also appears to increase as the concentration of NaOH and the etching time increase (Figures 5-26, 5-27), which is the same as the results of fixed concentration of NaOH at low value (Figures 5-28, 5-29).

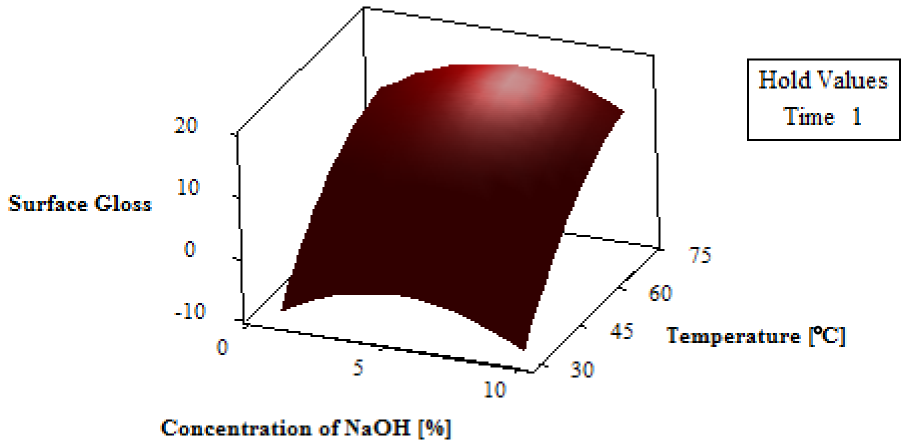

Figure 5-24: 3-D response surface plot for the influence of concentration of NaOH and the etching temperature when the etching time was fixed at 1 minute

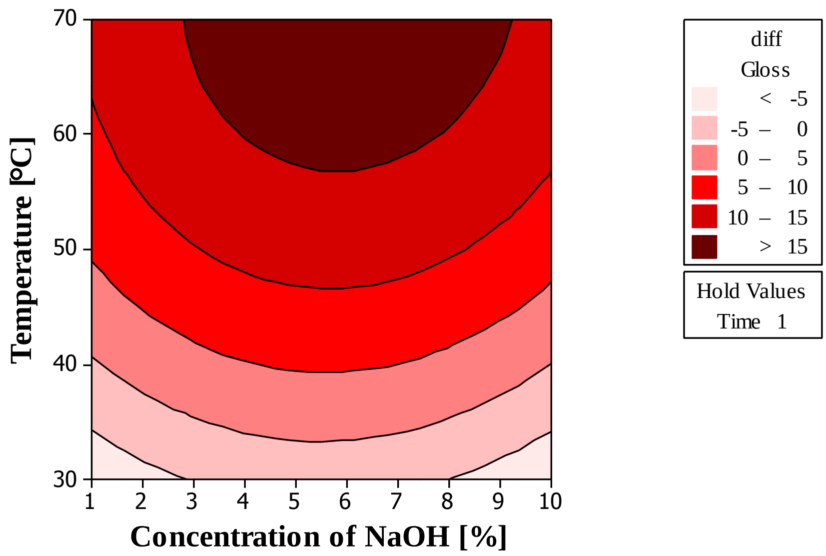

Figure 5-25: Contour plot for the influence of concentration of NaOH and the temperature when the etching time was fixed at 1 minute.

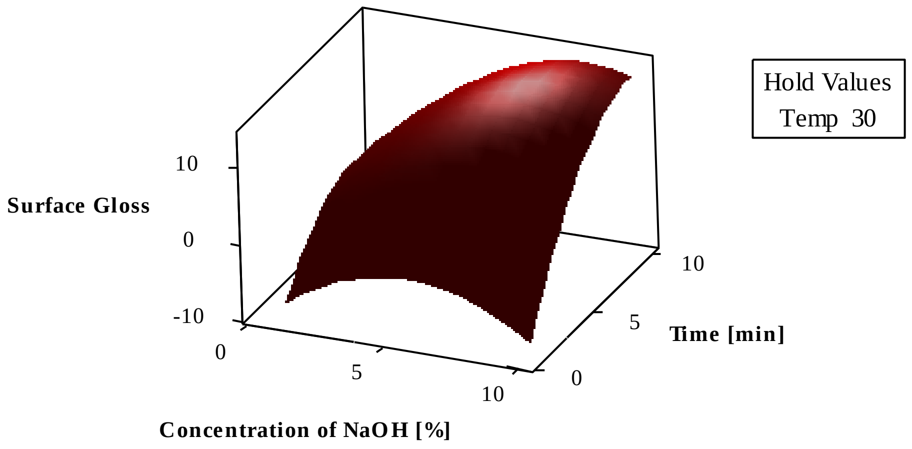

Figure 5-26: 3-D response surface plot for the influence of concentration of NaOH and the etching time when the etching temperature was fixed at 30°C.

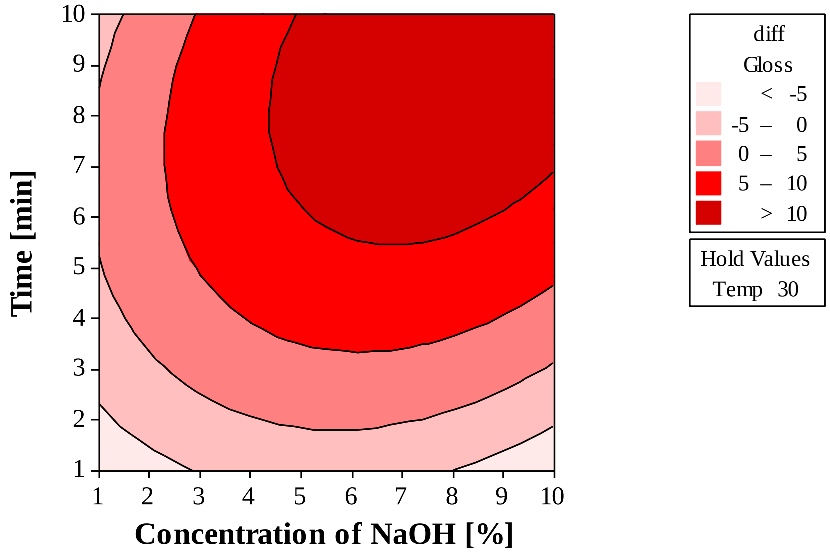

Figure 5-27: Contour plot for the influence of concentration of NaOH and the etching time when the etching temperature was fixed at 30°C.

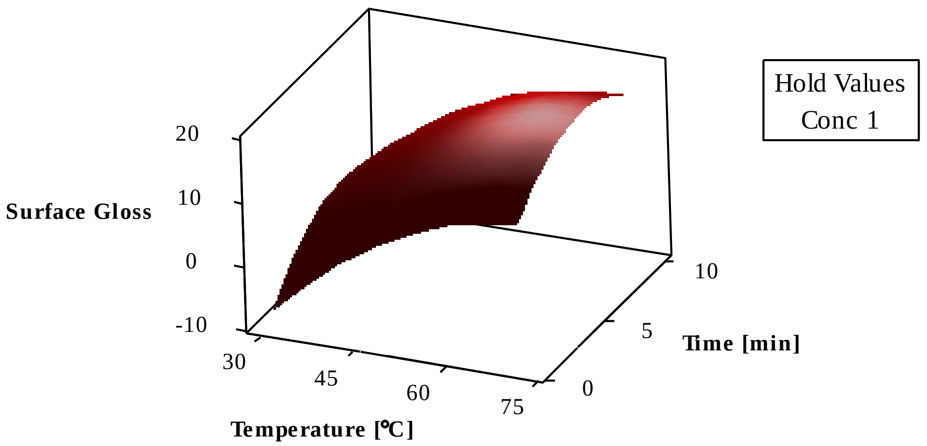

Figure 5-28: 3-D response surface plot for the influence of the etching temperature and the etching time when the concentration of NaOH was fixed at 1%.

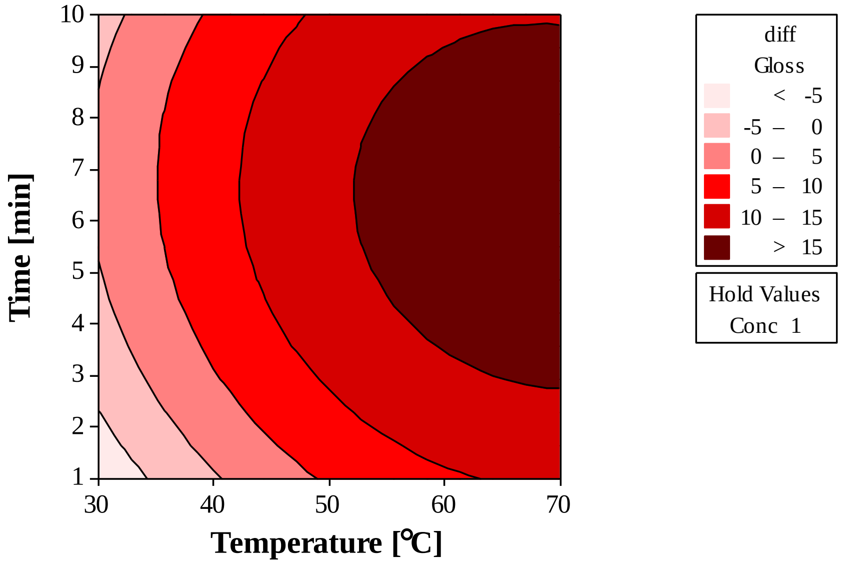

Figure 5-29: Contour plot for the influence of the influence of the etching temperature and the etching time when the concentration of NaOH was fixed at 1%.

5.4 Effect of Etching Process Parameters on Surface Roughness

The analysis of variance was used to study the significance of the effects of the three parameters (concentration of NaOH, etching temperature, and etching time) on the surface roughness, as shown in Table 5-8. The P-value for the model was found to be 0.573 which is more than the significant value. Therefore, the model is insignificant. Moreover, all factor terms have a P-value higher than the significant value (α=0.05), so it can be concluded that all terms are insignificant. This effect may occur from variance of roughness values due to the increase in all input parameters (in case of over etching) that causes formation and falling out of uneven particles on aluminum surface, which consequently influences the surface roughness.

Table 5-8: The ANOVA for response surface quadratic model of surface roughness.

Source	**DF**	**Seq SS**	**Adj SS**	**Adj MS**	**F-value**	**P-value**
Regression model	9	0.011	0.011	0.001	0.85	0.573
Linear	3	0.004	0.003	0.001	0.59	0.626
Conc	1	0.001	0.000	0.000	0.18	0.677
Temp	1	0.002	0.000	0.000	0.2	0.659
Time	1	0.001	0.002	0.002	1.15	0.288
Square	3	0.006	0.006	0.002	1.37	0.263
Conc*Conc	1	0.003	0.003	0.003	2.25	0.140
Temp*Temp	1	0.000	0.000	0.000	0.27	0.606
Time*Time	1	0.002	0.002	0.002	1.66	0.204
Interaction	3	0.001	0.001	0.000	0.28	0.838
Conc*Temp	1	0.000	0.000	0.000	0.14	0.708
Conc*Time	1	0.001	0.001	0.001	0.6	0.442
Temp*Time	1	0.000	0.000	0.000	0.1	0.748
Residual Error	50	0.072	0.072	0.001		
Lack-of-Fit	5	0.008	0.008	0.002	1.11	0.369
Pure Error	45	0.064	0.064	0.001		
Total	59	0.083				

Although etching can eliminate the streak appearance, over-etching, i.e., using high temperature and high concentration of NaOH, can affect the surface of aluminum. The effect of over-etching causes a large number of pitting on the surface that results from aluminum or other particles dissolved during etching. Figure 5-30 shows the surface of aluminum at streak regions before etching. With increasing etching temperature, the etched surfaces show more pits, as illustrated in Figure 5-31. Consequently, the measured surface roughness value of these etched specimens may not be the best parameter for the assessment of streak elimination because of the pits.

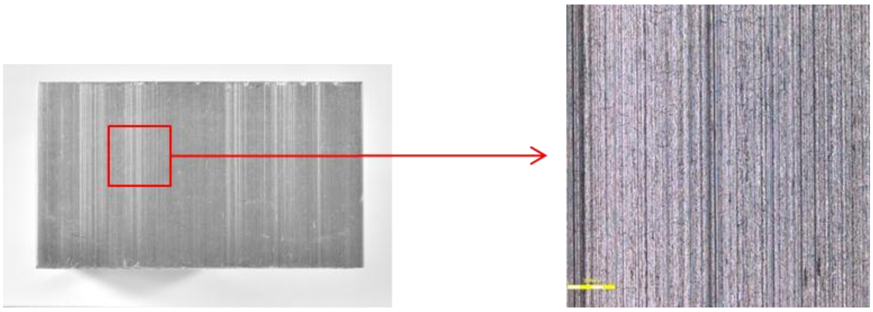

Figure 5-30: Aluminum specimen with streak before etching.

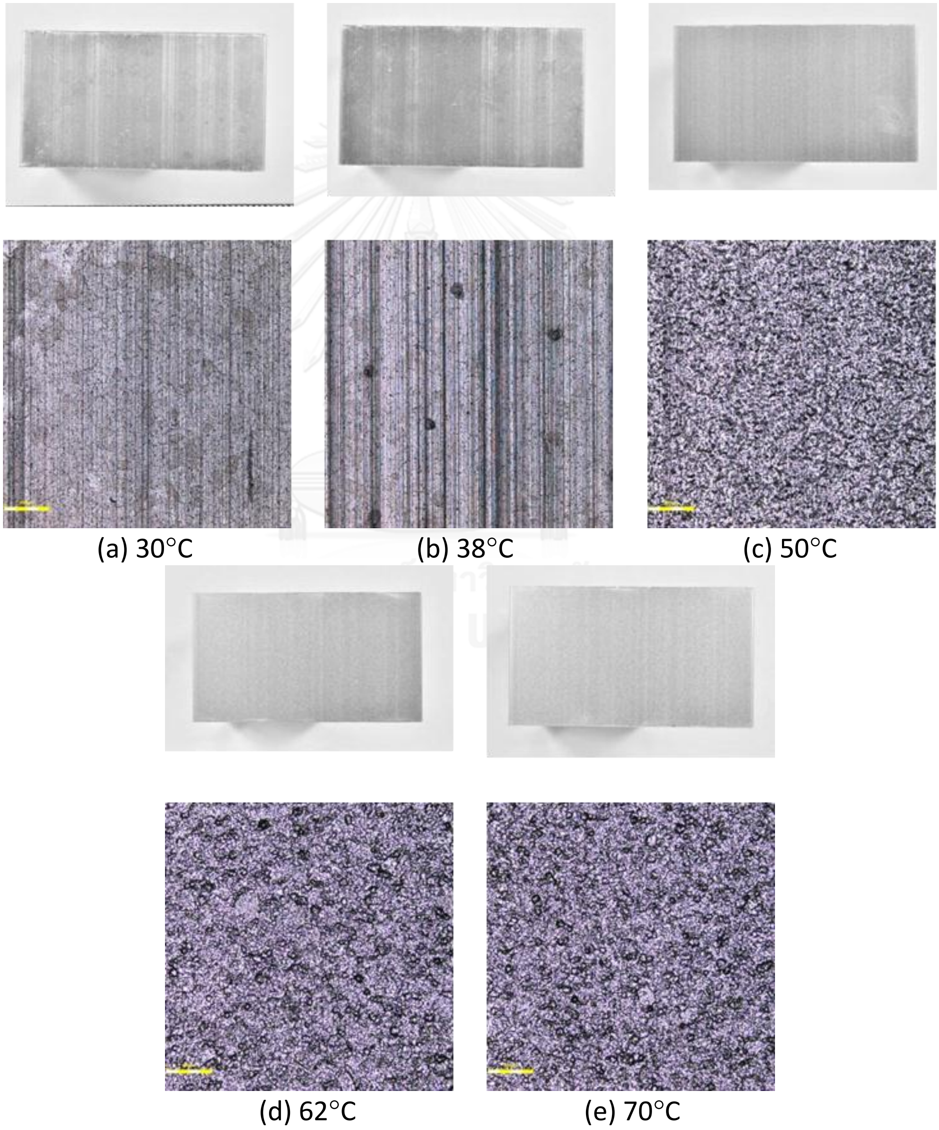

Figure 5-31: Aluminum specimens after etching at various etching temperatures.

5.5 Overlaid Contour Plots for Streak Elimination

From the CCD results (Tables 5-2, 5-5), the streak defect on etched aluminum was not observed in the range of 2.5 to 3.0% of weight loss and the surface gloss difference in the range of 14.9 to 30.0 GU. Therefore, these ranges were used to determine the ranges of etching process conditions to minimize streak defect using the overlaid contour plot function in MINITAB program. The relationships of the process conditions and the output constraints can be established as shown in Figures 5-32 to 5-34, each with different holding parameters. In these plots, the white regions are the optimum etching process condition ranges for streak defect elimination.

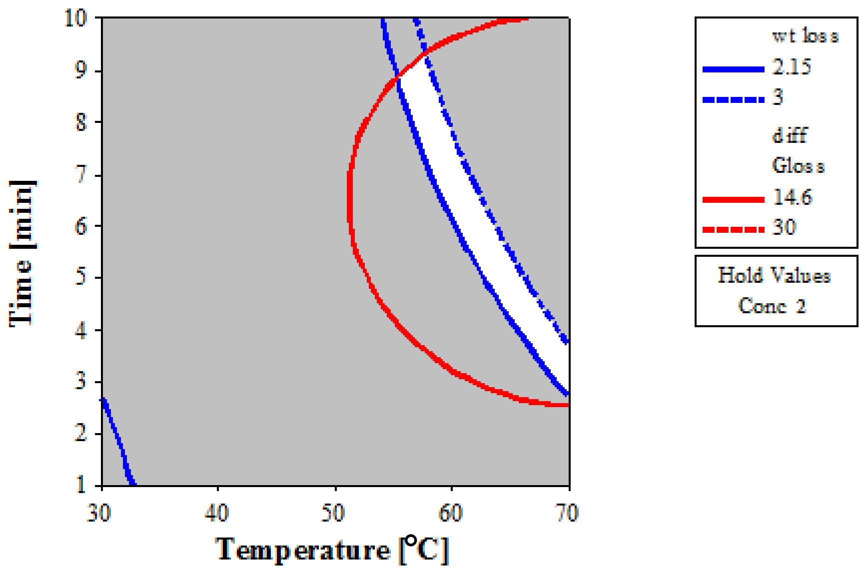

Figure 5-32: Overlaid contour plot for the influence of etching temperature on weight loss in the range of 2.5 to 3.0% and the surface gloss difference before and after etching in the range of 14.9 to 30.0 GU with holding at 2% NaOH.

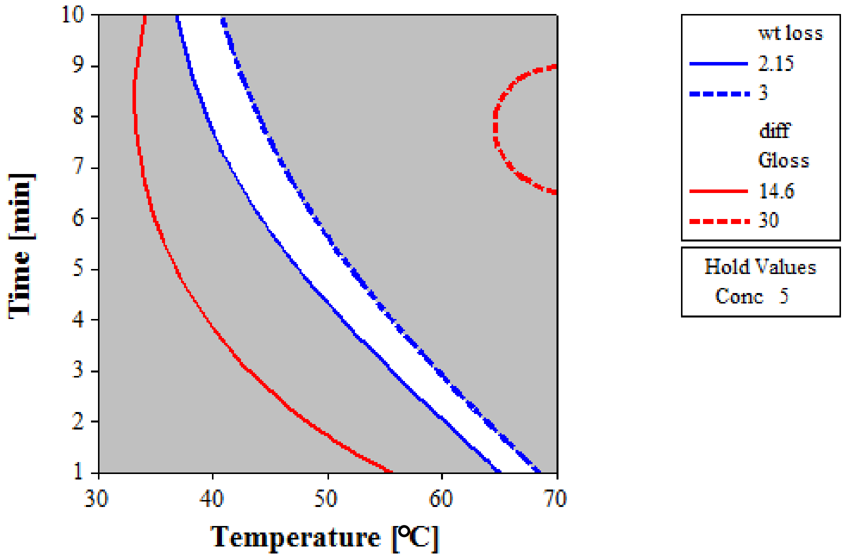

Figure 5-33: Overlaid contour plot for the influence of etching temperature on weight loss in the range of 2.5 to 3.0% and the surface gloss difference before and after etching in the range of 14.9 to 30.0 GU with holding at 5% NaOH.

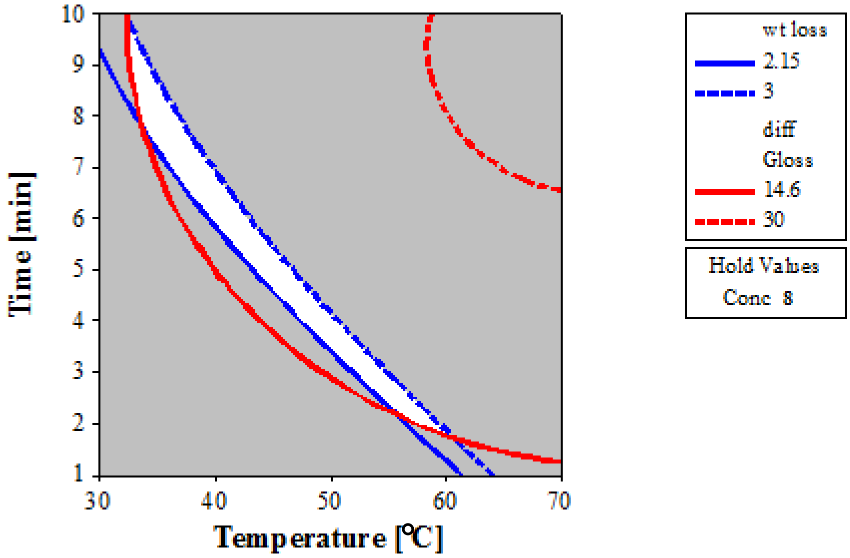

Figure 5-34: Overlaid contour plot for the influence of etching temperature on weight loss in the range of 2.5 to 3.0% and the surface gloss difference before and after etching in the range of 14.9 to 30.0 GU with holding at 8% NaOH.

5.6 Model Validation

The predictive model was built based on the CCD principle. In order to check these models, 3 conditions were tested: at a high concentration of NaOH (x_1 = 8 wt%, x_2 = 45°C, and x_3 = 5.1 min), at a medium concentration of NaOH (x_1 = 5 wt%, x_2 = 40°C, and x_3 = 9.3 min) and at a low concentration of NaOH (x_1 = 2 wt%, x_2 = 55°C, and x3 = 7.3 min) as shown in Table 5-9. The prediction results showed high accuracy at the high concentration of NaOH as illustrated in Figure 5-35, Figure 5-36. At the low concentration of NaOH, however, the prediction results provided approximately 0.55% in weight loss errors and 18% in the surface gloss difference errors. Moreover, the errors of the prediction results provided about 0.43% and 15% in weight loss and surface gloss difference, respectively. As a result, the prediction model could be used to accurately identify weight loss and possibly the surface gloss difference at high concentration levels of NaOH.

Table 5-9: Model validation results.

Run	**Un-coded levels**			**Wt loss [%]**	**ΔGloss [GU]**	**Predicted value from model equation**		**Error %wt loss**	**Error gloss**
	x_1	**x_2**	**x_3**			**%wt loss**	**Δgloss**		
1	2.0	55.0	7.3	2.0	22.5	2.51	19.44	0.55	13.6
	2.0	55.0	7.3	2.0	24.0	2.51	19.44	0.54	19.0
	2.0	55.0	7.3	2.1	24.9	2.51	19.44	0.46	21.9
2	5.0	40.0	9.3	1.9	23.5	2.32	18.65	0.37	20.6
	5.0	40.0	9.3	1.9	21.0	2.32	18.65	0.40	11.2
	5.0	40.0	9.3	1.8	22.1	2.32	18.65	0.52	15.6
3	8.0	45.0	5.1	1.9	20.5	2.41	20.74	0.46	1.2
	8.0	45.0	5.1	1.8	20.3	2.41	20.74	0.62	2.2
	8.0	45.0	5.1	1.7	21.0	2.41	20.74	0.66	1.2

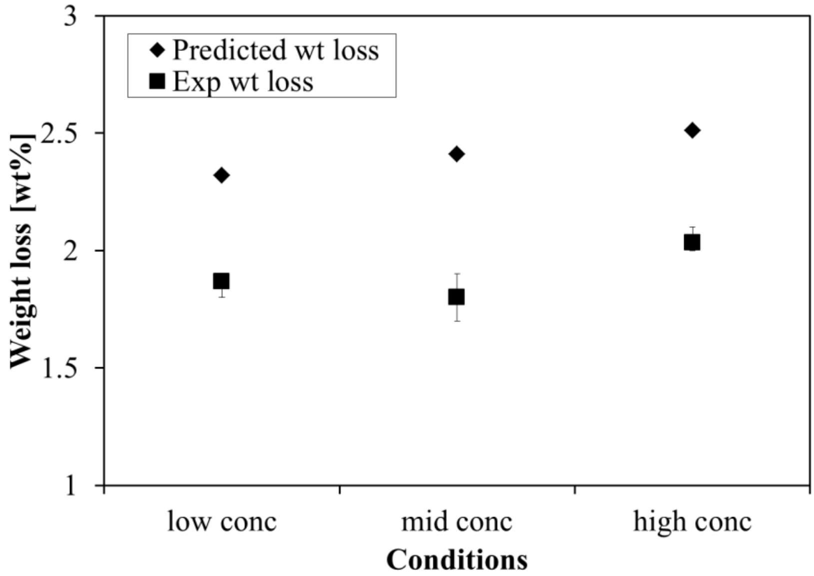

Figure 5-35: The prediction results of weight loss.

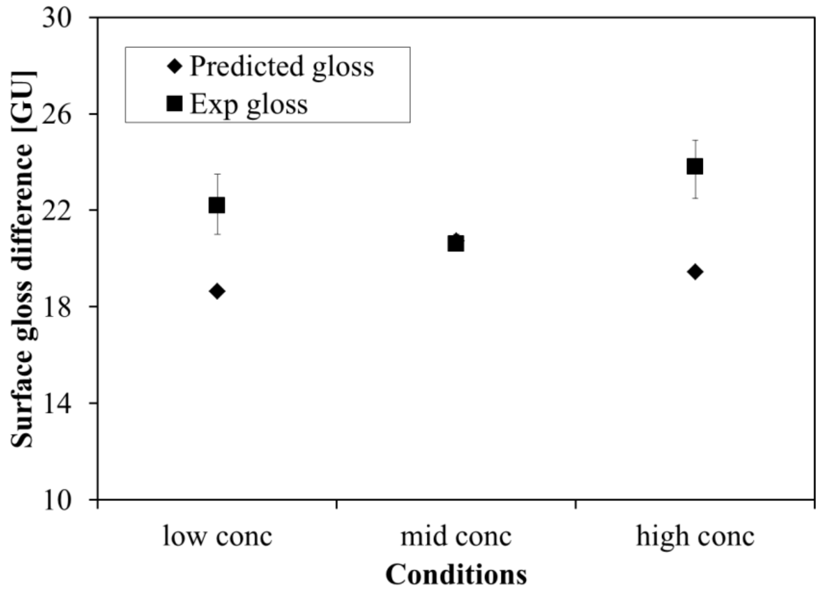

Figure 5-36: The prediction results of the surface gloss difference.

CHAPTER 6
CONCLUSIONS AND FUTURE WORKS

In this study, the effects of process parameters (concentration of NaOH, etching temperature and etching time) on response characteristics (weight loss, surface gloss, and surface roughness) of aluminum etching have been discussed. The optimum ranges of process parameters can be used to reduce the streak defect of extruded aluminum. The important conclusions from this work are summarized in this chapter.

6.1 Conclusions

1) For ANOVA results, it is observed that in all etching experiments, as expected, weight loss increases with concentration of NaOH, etching temperatures and etching time. Even though their main effects are significant, especially the etching temperature, the square terms (i.e., Conc*Conc, Time*Time) are insignificant since these parameters might not affect weight loss when the parameters increase. However, the accuracy results are proved in the higher concentration of NaOH and etching time in future work. Moreover, the difference in surface gloss before and after etching also tends to increase with these input parameters. All of the main effects are significant. Whereas the interaction effects of Conc*Temp and Temp*Time terms do not affect the difference in surface gloss.
2) The final surface roughness values are insignificant that occurred from the variance of roughness values due to the increase in all input parameters (in case of over etching) that causes formation and falling out of uneven particles on aluminum surface, which consequently influences the surface roughness
3) Based on the experimental results in this study, the predictive models for controlling the weight loss and difference in surface gloss by selecting a set of appropriate etching process parameters were provided for etching AA6063 application. The correlations between the experimental and predicted response values, i.e., weight loss and difference in surface gloss, were indicated by the model's R values of 0.9273 and 0.8286, respectively. Therefore, the predictive models can be used to guide the design of etching process parameters.
4) Three process parameters (concentration of NaOH, etching temperature and etching time) were optimized using the overlaid contour plots in CCD analysis for the removal of streak defect on extruded aluminum. From the experimental results, the streak defect cannot be observed in the minimized weight loss values in the range of 1.15 to 2.06% and difference in surface gloss in the range of 14.9 to 17.2 GU. Nonetheless, with careful selection of

the process parameters, the streak defect could be eliminated without removing too much of material from the surface of the extruded parts.

5) For the model validation, the prediction results showed high accuracy with maximum errors of 0.55% and 18% in weight loss and difference in surface gloss, respectively.

6.2 Future Works

- Evaluate the physical and chemical properties of the etched aluminum, i.e., microstructure, chemical compositions, thickness, and hardness.
- Determine the optimum etching process conditions and suitability for streak defect elimination.
- The effect of other process parameters such as type of etchant, shape of aluminum parts, etching rate etc. should also be investigated.

REFERENCES

1. Cobden R. Aluminium: Physical Properties, Characteristics and Alloys. Training in Aluminium Application Technologies; 1994.
2. Walker J. Streaking on Aluminium alloy extrusions: Auckland University of Technology; 2012.
3. Zhu H, Zhang X, Couper MJ, Dahle AK. The Foemation of Streak Defects on Anodized Aluminum Extrusions. Journal of Minerals, Materials Society. 2010;65(5):46-51.
4. Zhu H, Couper MJ, Dahle AK. Effect of Process Variables on the Formation of Streak Defects on Anodized Aluminum Extrusions: An Overview. High Temperature Materials and Processes. 2012;31:105-11.
5. Asensio-Lozano J, Suárez-Peña B, Voort GFV. Effect of Processing Steps on the Mechanical Properties and Surface Appearance of 6063 Aluminium Extruded Products. Materials. 2014;7:4224-42.
6. Technology MIo. Aluminium: Wikipedia; [cited 2017 15 March 2017]. Available from: https://en.wikipedia.org/wiki/Aluminium.
7. Rambabu P, Prasad NE, Kutumbarao VV, Wanhill RJH. Aluminium Alloys for Aerospace Applications. In: Prasad NE, Wanhill RJH, editors. Aerospace Materials and Material Technologies. Singapore: Springer Science; 2017. p. 29-52.
8. Aluminium billets: astrinas - Asian Trade and Investment Ltd.; 2017 [16 March 2017]. Available from: http://www.astrinas.com/en/product/raw-material/.
9. Extrusion Process: Sapa Profiles sponsors Aluminiumdesign.net; [16 March 2017]. Available from: http://www.aluminiumdesign.net/design-support/extrusion-process/.
10. Aluminium Profile Manufacturer in China: Shandong Huajian Aluminium; [17 March 2017]. Available from: http://www.alum-profile.com/1-aluminium-extrusion-profile/1-1b.jpg.
11. Beardmore R. Extruding Processes [17 March 2017]. Available from: http://www.roymech.co.uk/Useful_Tables/Manufacturing/Extruding.html.
12. Advantages of Aluminum Extrusions: Hoosier Trim Products; [18 March 2017]. Available from: http://www.hoosiertrim.com/advantages-of-aluminum-extrusions.htm.
13. Wernick S, Pinner R, Sheasby PG. The Surface Treatment and Finishing of Aluminum and its Alloys. Finishing Publications Ltd.1987.
14. Strauss J. Specular Reflectance of Anodized 6061-T6 Aluminum Alloy: Kansas State University; 2013.
15. Aluminum Surface Finishing User's Guide In: Africa AFoS, editor. 2004.
16. Cheng S. Effect of Aluminum Foil Etching Process on Graphene Super Capacitor. Chemical Engineering Transactions. 2015;46:655-60.
17. Short T. The Identification and Prevention of Defects on Anodized Aluminium Parts. Metal Finishing Information Services Ltd; 2003.
18. Which angle do you need to measure gloss? : Shenzhen 3NH Technology Co., Ltd.; [Available from: http://www.3nhcolor.com/news/160-685.html.
19. EXT OLS4000 Industrial Laser Confocal Microscopes: Olympus Coporation; [Available from: http://www.olympus-ims.com/en/metrology/ols4000/.

20. Agrawalla Y. Optimization of Maching Parameters in a Turning Operation of Austenitic Stainless Steel to Minimize Surface Roughness and Tool Wear: National Institute of Technology Rourkela; 2014.
21. Introduction to Design of Experiments: The Pennsylvania State University; 2017 [25 March 2017]. Available from: https://onlinecourses.science.psu.edu/stat503/node/5.
22. Response Surface Methods and Designs: The Pennsylvania State University; 2017 [25 March 2017]. Available from: https://onlinecourses.science.psu.edu/stat503/node/57.
23. Montoro SR, Medeiros SdF, Santos AM, Silva MB, Tebaldi ML. Application of 2K Experimental Design and Response Surface Methodology in the Optimization of the Molar Mass Reduction of Poly (3-Hydroxybutyrate-co-3Hydroxyvalerate) (PHBHV). Design of Experiments - Applications: Intech 2013. p. 94-119.
24. Trutna L, Spagon P, Castillo Ed, Moore T, Hartley S, Hurwitz A. Central Composite Designs (CCD). In: Enginerring Statistics Handbook [Internet]. National Institute of Standards and Technology. Available from: http://www.itl.nist.gov/div898/handbook/pri/section3/pri3361.htm.
25. Biau DJ, Jolles BM, Porcher R. P Value and the Theory of Hypothesis Testing: An Explanation for New Researchers. Clinical Orthopaedics and Relates Research. 2009;468(3):885-92.
26. Zhu H. Etching Behavior of Aluminum Alloy Extrusions. The Minerals, Metals & Materials Society. 2014;66(11):2222-8.
27. Ma Y, Zhou X, Thompson GE, Nilsson J-O, Gustavsson M, Crispin A. Origin of streaks on anodised aluminium alloy extrusions. The International Journal of Surface Engineering and Coatings. 2013;91(1):11-6.
28. Cakır O. Chemical etching of aluminium. Journal of Materials Processing Technology 2008;199:337-40.
29. Pálfi N, Geier N, editors. A comparative study of full factorial and central composite designs through the machining of aluminium alloy. 8th International Engineering Symposium; 2016; Bánki.

APPENDIX

APPENDIX A.

A.1 Experimental Results for Streak Appearances

A.1.1 Streak Appearance Table

Run	Concof NaOH [wt%], x_1	EtchingTemp [°C], x_2	Etching Time [min], x_3	Streak observation
1	2	38	2	observed
2	8	38	2	observed
3	2	62	2	observed
4	8	62	2	disappeared
5	2	38	8	observed
6	8	38	8	disappeared
7	2	62	8	disappeared
8	8	62	8	disappeared
9	1	50	5	observed
10	10	50	5	disappeared
11	5	30	5	observed
12	5	70	5	disappeared
13	5	50	1	observed
14	5	50	10	disappeared
15	5	50	5	disappeared
16	5	50	5	disappeared
17	5	50	5	disappeared
18	5	50	5	disappeared
19	5	50	5	disappeared
20	5	50	5	disappeared
21	2	38	2	observed
22	8	38	2	observed
23	2	62	2	observed
24	8	62	2	disappeared
25	2	38	8	observed

Run	Concof NaOH [wt%], x_1	EtchingTemp [°C], x_2	Etching Time [min], x_3	Streak observation
26	8	38	8	disappeared
27	2	62	8	disappeared
28	8	62	8	disappeared
29	1	50	5	observed
30	10	50	5	disappeared
31	5	30	5	observed
32	5	70	5	disappeared
33	5	50	1	observed
34	5	50	10	disappeared
35	5	50	5	disappeared
36	5	50	5	disappeared
37	5	50	5	disappeared
38	5	50	5	disappeared
39	5	50	5	disappeared
40	5	50	5	disappeared
41	2	38	2	observed
42	8	38	2	observed
43	2	62	2	observed
44	8	62	2	disappeared
45	2	38	8	observed
46	8	38	8	disappeared
47	2	62	8	disappeared
48	8	62	8	disappeared
49	1	50	5	observed
50	10	50	5	disappeared
51	5	30	5	observed
52	5	70	5	disappeared
53	5	50	1	observed
54	5	50	10	disappeared
55	5	50	5	disappeared

Run	**Concof NaOH [wt%], x_1**	**EtchingTemp [°C], x_2**	**Etching Time [min], x_3**	**Streak observation**
56	5	50	5	disappeared
57	5	50	5	disappeared
58	5	50	5	disappeared
59	5	50	5	disappeared
60	5	50	5	disappeared

A.1.2 Optical image aluminum specimen after etching for 60 run of CCD

Run	Optical Image	Run	Optical Image
1	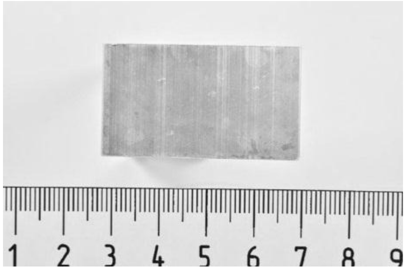 Streak: observed	2	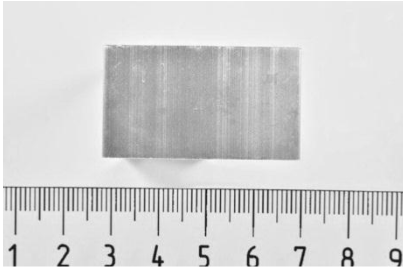 Streak: observed
3	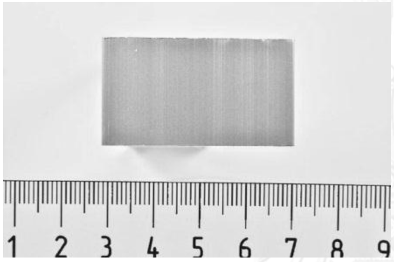 Streak: observed	4	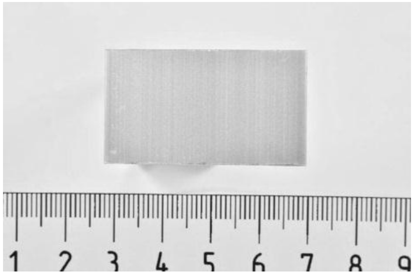 Streak: disappeared
5	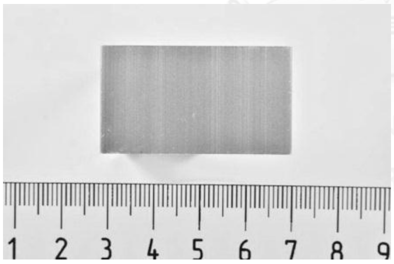 Streak: observed	6	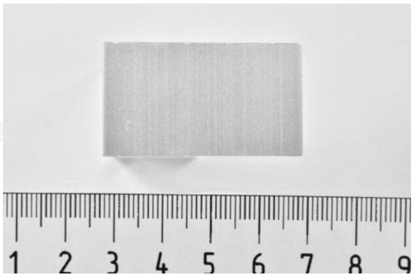 Streak: disappeared
7	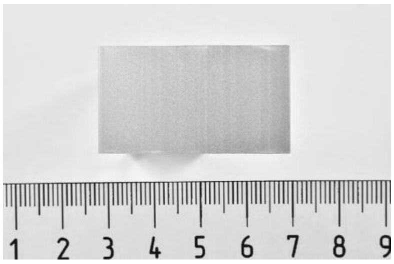 Streak: disappeared	8	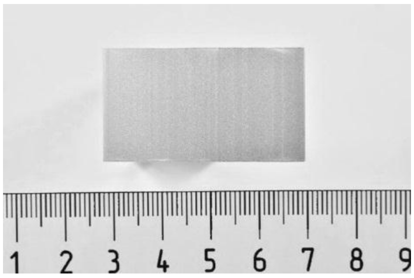 Streak: disappeared

9	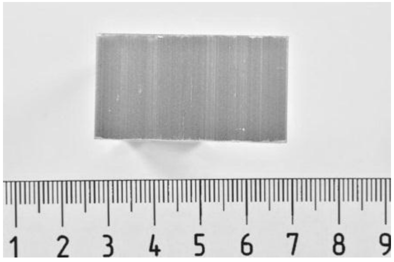 Streak: observed	10	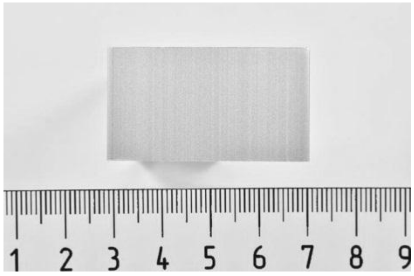 Streak: disappeared
11	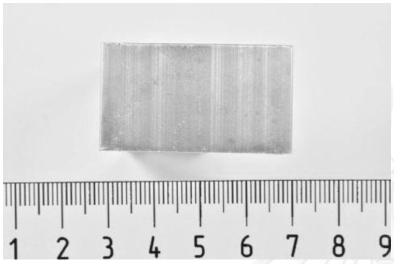 Streak: observed	12	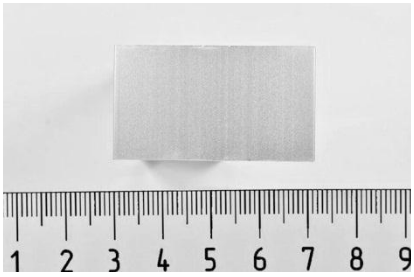 Streak: disappeared
13	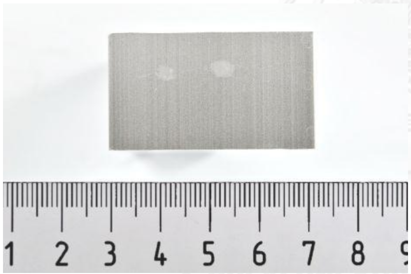 Streak: observed	14	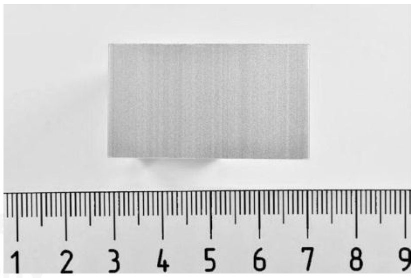 Streak: disappeared
15	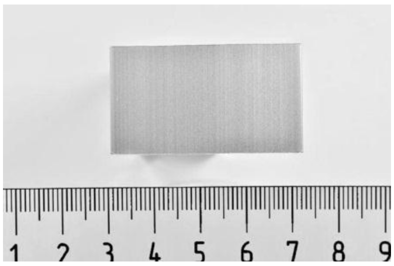 Streak: disappeared	16	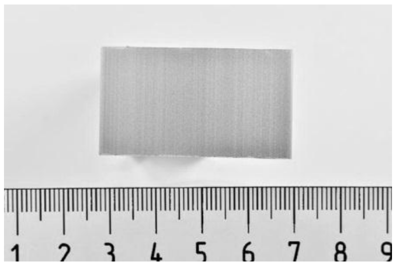 Streak: disappeared

17	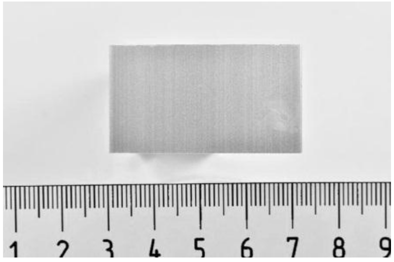 Streak: disappeared	18	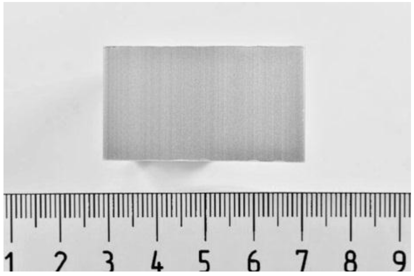 Streak: disappeared
19	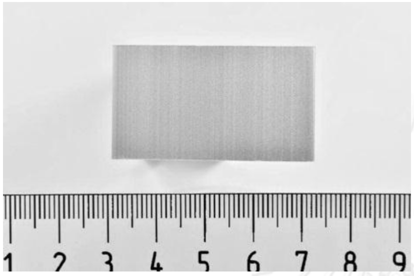 Streak: disappeared	20	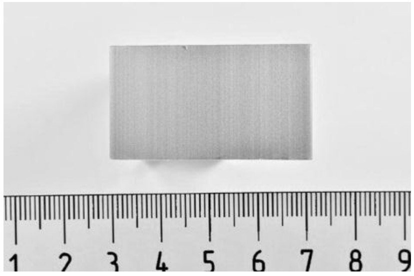 Streak: disappeared
21	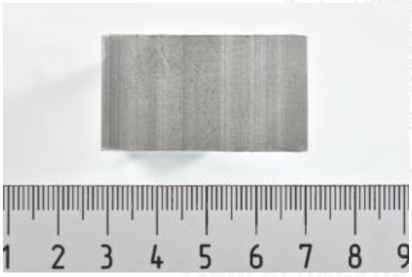 Streak: observed	22	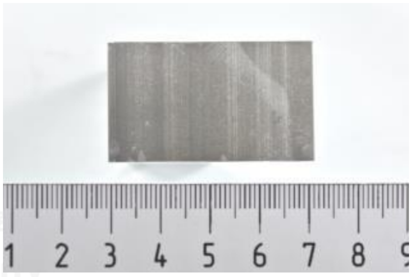 Streak: observed
23	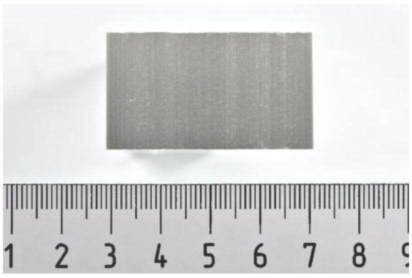 Streak: observed	24	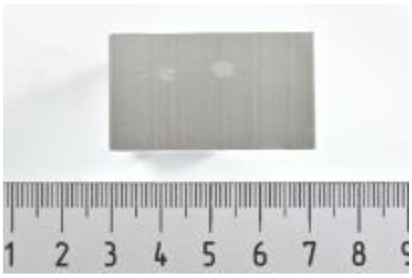 Streak: disappeared

25	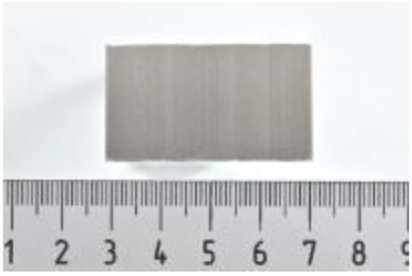 Streak: observed	26	 Streak: disappeared
27	 Streak: disappeared	28	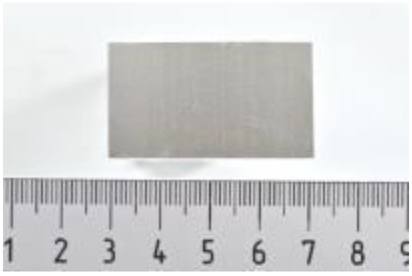 Streak: disappeared
29	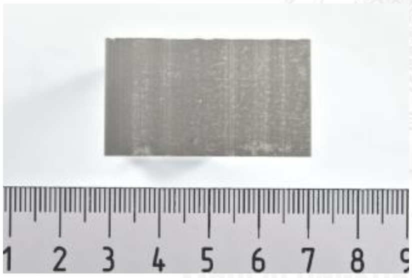 Streak: observed	30	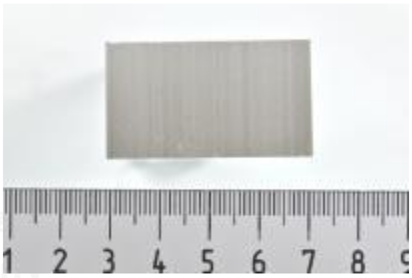 Streak: disappeared
31	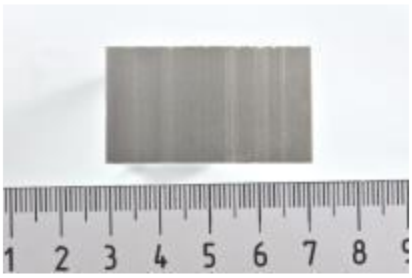 Streak: observed	32	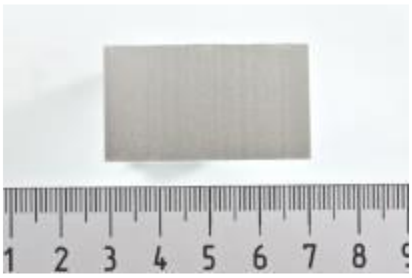 Streak: disappeared

33	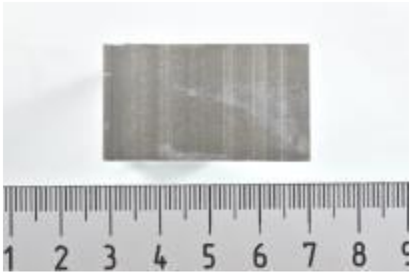 Streak: observed	34	 Streak: disappeared
35	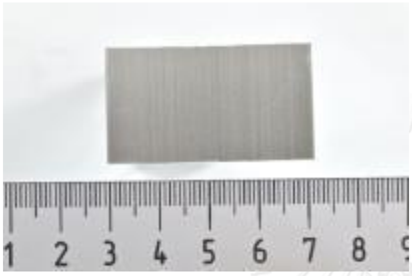 Streak: disappeared	36	 Streak: disappeared
37	 Streak: disappeared	38	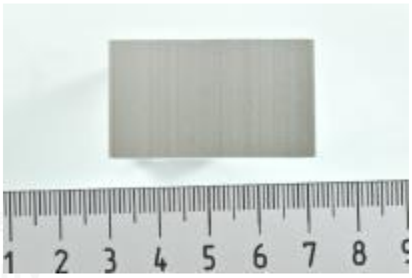 Streak: disappeared
39	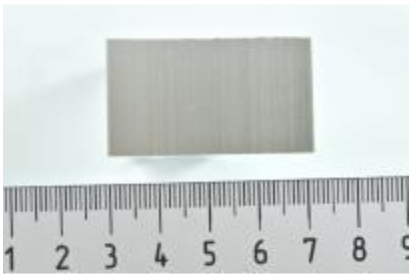 Streak: disappeared	40	 Streak: disappeared

41	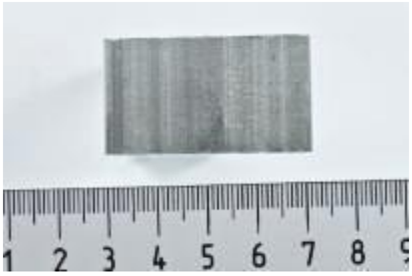 Streak: observed	42	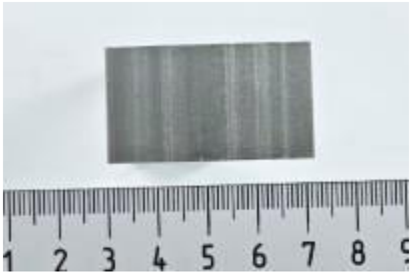 Streak: observed
43	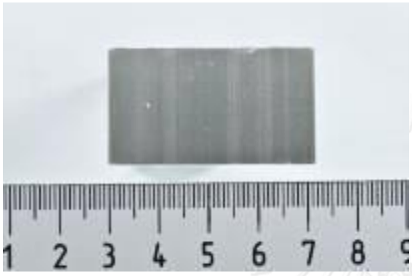 Streak: observed	44	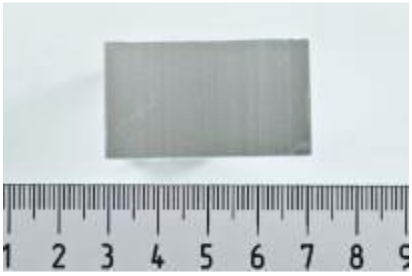 Streak: disappeared
45	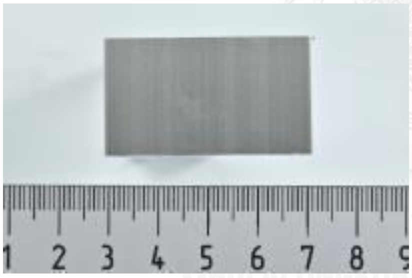 Streak: observed	46	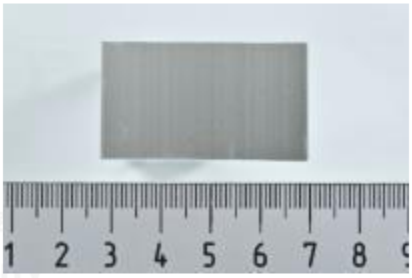 Streak: disappeared
47	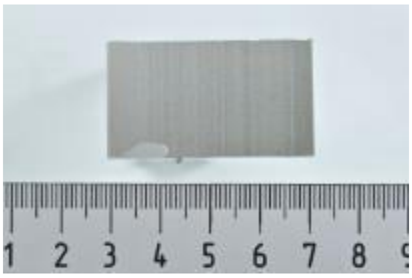 Streak: disappeared	48	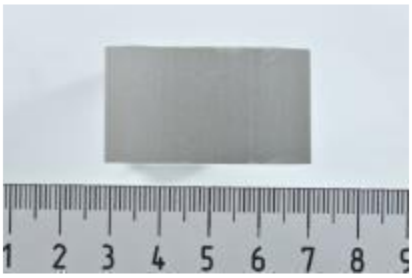 Streak: disappeared

49	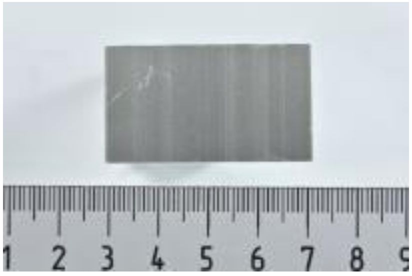 Streak: observed	50	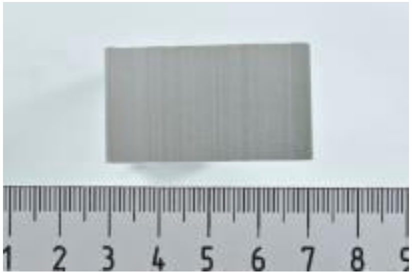 Streak: disappeared
51	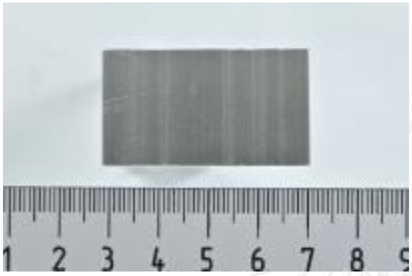 Streak: observed	52	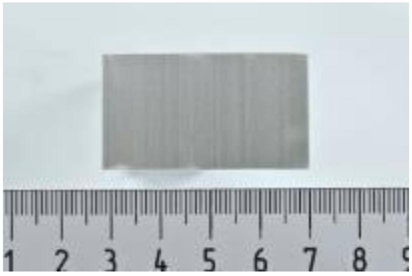 Streak: disappeared
53	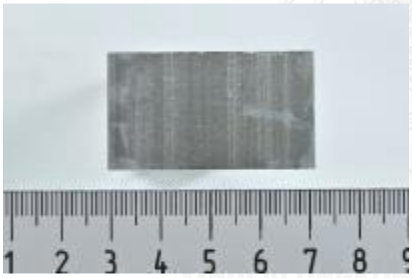 Streak: observed	54	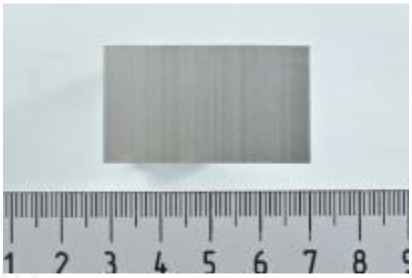 Streak: disappeared
55	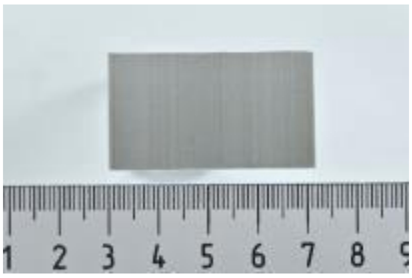 Streak: disappeared	56	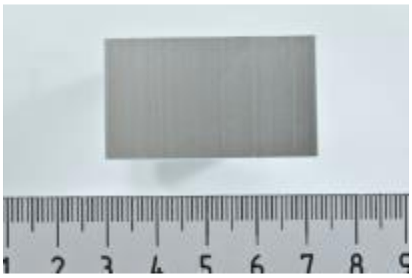 Streak: disappeared

57	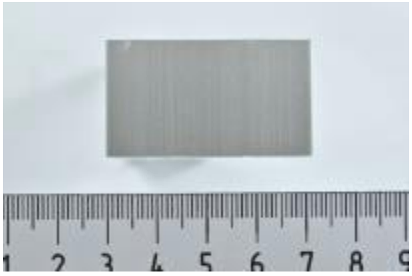 Streak: disappeared	58	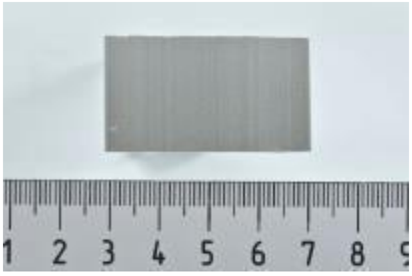 Streak: disappeared
59	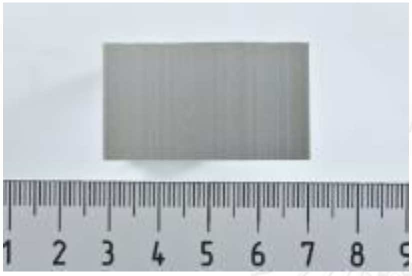 Streak: disappeared	60	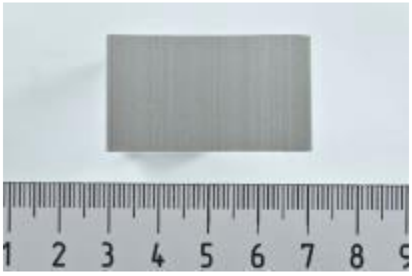 Streak: disappeared

A.2 Experimental Results for Weight Loss

A.2.1 Weight loss calculation

- Weight loss calculation (Y_1)

For example from (Run 1), weight loss is 0.17% that can be calculated from the below equation.

$$\text{Weight loss} = \left(\frac{wt_{before} - wt_{after}}{wt_{before}} \right) \times 100$$

Where,

wt_{before} is the initial weight of specimen.

wt_{after} is the weight of specimen after etching.

For experiment Run1,

$$\text{Weight loss of Run1} = \left(\frac{12.3864g - 12.3653g}{12.3864g} \right) \times 100 = 0.1703\%$$

A.2.2 Experimental data of weight loss for 60 runs CCD

Run	Conc of NaOH [wt%], x_1	Etching Temp [°C], x_2	Etching Time [min], x_3	Weight before etching [g]	Weight after etching [g]	Weight loss [%], Y_1
1	2	38	2	12.3864	12.3653	0.17
2	8	38	2	12.3843	12.3261	0.47
3	2	62	2	12.3604	12.2599	0.81
4	8	62	2	12.4377	12.0720	2.94
5	2	38	8	12.4183	12.3209	0.78
6	8	38	8	12.4278	12.1443	2.28
7	2	62	8	12.3123	11.8493	3.76
8	8	62	8	12.3982	11.0915	10.54
9	1	50	5	12.1887	12.1092	0.65
10	10	50	5	12.3374	11.9458	3.17
11	5	30	5	12.3149	12.2636	0.42
12	5	70	5	12.4693	11.2552	9.74
13	5	50	1	12.3110	12.2687	0.34

Run	Conc of NaOH [wt%], x_1	Etching Temp [°C], x_2	Etching Time [min], x_3	Weight before etching [g]	Weight after etching [g]	Weight loss [%], Y_1
14	5	50	10	12.4039	11.8372	4.57
15	5	50	5	12.3406	12.0753	2.15
16	5	50	5	12.3664	12.1049	2.11
17	5	50	5	12.3340	12.0687	2.15
18	5	50	5	12.3876	12.1423	1.98
19	5	50	5	12.4007	12.1450	2.06
20	5	50	5	12.3620	12.0923	2.18
21	2	38	2	12.3944	12.3698	0.20
22	8	38	2	12.6744	12.6136	0.48
23	2	62	2	12.3888	12.2744	0.92
24	8	62	2	12.3894	12.1129	2.23
25	2	38	8	12.4180	12.2754	1.15
26	8	38	8	12.3323	11.8827	3.65
27	2	62	8	12.3996	11.9089	3.96
28	8	62	8	12.3370	10.8280	12.23
29	1	50	5	12.3973	12.3056	0.74
30	10	50	5	12.3775	11.8833	3.99
31	5	30	5	12.3799	12.2919	0.71
32	5	70	5	12.3153	11.1995	9.06
33	5	50	1	12.3843	12.3371	0.38
34	5	50	10	12.2551	11.6379	5.04
35	5	50	5	12.3426	12.0728	2.19
36	5	50	5	12.413	12.1428	2.18
37	5	50	5	12.3770	12.0775	2.42
38	5	50	5	12.3983	12.0891	2.49
39	5	50	5	12.3671	12.0559	2.52
40	5	50	5	12.3413	12.0218	2.59
41	2	38	2	12.3775	12.3532	0.20
42	8	38	2	12.3764	12.3134	0.51

Run	Conc of NaOH [wt%], x_1	Etching Temp [°C], x_2	Etching Time [min], x_3	Weight before etching [g]	Weight after etching [g]	Weight loss [%], Y_1
43	2	62	2	12.3526	12.2401	0.91
44	8	62	2	12.3629	12.0835	2.26
45	2	38	8	12.4190	12.2810	1.11
46	8	38	8	12.4448	12.1843	2.09
47	2	62	8	12.4420	11.9350	4.07
48	8	62	8	12.4814	10.9824	12.01
49	1	50	5	12.3379	12.2260	0.91
50	10	50	5	12.3676	11.8749	3.98
51	5	30	5	12.3453	12.2669	0.64
52	5	70	5	12.3420	11.3910	7.71
53	5	50	1	12.3980	12.3553	0.34
54	5	50	10	12.3947	11.7009	5.60
55	5	50	5	12.3797	12.0964	2.29
56	5	50	5	12.8932	12.5850	2.39
57	5	50	5	12.3972	12.1116	2.30
58	5	50	5	12.2544	11.9541	2.45
59	5	50	5	12.4216	12.1025	2.57
60	5	50	5	12.3975	12.0744	2.61

A.3 Experimental Results for Surface Gloss Differences

A.3.1 Surface Gloss Difference Calculation

- Surface gloss difference measurement (Y_2)

The surface gloss was measured by glossmeter at two locations as shown in the below figure. Loc1 is the streak defect region and Loc2 is the surrounding region. So, the surface gloss difference, Δgloss, was measured the different surface gloss values between Loc1 ($gloss_{loc1}$) and Loc2 ($gloss_{loc2}$), then calculated the Δgloss from difference between $gloss_{loc1}$ and $gloss_{loc2}$.

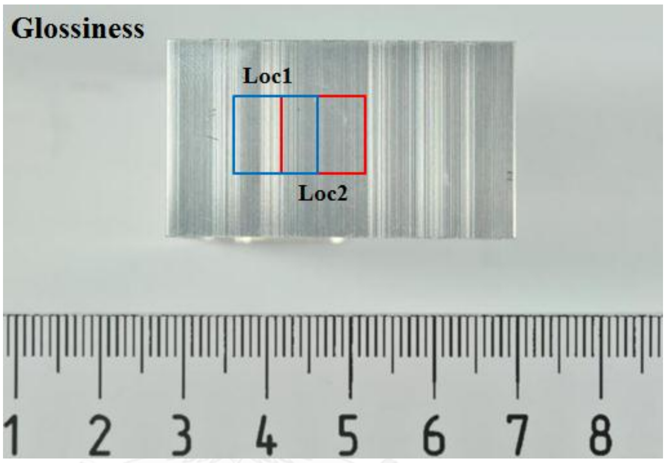

For example from (Run 1), the surface gloss difference is 6.0 GU that can be calculated from this equation:

$$\Delta \text{gloss} = \left| \left(\left| \text{gloss}_{\text{loc1}} - \text{gloss}_{\text{loc2}} \right| \right)_{\text{before}} - \left(\left| \text{gloss}_{\text{loc1}} - \text{gloss}_{\text{loc2}} \right| \right)_{\text{after}} \right|$$

From the Run1 results,

Before Etching			After Etching		
$gloss_{Loc1}$	**$gloss_{Loc2}$**	**$\Delta gloss_{before}$**	**$gloss_{Loc1}$**	**$gloss_{Loc2}$**	**$\Delta gloss_{after}$**
79.9	103.9	24.0	79.3	97.3	18.0

$$\Delta gloss_{Run1} = \left| \left(\left| 79.9 - 103.9 \right| \right)_{before} - \left(\left| 79.3 - 97.3 \right| \right)_{after} \right|$$

$$= \left| 24.0 - 18.0_{\text{after}} \right| = 6.0 \ \text{GU}$$

A.3.2 Experimental data of surface gloss difference for 60 runs CCD

Run	x_1	x_2	x_3	Surface gloss before etching [GU]			Surface gloss after etching [GU]			Δ Gloss [GU], Y_2
				Loc1	Loc2	ΔGloss before	Loc1	Loc2	ΔGloss after	
1	2	38	2	79.9	103.9	24.0	79.3	97.3	18.0	6.0
2	8	38	2	83.3	113.7	30.4	82.3	108.4	26.1	4.3
3	2	62	2	99.1	130.3	31.2	72.3	91.5	19.2	12.0
4	8	62	2	92.3	117.5	25.2	40.9	48.9	8.0	17.2
5	2	38	8	91.5	115.7	24.2	78.1	95.2	17.1	7.1
6	8	38	8	95.3	119.5	24.2	28.4	33.4	5.0	19.2
7	2	62	8	86.5	107.8	21.3	8.0	8.8	0.8	20.5
8	8	62	8	100.8	126.8	26.0	6.7	6.9	0.2	25.8
9	1	50	5	96.5	128.1	31.6	89.5	109.3	19.8	11.8
10	10	50	5	86.9	115.8	28.9	13.4	13.9	0.5	28.4
11	5	30	5	88.9	119.8	30.9	100.9	116.5	15.6	15.3
12	5	70	5	90.2	125.4	35.2	6.4	6.6	0.2	35.0
13	5	50	1	93.8	121.0	27.2	86.3	105.2	18.9	8.3
14	5	50	10	85.5	120.6	35.1	7.6	7.7	0.1	35.0
15	5	50	5	93.7	122.0	28.3	31.3	38.7	7.4	20.9
16	5	50	5	96.0	128.1	32.1	31.9	39.6	7.7	24.4
17	5	50	5	90.9	104.4	13.5	31.7	37.7	6.0	7.5
18	5	50	5	87.4	107.0	19.6	30.2	36.1	5.9	13.7
19	5	50	5	85.4	123.8	38.4	31.8	36.0	4.2	34.2
20	5	50	5	84.1	118.1	34.0	27.9	31.5	3.6	30.4
21	2	38	2	97.8	123.9	26.1	66.5	86.1	19.6	6.5
22	8	38	2	97.0	126.7	29.7	72.5	97.9	25.4	4.3
23	2	62	2	95.4	120.9	25.5	51.2	61.9	10.7	14.8
24	8	62	2	75.9	102.8	26.9	31.2	38.2	7.0	19.9
25	2	38	8	94.0	122.7	28.7	58.8	76.8	18.0	10.7
26	8	38	8	94.5	120.0	25.5	10.5	11.3	0.8	24.7
27	2	62	8	81.3	113.3	32.0	10.3	11.3	1.0	31.0
28	8	62	8	87.5	112.8	25.3	6.2	6.6	0.4	24.9
29	1	50	5	86.6	114.9	28.3	62.2	79.4	17.2	11.1

Run	x_1	x_2	x_3	Surface gloss before etching [GU]			Surface gloss after etching [GU]			Δ Gloss [GU], Y_2
				Loc1	Loc2	ΔGloss before	Loc1	Loc2	ΔGloss after	
30	10	50	5	90.9	117.8	26.9	9.6	10.0	0.4	26.5
31	5	30	5	88.7	111.5	22.8	80.7	95.8	15.1	7.7
32	5	70	5	95.3	119.6	24.3	5.3	5.4	0.1	24.2
33	5	50	1	90.4	121.5	31.1	64.1	83.4	19.3	11.8
34	5	50	10	80.0	109.3	29.3	6.0	5.9	0.1	29.2
35	5	50	5	100.8	133.6	32.8	30.5	37.8	7.3	25.5
36	5	50	5	85.2	108.9	23.7	29.6	36.1	6.5	17.2
37	5	50	5	74.5	102.5	28.0	23.0	28.2	5.2	22.8
38	5	50	5	74.4	100.8	26.4	21.8	26.9	5.1	21.3
39	5	50	5	74.4	99.1	24.7	22.8	27.6	4.8	19.9
40	5	50	5	85.2	111.9	26.7	19.8	23.7	3.9	22.8
41	2	38	2	82.9	108.3	25.4	72.3	91.6	19.3	6.1
42	8	38	2	69.3	101.0	31.7	64.8	92.1	27.3	4.4
43	2	62	2	77.2	102.8	25.6	62.0	70.6	8.6	17.0
44	8	62	2	76.8	105.5	28.7	28.5	35.6	7.1	21.6
45	2	38	8	81.9	106.9	25.0	57.1	73.8	16.7	8.3
46	8	38	8	85.7	111.1	25.4	34.2	41.5	7.3	18.1
47	2	62	8	91.0	113.8	22.8	7.2	7.9	0.7	22.1
48	8	62	8	84.1	104.6	20.5	6.9	7.2	0.3	20.2
49	1	50	5	80.6	109.6	29.0	60.5	78.9	18.4	10.6
50	10	50	5	63.3	94.3	31.0	9.5	9.9	0.4	30.6
51	5	30	5	88.6	114.0	25.4	78.7	94.5	15.8	9.6
52	5	70	5	85.9	115.4	29.5	6.8	6.7	0.1	29.4
53	5	50	1	89.2	102.4	13.2	68.2	87.6	19.4	6.2
54	5	50	10	101.0	126.4	25.4	6.8	6.7	0.1	25.3
55	5	50	5	68.6	86.2	17.6	26.0	32.4	6.4	11.2
56	5	50	5	85.9	122.9	37.0	25.3	32.7	7.4	29.6
57	5	50	5	80.0	99.2	19.2	27.9	34.2	6.3	12.9
58	5	50	5	97.0	124.3	27.3	24.8	30.2	5.4	21.9
59	5	50	5	86.4	111.2	24.8	24.0	29.7	5.7	19.1

Run	x_1	x_2	x_3	Surface gloss before etching [GU]			Surface gloss after etching [GU]			Δ Gloss [GU], Y_2
				Loc1	Loc2	ΔGloss before	Loc1	Loc2	ΔGloss after	
60	5	50	5	98.0	120.4	22.4	21.2	25.4	4.2	18.2

A.4 Experimental Results for Final Surface Roughness

A.4.1 Surface roughness measurement

- Surface roughness measurement (Y_3)

The final surface roughness (Y_3) was measured by 3D Lasor Confocal Microscope into 10 mm long distance of measurement as shown in the below figure.

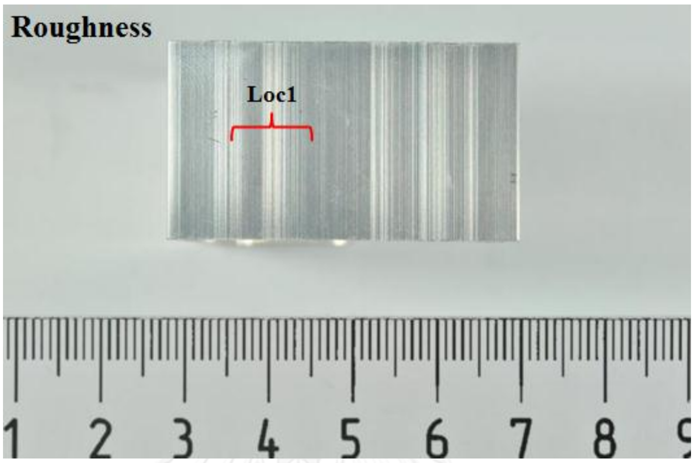

A.4.2 Experimental data of final surface roughness for 60 runs CCD

Run	Conc of NaOH [wt%], x_1	Etching Temp [°C], x_2	Etching Time [min], x_3	Surface roughness before etching [µm]	Surface roughness after etching [µm], Y_3
1	2	38	2	0.213	0.216
2	8	38	2	0.211	0.233
3	2	62	2	0.228	0.216
4	8	62	2	0.210	0.393
5	2	38	8	0.235	0.308
6	8	38	8	0.215	0.440
7	2	62	8	0.198	0.616
8	8	62	8	0.216	0.790
9	1	50	5	0.213	0.267
10	10	50	5	0.216	0.498
11	5	30	5	0.212	0.258
12	5	70	5	0.232	0.898

Run	Conc of NaOH [wt%], x_1	Etching Temp [°C], x_2	Etching Time [min], x_3	Surface roughness before etching [µm]	Surface roughness after etching [µm], Y_3
13	5	50	1	0.231	0.258
14	5	50	10	0.219	0.642
15	5	50	5	0.204	0.443
16	5	50	5	0.207	0.366
17	5	50	5	0.213	0.431
18	5	50	5	0.217	0.421
19	5	50	5	0.239	0.411
20	5	50	5	0.223	0.415
21	2	38	2	0.196	0.212
22	8	38	2	0.205	0.242
23	2	62	2	0.198	0.288
24	8	62	2	0.228	0.432
25	2	38	8	0.212	0.300
26	8	38	8	0.218	0.567
27	2	62	8	0.217	0.255
28	8	62	8	0.223	0.558
29	1	50	5	0.238	0.938
30	10	50	5	0.230	0.268
31	5	30	5	0.225	0.539
32	5	70	5	0.230	1.060
33	5	50	1	0.193	0.221
34	5	50	10	0.229	0.643
35	5	50	5	0.243	0.421
36	5	50	5	0.248	0.432
37	5	50	5	0.204	0.466
38	5	50	5	0.232	0.462
39	5	50	5	0.220	0.446
40	5	50	5	0.219	0.488
41	2	38	2	0.256	0.222

Run	Conc of NaOH [wt%], x_1	Etching Temp [°C], x_2	Etching Time [min], x_3	Surface roughness before etching [µm]	Surface roughness after etching [µm], Y_3
42	8	38	2	0.233	0.239
43	2	62	2	0.222	0.330
44	8	62	2	0.230	0.396
45	2	38	8	0.227	0.318
46	8	38	8	0.232	0.412
47	2	62	8	0.227	0.673
48	8	62	8	0.206	0.947
49	1	50	5	0.223	0.324
50	10	50	5	0.223	0.585
51	5	30	5	0.22	0.263
52	5	70	5	0.223	0.748
53	5	50	1	0.197	0.242
54	5	50	10	0.205	0.725
55	5	50	5	0.232	0.435
56	5	50	5	0.226	0.443
57	5	50	5	0.224	0.413
58	5	50	5	0.251	0.437
59	5	50	5	0.235	0.471
60	5	50	5	0.222	0.431

APPENDIX B.

B.1 Surface Response Plots for Weight Loss

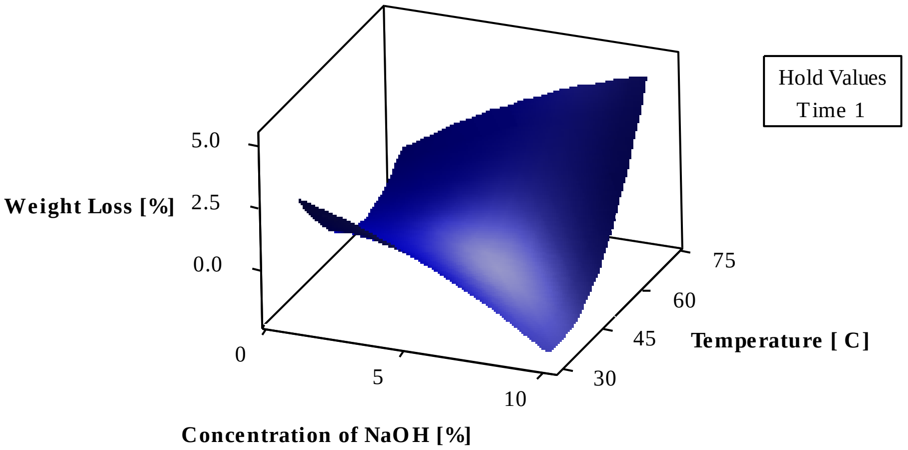

Figure B-1: 3-D response surface plot for the influence of concentration of NaOH and the etching temperature when the etching time was fixed at 1 min.

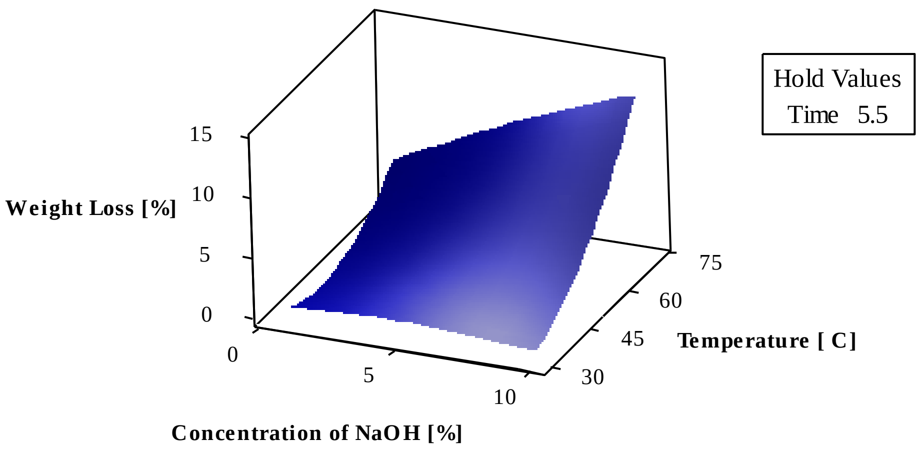

Figure B-2: 3-D response surface plot for the influence of concentration of NaOH and the etching temperature when the etching time was fixed at 5 min.

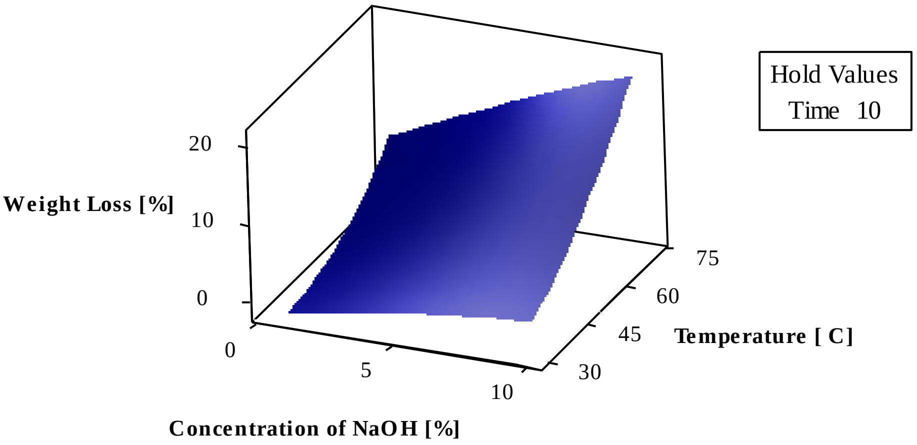

Figure B-3: 3-D response surface plot for the influence of concentration of NaOH and the etching temperature when the etching time was fixed at 10 min.

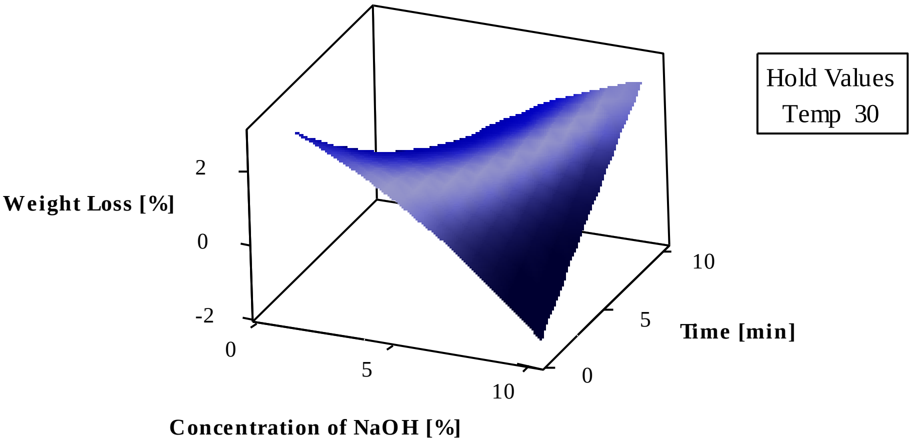

Figure B-4: 3-D response surface plot for the influence of concentration of NaOH and the etching time when the etching temperature was fixed at 30°C.

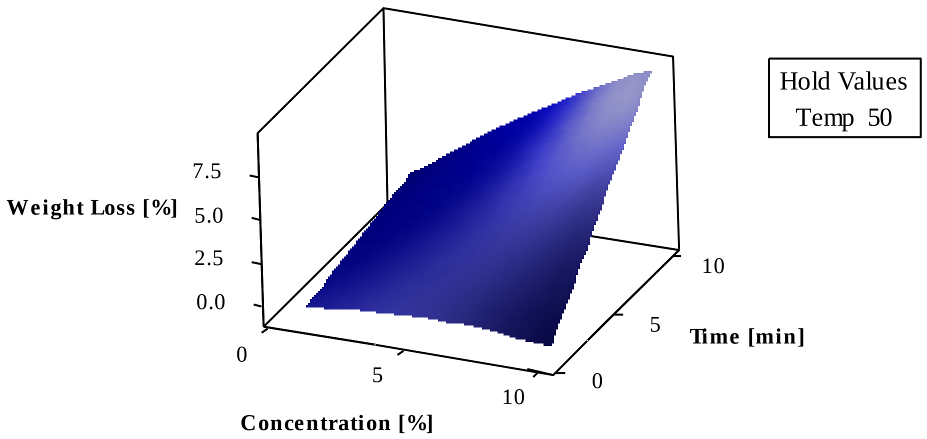

Figure B-5: 3-D response surface plot for the influence of concentration of NaOH and the etching time when the etching temperature was fixed at 50°C.

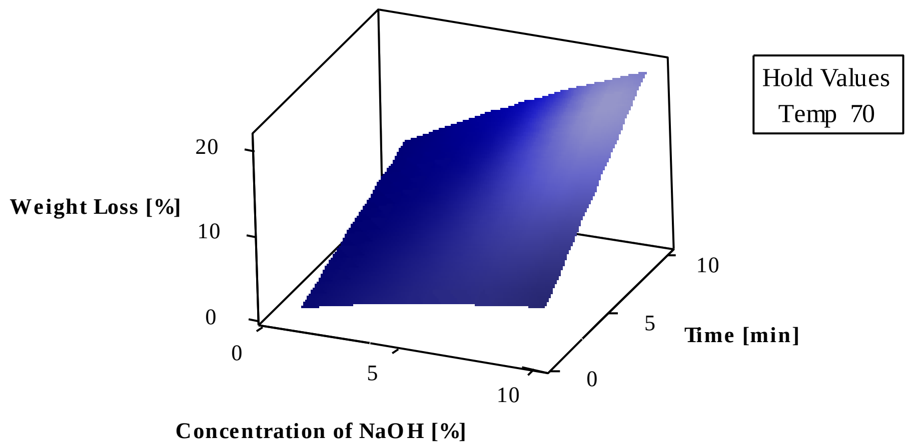

Figure B-6: 3-D response surface plot for the influence of concentration of NaOH and the etching time when the etching temperature was fixed at 70°C.

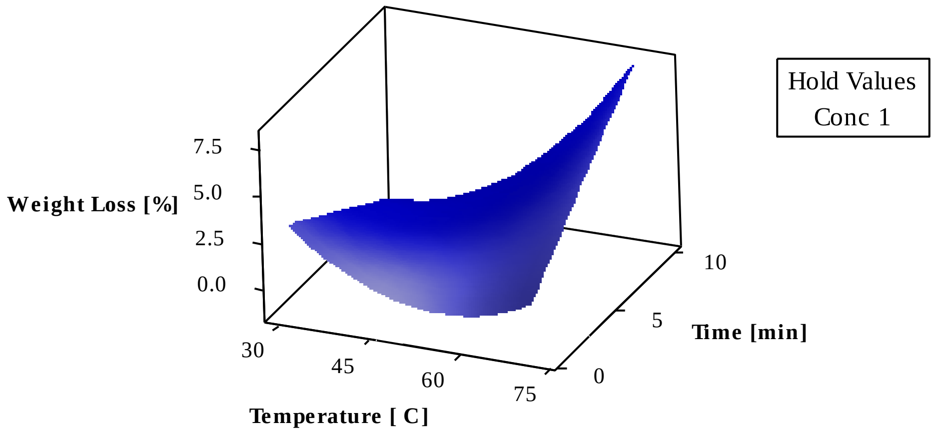

Figure B-7: 3-D response surface plot for the influence of the etching temperature and the etching time when the concentration of NaOH was fixed at 1%.

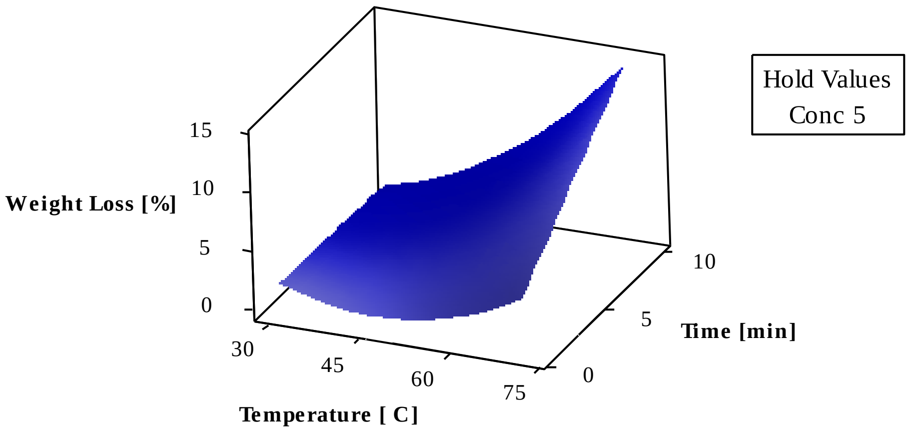

Figure B-8: 3-D response surface plot for the influence of the etching temperature and the etching time when the concentration of NaOH was fixed at 5%.

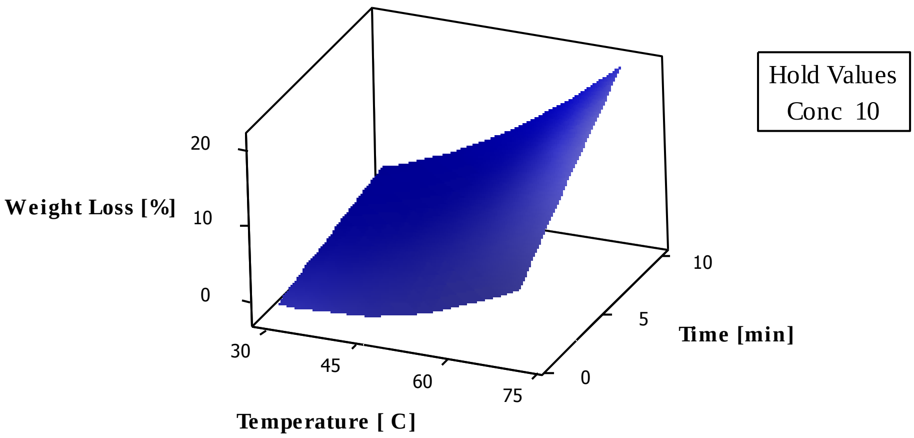

Figure B-9: 3-D response surface plot for the influence of the etching temperature and the etching time when the concentration of NaOH was fixed at 10%.

B.2 Surface Response Plots for Surface Gloss Difference

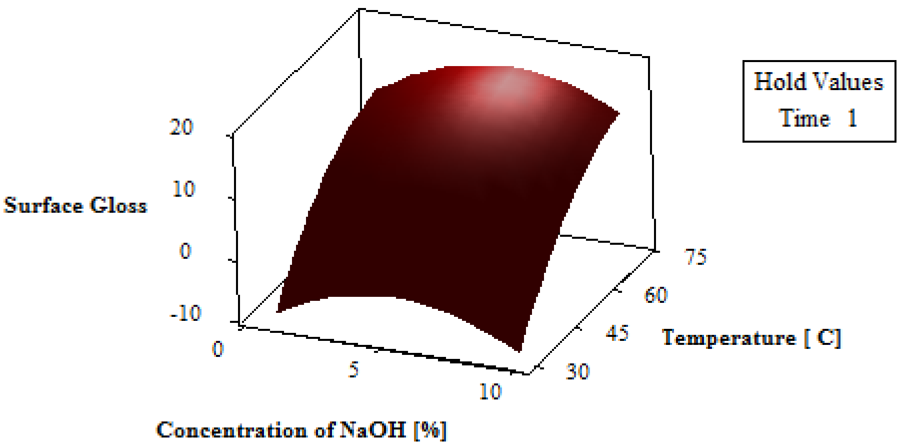

Figure B-10: 3-D response surface plot for the influence of concentration of NaOH and the etching temperature when the etching time was fixed at 1 min.

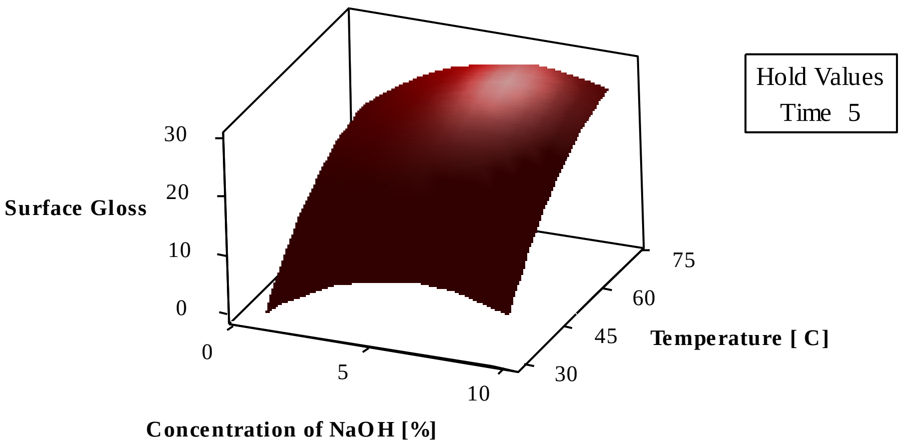

Figure B-11: 3-D response surface plot for the influence of concentration of NaOH and the etching temperature when the etching time was fixed at 5 min.

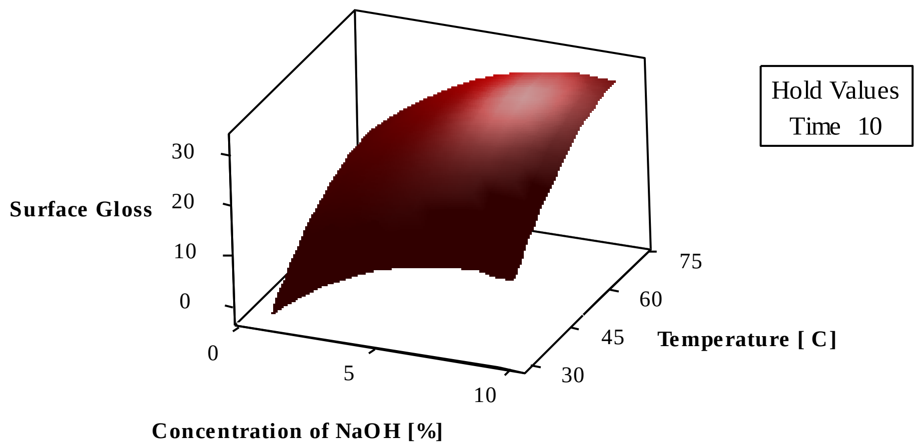

Figure B-12: 3-D response surface plot for the influence of concentration of NaOH and the etching temperature when the etching time was fixed at 10 min.

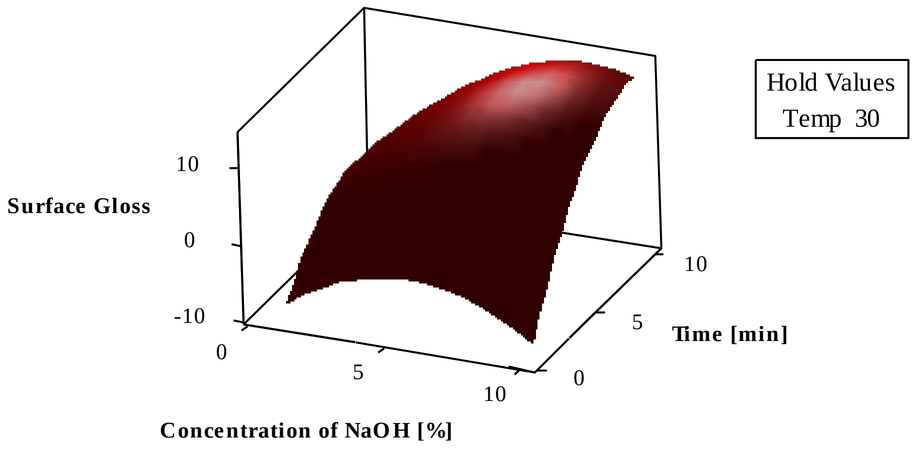

Figure B-13: 3-D response surface plot for the influence of concentration of NaOH and the etching time when the etching temperature was fixed at 30°C.

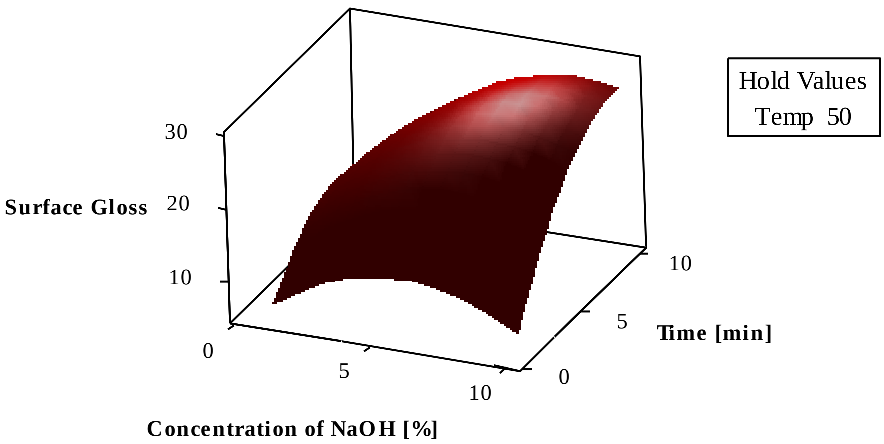

Figure B-14: 3-D response surface plot for the influence of concentration of NaOH and the etching time when the etching temperature was fixed at 50°C.

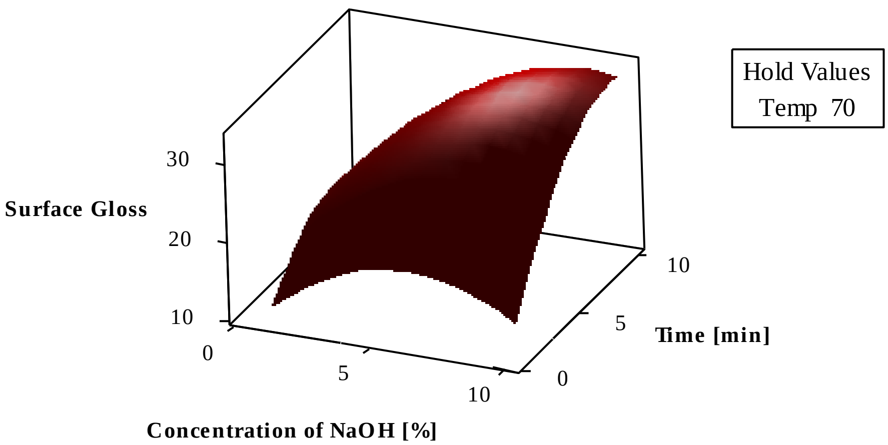

Figure B-15: 3-D response surface plot for the influence of concentration of NaOH and the etching time when the etching temperature was fixed at 70°C.

B.3 Contour Plots for Weight Loss

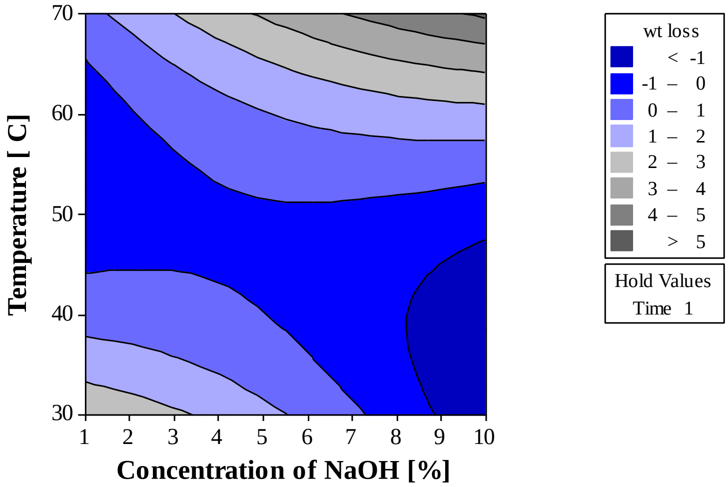

Figure B-16: Contour plot for the influence of concentration of NaOH and the temperature when the etching time was fixed at 1 min.

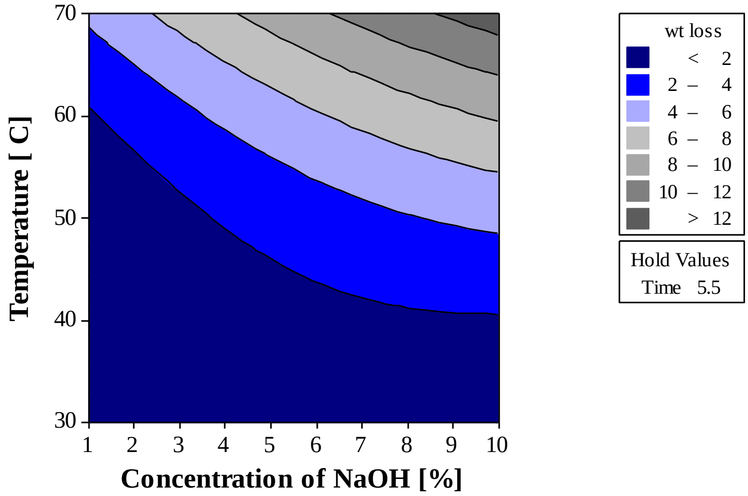

Figure B-17: Contour plot for the influence of concentration of NaOH and the temperature when the etching time was fixed at 5 min.

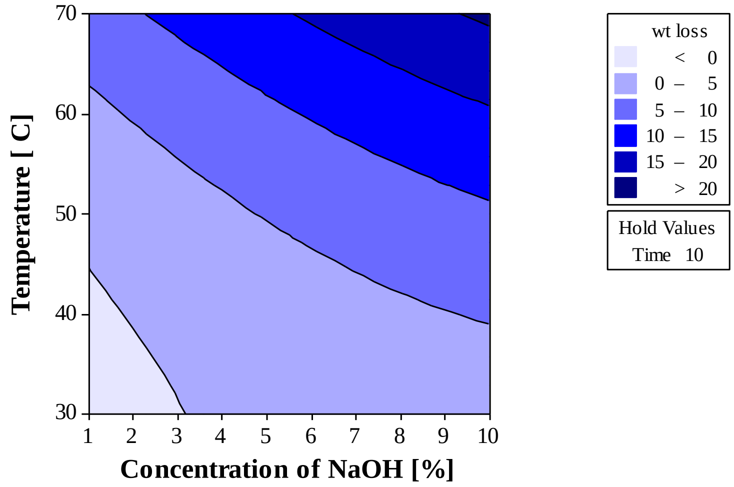

Figure B-18: Contour plot for the influence of concentration of NaOH and the temperature when the etching time was fixed at 10 min.

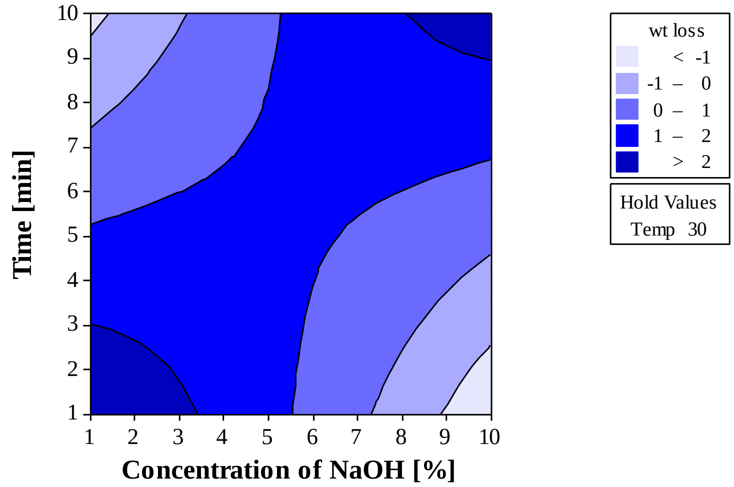

Figure B-19: Contour plot for the influence of concentration of NaOH and the etching time when the etching temperature was fixed at 30°C.

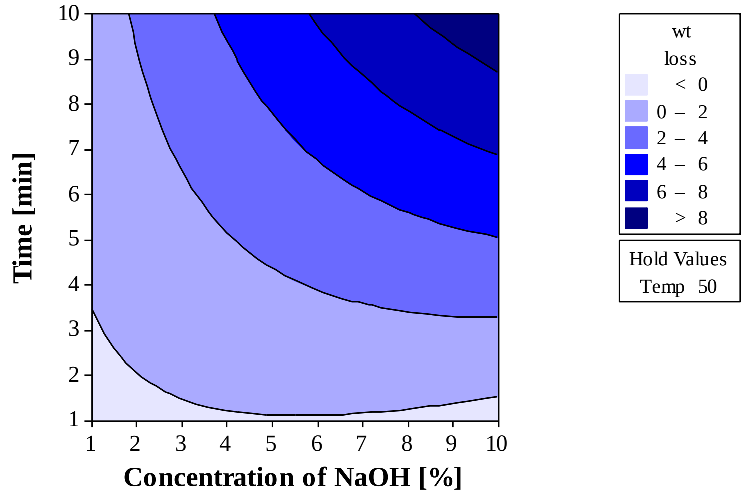

Figure B-20: Contour plot for the influence of concentration of NaOH and the etching time when the etching temperature was fixed at 50°C.

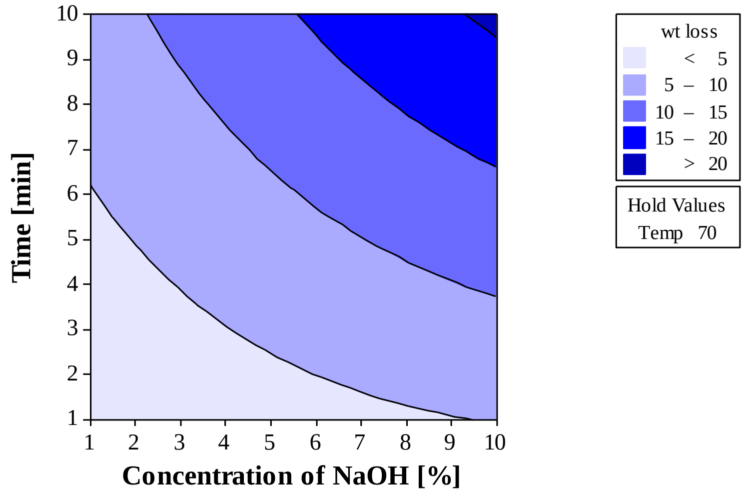

Figure B-21: Contour plot for the influence of concentration of NaOH and the etching time when the etching temperature was fixed at 70°C.

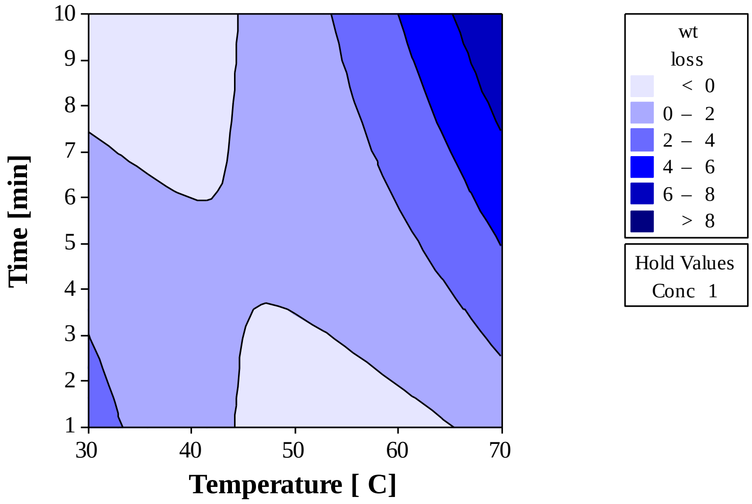

Figure B-22: Contour plot for the influence of the influence of the etching temperature and the etching time when the concentration of NaOH was fixed at 1%.

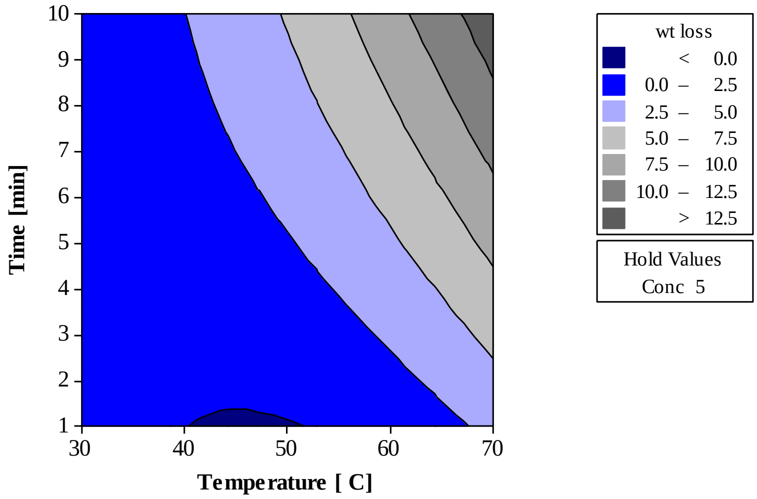

Figure B-23: Contour plot for the influence of the influence of the etching temperature and the etching time when the concentration of NaOH was fixed at 5%.

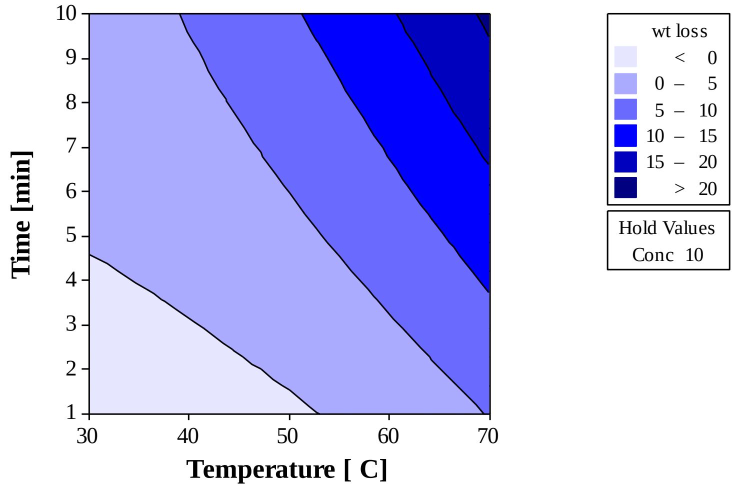

Figure B-24: Contour plot for the influence of the influence of the etching temperature and the etching time when the concentration of NaOH was fixed at 10%.

B.4 Contour Plots for Surface Gloss Difference

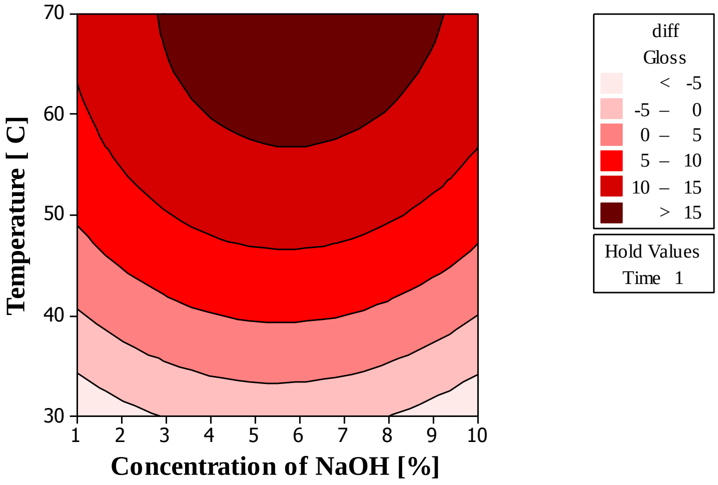

Figure B-25: Contour plot for the influence of concentration of NaOH and the temperature when the etching time was fixed at 1 min.

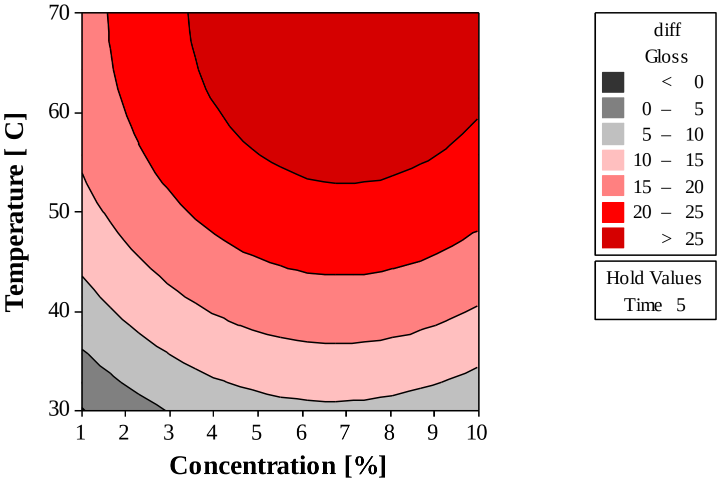

Figure B-26: Contour plot for the influence of concentration of NaOH and the temperature when the etching time was fixed at 5 min.

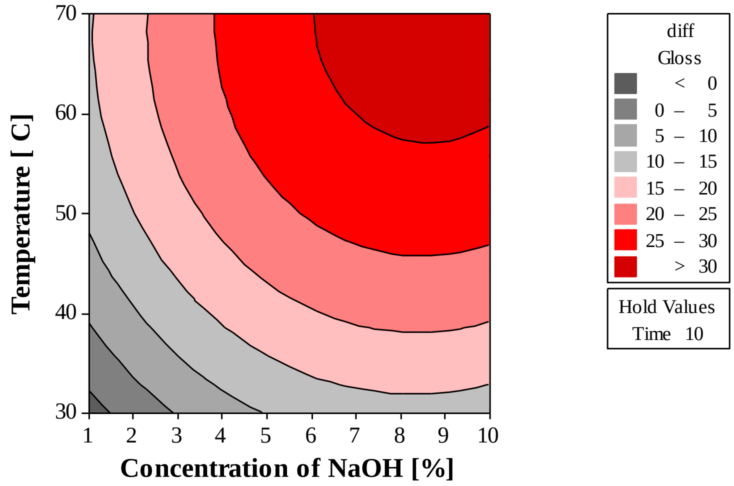

Figure B-27: Contour plot for the influence of concentration of NaOH and the temperature when the etching time was fixed at 10 min.

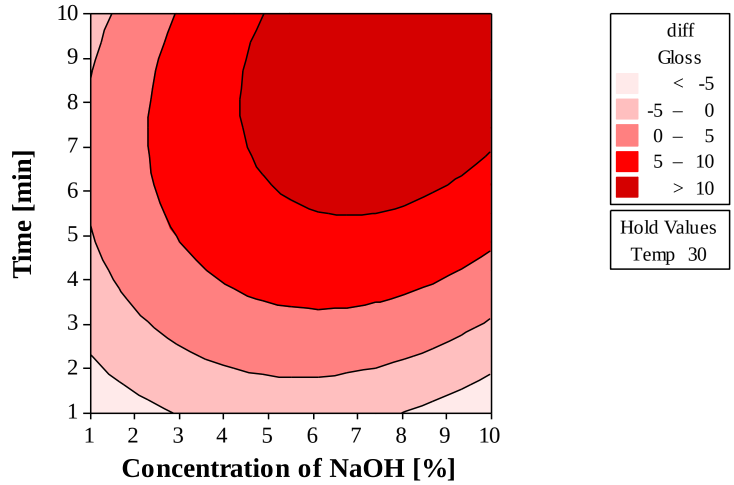

Figure B-28: Contour plot for the influence of concentration of NaOH and the etching time when the etching temperature was fixed at 30°C.

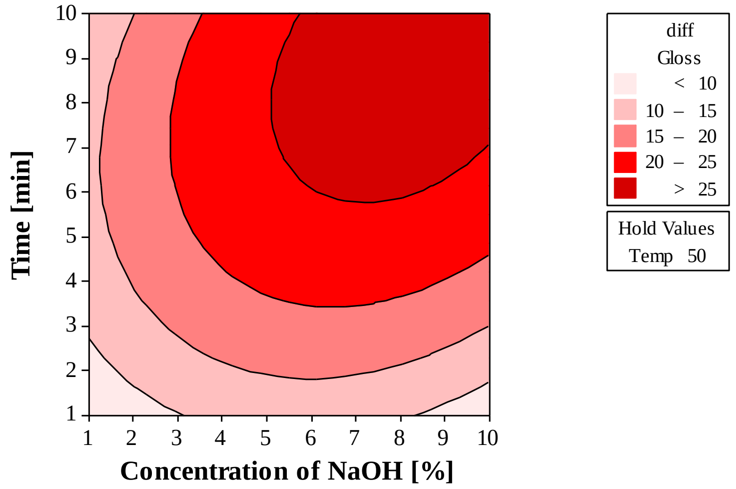

Figure B-29: Contour plot for the influence of concentration of NaOH and the etching time when the etching temperature was fixed at 50°C.

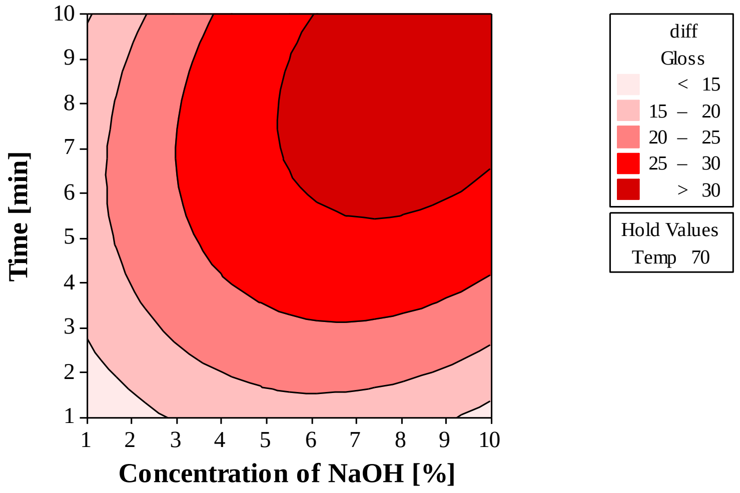

Figure B-30: Contour plot for the influence of concentration of NaOH and the etching time when the etching temperature was fixed at 70°C.

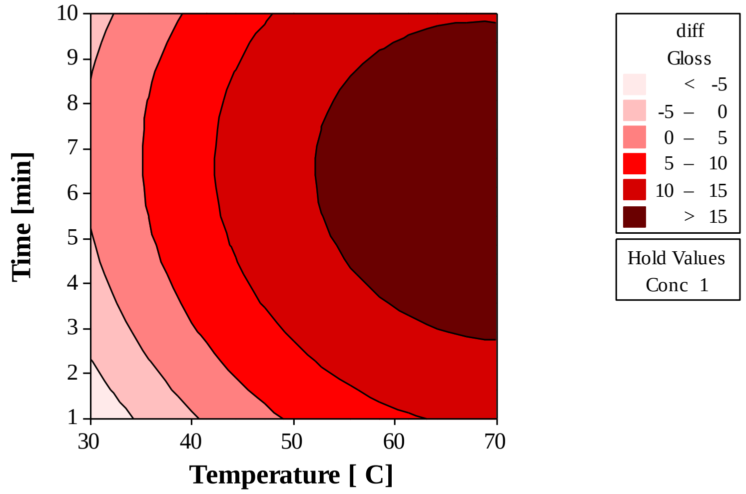

Figure B-31: Contour plot for the influence of the influence of the etching temperature and the etching time when the concentration of NaOH was fixed at 1%.

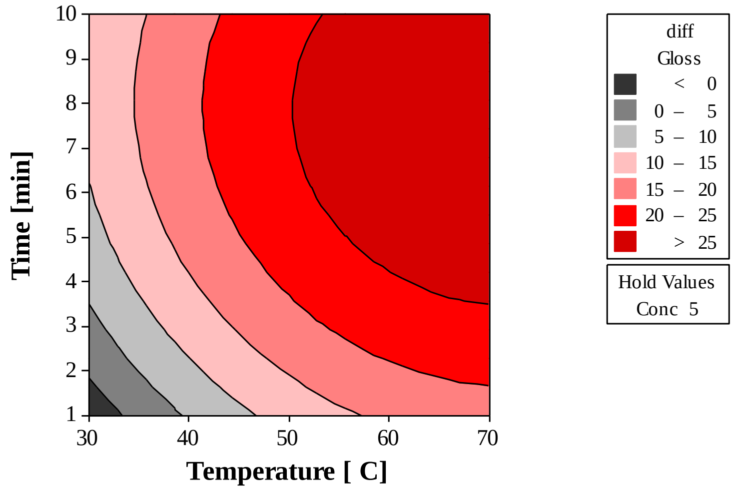

Figure B-32: Contour plot for the influence of the influence of the etching temperature and the etching time when the concentration of NaOH was fixed at 5%.

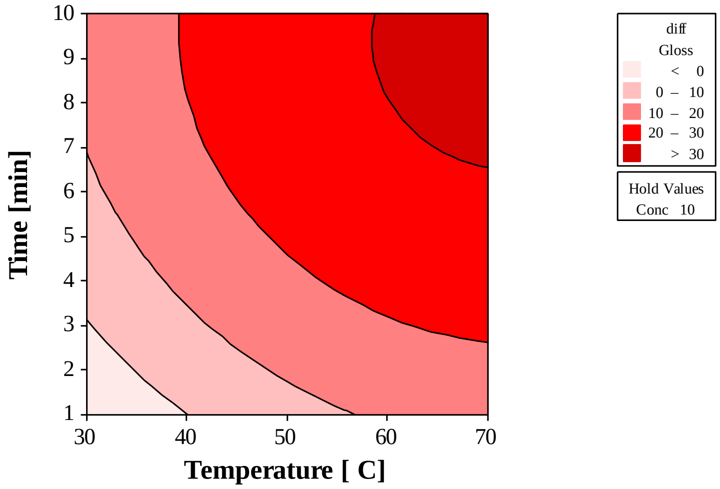

Figure B-33: Contour plot for the influence of the influence of the etching temperature and the etching time when the concentration of NaOH was fixed at 10%.

VITA

Ms. Sirikarn Sattawitchayapit was born on October 23, 1988, in Chonburi, Thailand. She completed a high school from Rayong Wittayakhom School in 2008 and received the Bachelor degree from Department of Chemical Technology, Faculty of Science, Chulalongkorn University, Bangkok, Thailand in 2012. After graduation, she has been working as a research assistant at The National Metals and Material Technology Center (MTEC), The National Science and Technology Development Agency (NSTDA), Thailand. Since 2014, she entered the graduate school of Chulalongkorn University and received her Master's Degree in Chemical Engineering from Department of Chemical Engineering, Faculty of Engineering, Chulalongkorn University in 2017. During her graduate study, she gave a poster presentation at The Pure and Applied Chemistry International Conference 2016 (PACCON2016). Details are given as follows:

- Sattawitchayapit S, Mahabunphachai S, Arpornwichanop A. Effect of Etching Process Parameters on Streak Defect in Anodized Aluminum. The Pure and Applied Chemistry International Conference 2016, February 9-11, 2016, BITEC Bangna, Bangkok, Thailand.